

Application of Solid Phase Microextraction for Lipid Analysis and Lipidomics

by

Afsoon Pajand Birjandi

A thesis
presented to the University of Waterloo
in fulfillment of the
thesis requirement for the degree of
Doctor of Philosophy
in
Chemistry

Waterloo, Ontario, Canada, 2015

© Afsoon Pajand Birjandi 2015

Author's Declaration

I hereby declare that I am the sole author of this thesis. This is a true copy of the thesis, including any required final revisions, as accepted by my examiners.

I understand that my thesis may be made electronically available to the public.

Abstract

Although the latest advancements in lipid analysis technology provide an excellent opportunity for the comprehensive study of lipidome, fulfilling the analytical requirements at the desired quality is still a major challenge. In lipidomic workflow, sample treatment and extraction for simultaneous analysis of endogenous lipids is of a great interest, especially when a number of undesirable circumstances such as ionization suppression are the matter of concern. In this thesis, I describe several approaches for both in vivo and high throughput in vitro sample preparation for molecular lipidomics based on solid phase microextraction (SPME) in the direct extraction mode.

The initial research presented in this thesis focused on the analysis of fatty acids (FA) as the major building block and most fundamental category of entire lipid family. In this study, we present a direct immersion solid phase microextraction method coupled to a liquid chromatography-mass spectrometry platform (DI-SPME- HPLC-ESI-MS) for determination of unconjugated fatty acids (FA) in fish and human plasma. The proposed method was fully validated according to bioanalytical method validation guidelines. The affinity constant (K_a) of individual FAs to protein albumin was determined to be 9.2×10^4 to $4.3 \times 10^5 \text{ M}^{-1}$. The plasma protein binding (PPB%) was calculated and found to be in the range of 98.0–99.7% for different polyunsaturated fatty acids (PUFAs). The PUFAs under study were found at a high concentration range in fish plasma, whereas only a few were within quantification range in control human plasma. The method was successfully applied for monitoring PUFA changes in plasma samples obtained during operation of a group of patients undergoing

cardiac surgery with the use of cardiopulmonary bypass (CPB). The most significant alteration induced by surgery was noticed in the concentration level of α -linolenic acid (18:3, ALA), arachidonic acid (20:4, AA), and docosahexanoic acid (22:6, DHA) soon after inception of CPB in all cases.

The quantitative results obtained for fatty acid measurement have encouraged me to expand my study for analyzing a broad spectrum of complex lipids as the next step. Therefore, in Chapter 3 biocompatible thin film SPME technique is introduced for quantitative analysis of lipids from human plasma in a high throughput manner. Robotic assisted 96-blade thin-film SPME was employed for the extraction of a group of non-endogenous lipids from plasma, and satisfactory results for recovery and reproducibility were achieved. In addition, the new extraction method eliminated the need for multi-step sample handling including centrifugation, filtering, solvent evaporation, and reconstitution. The total preparation time was reduced to less than 2 min per sample, while artifacts and sample loss were minimized due to the simplified method. Absolute recoveries were typically 1-2%, thereby avoiding sample disturbance while providing proper sensitivity. Furthermore, endogenous and non-endogenous groups of target lipids were quantified, and excellent linearity and method precision were obtained. The regression calibrations obtained from five different plasma batches represents RSD less than 5% in all cases, clearly indicating the absence of matrix effects and lot-to-lot variations of the proposed method. The linearity ($R^2 > 0.99$), inter and intra-day reproducibility (2-7%), and precision (1-12%) provided verification of method validity.

Finally, the evaluated SPME method was compared to the conventional Bligh & Dyer technique for the untargeted lipidomic study of human hepatocellular carcinoma (HCC) cell lines. Cells were cultured under standard conditions in two individual groups; one cultivated normally as a control group and another supplemented by eicosapentanoic acid (20:5), as a highly polyunsaturated fatty acid, to study the effect of treatment on the lipidome pattern of cancerous cells. The obtained results provided a list of up-regulated and down-regulated lipids through a comparison between control versus treated cells. Method precision for the SPME approach was excellent (5-18% RSD) for all detected lipids. The relative LOD range was 0.5-1 ng/ml for the proposed SPME method, while for Bligh & Dyer, it was found to range between 0.05-0.1 ng/ml. Automated 96-blade sample handling enhanced extraction rates by approximately 2 min per sample, while generating comparable or enhanced product yields in comparison to conventional methods

This study highlights important advantages of both SPME approaches using the rod fiber and thin-film geometries to capture fatty acids and lipids from different biological media including human and fish plasma as well as cell culture. The experimental results confirm the suitability of SPME for both in vitro and in vivo study in clinical samples as a new tool for lipidomic analysis.

Acknowledgements

I have enjoyed working on various interesting yet challenging research projects during my PhD journey and am grateful for all the ideas and insights provided by many people who have worked with me. First and foremost, I would like to thank my supervisor, Professor Janusz Pawliszyn, for supplying with the facilities at his laboratory and for the possibility to work on this thesis under his supervision, for providing me with the situation in which I got to learn more about myself and to prove to myself that I am not the one who gives up on her goals and dreams in the extreme hardship.

I also give my heartfelt thanks to all those others who have helped make this accomplishment possible: to Dr. Michael Palmer, Dr. Marcin Wąsowicz, and Dr. Wojciech Gabryelski who despite their busy schedules served as my committee. To Professor Danel Figeys and Dr. Zhibin Ning at the Ottawa Institute of System Biology for the work we have done together, for providing the cell samples and the insightful discussions we had concerning statistical data processing and interpretation which considerably enriched my work. I am also grateful to Dr. Ken Stark for his willingness to provide valuable input on the biological aspect of my experimental data.

I gratefully acknowledge the support and friendship of our group lab manager, Dr. Fatemeh Sadat Mirnghi, her openness and welcoming for questions, problems and discussions which largely helped me to accomplish my learning curve and get me prepared for more profound phases of my research projects. Dr. Vincent Bessonneau is highly appreciated for training me with different professional software and algorithms used in multivariate data analysis and

“omic” studies. Dr. Barbara Bojko is appreciated for providing feedback. Appreciation is extended to all other colleagues and persons in the lab who have been responsible for the equipment and logistics.

On an entirely different level, my deepest love, thanks and gratitude to my beloved Del-o-Jan Choir group members, especially to Dr. Ali Tehrani as a compassionate mentor and vocal trainer. I had such relieving moments when experiencing the glamour of singing along with a affectionate team for more than three years. Together we accomplished a journey of not only learning and performing music but also loving and supporting each other despite our differences. It was an amazing and heartwarming experience to be accepted as a trusted team member when most felt abandoned and isolated at work. You are my new family and the best thing that has happened to me in this country. I love each and every of you!

In addition, I would like to express my sincere gratitude to Mr. Mehran Rad who I enjoyed his afternoon sessions of Persian literature and poetry, that delightful moment of leaving the cold and sullen laboratory environment to refresh and reconnect with the delightful elegance of my Persian roots and culture.

Most importantly, I wish to express my deepest love and gratitude to my beloved parents, Firouzeh and Hamid who has enlighten my path with their notable passion for education and reading and their heartfelt support and endless encouragement which has enabled me to survive the challenges of these years; also to my brothers Omid, Arash and Atta, I miss our moments together, specially the fighting ones.

Dedication

To my mom, whose wise words kept me going through the hardship of these years:

"Never dare to ride a wild horse, but if you did, be brave enough and do not let it throw you off!"

Table of Contents

Author's Declaration	ii
Abstract	iii
Acknowledgements	vi
Dedication	viii
Table of Contents	ix
List of Figures	xiii
List of Tables	xix
List of Abbreviations and Symbols.....	xxi
Chapter 1 Introduction	1
1.1 Lipid chemistry and general classification	1
1.1.1 Fatty Acid	2
1.1.2 Glycerophospholipids	3
1.1.3 Sphingolipids	5
1.1.4 Glycerolipids	6
1.2 Lipid Distribution and interaction with proteins	7
1.3 Necessity of lipid analysis and lipidomics	8
1.3.1 Trends in lipid analysis.....	9
1.4 Lipid analysis and lipidomics: miscellaneous platforms	10
1.4.1 Direct infusion and shotgun lipidomics.....	10
1.4.2 GC and GC-MS	11
1.4.3 LC and LC-MS	13
1.5 Sample preparation and extraction for lipidomics.....	15
1.5.1 Liquid-Liquid Extraction	16
1.5.2 Solid-phase extraction (SPE).....	17

1.5.3 Other emerging extraction techniques	18
1.6 Solid-phase microextraction	20
1.6.1 Thin-film microextraction	24
1.6.2 SPME for metabolomic studies	25
1.7 Research objectives.....	27
Chapter 2 Application of Solid Phase Microextraction for Quantitation of Polyunsaturated	
Fatty Acids in Biological Fluids	29
2.1 Preamble and introduction	29
2.1.1 Preamble	29
2.1.2 Introduction	29
2.2 Experimental.....	33
2.2.1 Chemical and Materials	33
2.2.2 Plasma Sample Preparation	34
2.2.3 Optimization of SPME Procedure	35
2.2.4 LC-ESI-MS Operating Conditions	36
2.2.5 Determination of Matrix Effect and Ionization Suppression.....	37
2.2.6 Determination of Protein Affinity Constant	37
2.2.7 Determination of plasma protein binding: investigation of free and total	
concentrations	38
2.3 Results and Discussions	38
2.3.1 HPLC-ESI-MS.....	38
2.3.2 SPME method development	40
2.3.3 Extraction efficiency of the SPME method in PBS.....	44
2.3.4 Evaluation of matrix effect and ionization suppression	45
2.3.5 Evaluation of matrix effect using Sample Extract Dilution Method	46
2.3.6 Determination of albumin affinity constant by SPME	47
2.3.7 Plasma protein binding (PPB %)	49
2.3.8 Fatty acids quantification in plasma samples	51

2.3.9 Comparison of NEFA composition in fish and human plasma	52
2.3.10 Clinical data analysis	53
2.4 Conclusions and Future Directions	57
2.5 Addendum and Acknowledgment	58
Chapter 3 Methodological modifications on quantitative analysis of plasma lipids using high throughput solid phase microextraction.....	59
3.1 Introduction	59
3.2 Experimental	63
3.2.1 Reagents and materials	63
3.2.2 Preparation of standard solutions and plasma samples	64
3.2.3 Preparation of C18-PAN 96-Blade coatings	65
3.2.4 Optimization of the SPME procedure	65
3.2.5 LC-ESI-MS Operating Conditions	66
3.2.6 Data analysis and calculations	67
3.3 Results and Discussion.....	69
3.3.1 Chromatographic Method Validation.....	69
3.3.2 Extraction phase: Comparison of C18 fiber and thin film.....	74
3.3.3 Optimization of extraction and desorption conditions	75
3.3.4 Mass balance and distribution; Investigation of suitability of PBS buffer for free concentration determination	78
3.3.5 Matrix free calibration	81
3.3.6 Evaluation of matrix effects	83
3.3.7 Evaluation of non-depletive extraction recovery by sequential SPME extractions	86
3.3.8 High throughput 96-blade SPME system for Plasma Protein Binding (PPB %) ...	89
3.3.9 Summary of method performance	94
3.3.10 Conclusions and future directions	99
Chapter 4 Discovery Lipidomic of Hepatic Cancer Cells in Response to Treatment by a Polyunsaturated Fatty Acid: Eicosapentaenoic Acid.....	101

4.1 Introduction.....	101
4.2 Experimental.....	102
4.2.1 Cell culture	102
4.2.2 Lipid extraction by Bligh & Dyer protocol	103
4.2.3 Preparation of C18-PAN 96-Blade coatings	104
4.2.4 SPME procedure.....	105
4.2.5 LC-ESI-MS operating conditions	108
4.2.6 Data processing.....	109
4.2.7 Data analysis.....	109
4.2.8 Data Quality Assurance	110
4.3 Results and discussion	111
4.3.1 LC-MS method assessment	111
4.3.2 Comparison of sample preparation methods for known identified lipids	117
4.3.3 Lipidomics - SPME results versus conventional Bligh & Dyer	118
4.3.4 Quality control (QC) Monitoring- assessment of instrumental response robustness	123
4.3.5 Statistical analysis.....	125
4.3.6 Feature Identification.....	128
4.3.7 Comparison of extraction efficiency of two methods for the group coverage	131
4.3.8 Control vs. Treated Cells- Up-regulated lipids.....	132
4.3.9 Control vs. Treated Cells - Down-regulated lipids.....	138
4.3.10 Matrix effect evaluation.....	143
4.4 Conclusion	144
Chapter 5 Summary and future directions	147
5.1 Summary	147
5.2 Future directions	151
Bibliography	154

List of Figures

Figure 1-1 Schematic representation of a typical SPME workflow from a given biological sample to LC-MS. Small arrows indicate the direction of mass transfer.	21
Figure 2-1 schematic of the experimental model for the equilibrium extraction of free fatty acids from plasma using the SPME fiber. Figure reprinted from reference with the permission of the publisher. ⁵⁹	33
Figure 2-2 Examples of XIC chromatograms for SPME-LC-MS analysis of 2µg/mL of fatty acids from human plasma; DHA: 327.3, DPA: 329.3, ADR: 332.3, DTA: 333.3, EPA: 301.3, ARA: 303.3, EPA: 305.3, SDA: 275.2 and 10-ALA: 277.2 respectively)	40
Figure 2-3 Extraction time profile for extraction of (3000 ng/mL) fatty acids spiked in plasma, the second plateau is an unusual observation due to the initiation of protein aggregation around the fiber after 4 hours extraction with aggressive vortex.....	41
Figure 2-4 Evaluation of analyte loss using different washing strategies, extraction from spiked PBS (30ng/ml)	42
Figure 2-5 Desorption solution composition containing acetonitrile, ACN/MOH/W (40:40:20) plain or with additives of NH ₄ OH (pH 7.8), Formic acid (pH 3.2) or tributylamin (pH 9.2), extraction from spiked PBS (30ng/ml)	43
Figure 2-6 Plasma sample dilution effect on normalized ion current intensity for fatty acids extracted from spiked plasma at a concentration of 2µg/ml of standard fatty acids.....	47

Figure 2-7 Albumin concentration-dependent NEFA recovery; y-axis represents the extraction recovery percentage of fatty acids vs albumin concentrations after 2 hr of extraction. Figure reprinted from reference with the permission of the publisher. 49

Figure 2-8 Scheme of cardiac surgery with the use of extracorporeal circulation (CPB) indicating the sample collection over the time of surgery. Figure reproduced from reference with the permission of the publisher¹⁵⁸ 54

Figure 2-9 Metabolic profile of FAs in patients undergoing cardiac surgery with the use of CPB; the most significant increase of FAs was observed for patient 7, in which the level of ALA reaches to 75 ± 4 μg . Based on Table 2-3, concentration of ALA in the normal human plasma is only 2.8 ± 0.2 μg . Figure reprinted from reference with the permission of the publisher..... 56

Figure 3-1 Extracted ion chromatograms (XIC) of PC and TG using acidic buffer in elution 72

Figure 3-2 Example of extracted ion chromatograms (XIC) for 3 mg/mL odd lipid standard in blood plasma; mobile phase A consist of ACN/ W (90:10) Containing 0.1 % Acetic acid and mobile phase B consist of IPA 100% 0.15 mM amonium acetate..... 73

Figure 3-3 Evaluation of different SPME coatings for the extraction of lipids from PBS; comparison of coatings (C18 vs. HLB) and geometries (rod fiber vs. Thin-Film) 74

Figure 3-4 Evaluation of desorption solvent for C18-PAN coatings for equilibrium extraction from PBS buffer solutions containing 200 ng/mL lipids 75

Figure 3-5 Evaluation of the optimized desorption time profile in 1ml MOH/IPA desorption solution.....	76
Figure 3-6 Extraction time profile obtained for lipid standards using Thin-Film C18 coating. Extraction conditions: (3500ng/ml) standards of odd lipids spiked in human plasma	77
Figure 3-7 Example of matrix-free calibration curves obtained in PBS in a) low and b) high concentration ranges; the slope of calibration as well as linearity regression of each lipid are displayed beside the plots	82
Figure 3-8 Matrix effect of SPME method using the sample extract dilution method; for some lipids signal was not detected in higher dilution levels. No dilution was required for SPME extracts for any of the studied lipids.	85
Figure 3-9 Measured concentrations (n = 3) of consecutive SPME measurements for a) spiked odd lipid standards and b) natural non-spiked lipids. The extraction uptake was monitored for the 1 st , 2 nd , 3 rd , 4 th , 5 th and 6 th successive extractions.	87
Figure 3-10 Extraction recovery after 6 sequential extractions from spiked plasma (3000ng)	89
Figure 3-11 Schematic of different lipid-binding proteins in interaction with lipids in plasma. Binding is a complex function of the affinity of proteins to different lipids.	92
Figure 3-12 Human plasma samples (n = 3 lots) were analyzed by SPME-LC-MS/MS; a) example calibration curve of class-specific lipid standards for PC (17:0/17:0) and PC (14:0/18:1) at equimolar concentration range (500-5000 ng/mL; n=3 each point). Linear	

regression and correlation coefficient (R^2) are compared; b) Correlation between data obtained for measurement of PCs of different aliphatic chains.....	97
Figure 4-1 Thin-film C18 blade set/ MixMode SPME fiber assembly for simultaneous extraction of lipids and polar metabolites of HuH7 cell sample placed in the same well	105
Figure 4-2 Schematic of sampling order for SPME and B&D procedure for the cell suspension of HuH7; Each replicate tube contained approximately 8.4×10^6 cells.....	107
Figure 4-3 XIC chromatogram of lipid standards in A) positive and B) negative ion mode. Variations in retention time are expected for lipids of the same class and sub-class dependent on their structural orientation and acyl chain length.....	113
Figure 4-4 Total ion count (TIC) chromatograms from control HUH7 cell lines obtained by: panels A and C) SPME and panels B and D) Bligh & Dyer extraction methods in positive and negative ion modes respectively	116
Figure 4-5 Comparison of method precision (expressed as % RSD for n=5 replicates) obtained for Bligh & Dyer with methanol/ chloroform and the validated SPME technique using C18 coatings.....	118
Figure 4-6 (a) Ion map (m/z versus retention time) for HUH7 cell samples extracted by Bligh&Dyer and SPME and analyzed using positive ESI-LC-MS method. (b) Number of peaks with given % RSD obtained for the two independent data sets.....	121
Figure 4-7 (a) Ion map (m/z versus retention time) for HUH7 cell samples extracted by Bligh&Dyer and SPME and analyzed using negative ESI-LC-MS method. (b) Number of peaks with given % RSD obtained for the two independent data sets.....	122

Figure 4-8 Instrumental response variability for several QC injections randomized within the run sequence for selected compounds (a) CE, MG, and TG (b) SM and PE (c) PC and LPC; compounds with different signal intensity ranges are represented in separate charts. 124

Figure 4-9 Score plots of PCA performed on samples of control and treated cells extracted by SPME (red and violet dots); and samples of control and treated cells extracted by Bligh & Dyer (blue and green dots), QCs (yellow dots) and standard lipids (tiffany blue). Clustering of the QC samples demonstrates the repeatability of the analytical system used. X-axis and Y-axis represent the score of the first and second principal component, respectively. This plot is run for the pool of ion features unselectively..... 126

Figure 4-10 Example OPLS-Da models (right) and representative S-plots (left) in positive mode comparing control and treated cell samples by using: 1) SPME (top) and 2) Bligh & Dyer (bottom) extraction methods. Green and blue markers in the OPLS-DA models (right panels) represent the significant difference between profile of control and treated groups, respectively using both methods; each green dot on the S-plots (left panels) represents an ion feature that was detected. The green dots inside red boxes were the ions that drive group separation and screened for further identification 127

Figure 4-11 Example XIC chromatograms illustrates the ion 962.72301 in control vs. treated groups using SPME and B&D. The chromatograms clearly confirm the changes of this species which were not detectable in the control HUH7 cells cultured in normal condition. However, when the same cells were cultured while supplemented with EPA, this metabolite

increased greatly and created a significant discrimination between cell groups in statistical analysis..... 130

Figure 4-12 Comparison of extraction efficiency of a) Bligh & Dyer and b) SPME in covering a broad range of class-specific lipids. 132

Figure 4-13 Comparison between control and treated cells which illustrate the significant increase in the level of the above listed lipid species with application of a) Bligh & Dyer and b) SPME extraction technique 137

Figure 4-14 The two graphs illustrate the significant decrease of the above listed lipids in the treated cells extracted by top) Bligh & Dyer and bottom) SPME method. 139

Figure 4-15 Score plots of PCA performed on the lipid features of most significant difference listed in Table 4-2, Table 4-3 and Table 4-4. Plot illustrates a clear separation between BD-control and SPME-control, BD-Treat and SPME-Treat. The x-axes and y-axes represent the score of the first and second principal component contributing 72.6% and 20.3% variances, respectively. 140

Figure 4-16 Example Box-whisker plots representing four potential lipid candidates with lowest p values between the control and treated cell groups: m/z 780.55338 for PC (20:5/16:0) or PE (20:5/19:0); m/z 916.738626 for TG (20:5/20:5/16:0), m/z 838.56301 for PS (22:4/18:0) and m/z 329.24916 for docosapentaenoic acid (22:5)..... 141

Figure 4-17 Evaluation of ionization suppression involved in the extraction of cell samples 143

List of Tables

Table 1-1 Representative chemical structures of saturated and polyunsaturated fatty acids....	3
Table 1-2 Representative chemical structures of glycerophospholipids and lysophospholipids	4
Table 1-3 Representative chemical structures of sphingolipid family sub-classes.....	5
Table 1-4 Representative chemical structures of glycerolipid family sub-classes	6
Table 2-1 Evaluation of SPME method efficiency for extraction of FAs from physiological buffer solution (pH=7.4)	45
Table 2-2 Evaluation of albumin affinity constant and % plasma protein binding	50
Table 2-3 Linear dynamic range of fatty acid concentration in human and fish plasma samples.....	53
Table 3-1 Summary of LC-MS/MS parameters for analysis of lipids.....	70
Table 3-2 Automated LC-MS/MS method validation and instrumental robustness results ...	73
Table 3-3 Evaluation of Mass balance and total absolute recovery (%) from PBS solution containing 200ng lipid mixture using SPME extraction under optimized conditions; the total extraction recovery is compared to the recovery percentage reported in the literature	79
Table 3-4 Evaluation of matrix effect and ionization suppression in two different concentration levels	86
Table 3-5 different plasma lots by solid phase microextraction (SPME).....	94

Table 3-6 Summary of linearity results obtained for C18 coatings in 3 different pooled plasma lots. Each point of each calibration set was obtained using different sets of coatings (n=3 determination for each concentration level)..... 98

Table 4-1 A breakdown of the lipid classes surveyed in the BIoSTD using the LC-MS system developed on orbitrap mass spectrometr 112

Table 4-2 List of upregulated lipids with use of SPME and Bligh & dyer methods - positive mode; the input mz is the extracted mz ions by R program and the exact mass is the mass of lipid feature reported in Lipid Map Database and Metlin Database 135

Table 4-3 List of upregulated lipids obtained with use of SPME and Bligh & dyer methods- negative mode 136

Table 4-4 List of down-regulated lipids obtained with use of SPME and Bligh & dyer - positive mode 138

List of Abbreviations and Symbols

AA	Arachidonic acid (20:4)
ALA	α -linolenic acid (18:3)
ATP	Adenosine triphosphate
B&D	Bligh & Dyer extraction technique
C	Equilibrium concentration of analyte on the coating
C₀	Initial analyte concentration
C₁₈	Octadecyl
CE	Ceramide
CE	Collision energy
CFREE	Free (unbound) concentration of analyte
CL	Cardiolipin
C_p	Protein concentration
CPB	Cardiopulmonary bypass
C_s	Analyte concentration in the bulk of the sample matrix
CTOTAL	Total (bound + unbound) concentration of analyte
CV	Correlation variance
DG	Diacylglycerol
DHA	Docosahexanoic acid (22:6)

DPA	Docosapentanoic acid (22:5)
DTA	Docosaterionic acid (22:3)
EPA	Eicosapentanoic acid (20:5)
ESI	Electrospray ionization
ETA	Eicosaterionic acid (20:3)
FA	Fatty acyls
FDA	Food and Drug Administration
FFA	Free fatty acids
F_{up}	Unoccupied fraction of protein (no ligand bonding)
GC	Gas chromatography
HAS	Human serum albumin
HCC	Hepatocellular carcinoma
HMDB	Human metabolome database
HPLC	High pressure liquid chromatography
HS	Headspace
IPA	Isopropyl alcohol
IS	Ionization suppression
K_{fs}	Distribution constant of the analyte between SPME coating and sample at equilibrium
LC	Liquid chromatography
LDL	Low-density lipoprotein
LLE	Liquid-liquid extraction

LOD	Limit of detection
Log P	Log of octanol/water partition coefficient
LOQ	Limit of quantitation
Lyso	Lysophospholipids
MALDI	Matrix-assisted laser desorption ionization
MDA	Multivariate data analysis
ME	Matrix effect
MG	Monoacylglycerol
MRM	Multiple reaction monitoring mode
MRM	Multiple reaction monitoring
MS	Mass spectrometer/spectrometry
MS/MS	Tandem mass spectrometry
MUFA	Mono unsaturated fatty acids
M/Z	Mass to charge ratio
n	Amount of analyte extracted by SPME fiber at equilibrium
NA	Not applicable
ND	Not detected
NEFA	Nonesterified fatty acids
OPLS-DA	Orthogonal partial least squares-discriminant analysis
PBS	Physiological buffer saline
PC	Phosphocholine

PCA	Principal component analysis
PDMS	Polydimethylsiloxane
PE	Phosphoethanolamine
PEEK	Polyether ether ketone
PG	Phosphoglycerol
PI	Phosphoinositol
PPB	Plasma protein binding
ppb	Parts per billion
ppm	Parts per million
PS	Phosphoserine
PUFA	Polyunsaturated fatty acids
QC	Quality control
R²	Linear regression coefficient
rpm	Revolutions per minute
RSD	Relative standard deviation
RT	Retention time
S/N	Signal-to-noise ratio
SEM	Scanning electron microscopy
SM	Sphingomyelin
SPE	Solid phase extraction
SPME	Solid-phase microextraction

STA	Stearidonic acid (18:4)
TG	Triacylglycerol
TIC	Total ion chromatogram
TOF	Time-of-flight mass spectrometer
UV	Ultraviolet
V_f	Volume of fibre coating
V_f	Volume of SPME coating
V_s	Volume of sample matrix
XIC	Extracted ion chromatogram

Chapter 1

Introduction

1.1 Lipid chemistry and general classification

A variety of definitions exist for the term “lipid”; some describe its molecular structure, while others designate shared physical properties. As an extensive definition, “lipids” are said to be a set of naturally occurring molecules that mainly contain fatty acids (FAs) in their structure, and come in a diversity of structures and functionalities. Based on their molecular structure similarities, they can be further categorized into a range of substituent classes and sub-classes. All lipids within a category contain the same functional head group, but differ in the number of carbon atoms (usually C¹⁴), and double bonds incorporated into their aliphatic chains. Based on their functional backbone and associated physicochemical properties, lipids are generally classified into eight categories, each with its own sub-classification hierarchy. This grouping scheme is driven by the discernible hydrophobic and hydrophilic elements that compose the chemical structure of lipids. The main lipid classes are comprised of fatty acyls, glycerolipids, glycerophospholipids, sphingolipids, sterol lipids, prenol lipids, saccharolipids, and polyketides.^{1,2} This global classification is fairly comprehensive and referred to as a guide. In the following sections, the abovementioned lipid classes and their subclasses, which have been studied in the current thesis, are introduced and described in detail. Comprehensive information about lipids, including their systematic cataloguing and related nomenclature is provided in online databases such as LIPID MAPS (<http://www.lipidmaps.org/>), Lipid Library (<http://lipidlibrary.aocs.org>), Lipid Bank (<http://www.lipidbank.jp>) and Cyberlipids (<http://www.cyberlipid.org>).³⁻⁵

1.1.1 Fatty Acid

Fatty acids are a diverse group of molecules composed of a carboxylic acid head group attached to a long linear or branched aliphatic chain, which can vary in regards to the number of carbon atoms it carries, as well as its level of saturation. The chain length usually ranges from 4 to 28 carbons. Fatty acids are synthesized by chain elongation of an acetyl-CoA primer with malonyl-CoA (or methylmalonyl-CoA) groups. The "free fatty acids", i.e. not attached to other molecules, are mainly produced from hydrolysis of other major groups of lipids, such as triglycerides or phospholipids. FFA in the blood plasma arises mainly from lipolysis (TG hydrolysis) while the intracellular FFA may have been taken up from the blood, or they may have been synthesized in the cell; this varies with cell type. They serve as a source of fuel by producing adenosine triphosphate (ATP) through beta oxidation, particularly for heart and skeletal muscle. Saturated fatty acids have no double bonds, while unsaturated fatty acids have one (monounsaturated) or more double bonds (polyunsaturated); and the most naturally occurring unsaturated fatty acids are in the *cis* configuration. Polyunsaturated fatty acids (PUFA) can be classified into two groups, n-6 or n-3, depending on the position (n) of the double bond that is nearest to the methyl end of the fatty acid. Polyunsaturated fatty acids can be defined as fatty acids with 18 carbons or more in length that contain two or more double bonds. Typically, a mammalian diet requires a large intake of PUFA; this is due to the fact that although primary linoleic acid (18:2, n-6) is required for normal development, most mammals, including humans lack the desaturase enzymes needed for their production.⁶⁻⁸ Due to the great importance of this group of lipids, the development of a new analytical technique for their quantification is the subject of focus in

Chapter 2 of the currently presented thesis. Table 1-1 illustrates the example structure of different fatty acids.

Table 1-1 Representative chemical structures of saturated and polyunsaturated fatty acids

Name	Feature	Abbreviation	Chemical structure
Stearic acid	(18:0)	Saturated	
Oleic acid	(18:1)	Monounsaturated	
α -Linolenic acid	(18:3)	Polyunsaturated Essential	
Eicosapentaenoic acid	(20:5)	Polyunsaturated Essential	
Docosahexaenoic Acid	(22:6)	Polyunsaturated Essential	

1.1.2 Glycerophospholipids

A large majority of membrane lipid content consists of glycerophospholipids. This varies with cell type and cell organelle. A molecular species of a glycerophospholipid is characterized by its phospholipid class, subclass, and its fatty acyl content. The molecular structure of this group of lipids is composed of a glycerol backbone linked to a phosphate moiety in the sn3 position, and hydrocarbon chains esterified to the sn1 and sn2 positions. Modification of the glycerol backbone, head group, or stereospecificity of the aliphatic chain substantially alters the biological activity of the molecule. Based on the nature of the polar head group at the sn3 position of the glycerol backbone, glycerophospholipids are subdivided

into individual sub-categories. Due to variations in head group as well as diversity in the length and number of double bonds, glycerophospholipids are comprised of a great number of molecular species.^{9,10} The most abundant sub-categories of phospholipids includes phosphatidylcholine (PC) and phosphatidylethanolamine (PE), which together with other lipids construct the biomembrane structures.¹¹ Chemical structures of various phospholipid classes and sub-classes are shown in Table 1-2.

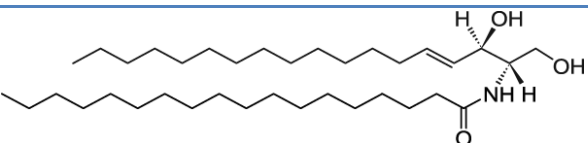
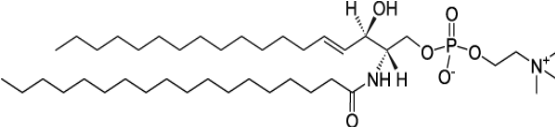
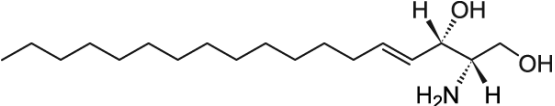
Table 1-2 Representative chemical structures of glycerophospholipids and lysophospholipids

Name	Abbreviation	Chemical structure
Lysophosphatidylcholine	LPC	
Phosphatidylcholine	PC	
Phosphatidylethanolamine	PE	
Phosphatidylglycerol	PG	
Phosphatidylinositol	PI	
Phosphatidylserine	PS	
Cardiolipin	CL	

1.1.3 Sphingolipids

Sphingolipids (SM) are a complex family of compounds that share a sphingosine base backbone and a long chain fatty acid; they are considered the second largest category of polar lipids. Major subdivisions of sphingolipids include sphingomyelins and ceramides, as well as other glycosphingolipids that contain multiple sugar rings. Similarly to PCs, sphingomyelins consist of a choline head group, and as a result, these two groups share many physical properties. Both PC and SM are located in the outer leaflet of plasma membranes, although they are also found in various other biological structures such as lipoproteins.^{12,13} Sphingolipids are particularly abundant in the central nervous system, representing approximately 5-10% of total lipid mass in most brain cells.^{14,15} In addition to playing structural roles in cellular membranes, sphingolipid metabolites act as bioactive signaling molecules involved in the regulation of cell growth, differentiation, senescence, and apoptosis. The main sphingolipids relevant to this study are shown in Table 1-3.

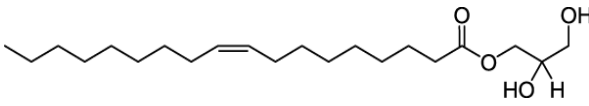
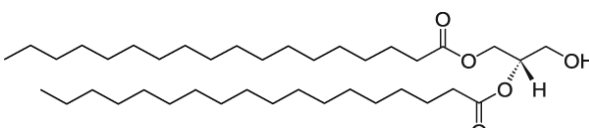
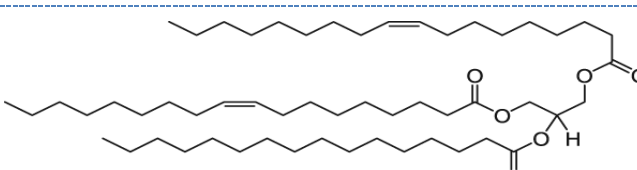
Table 1-3 Representative chemical structures of sphingolipid family sub-classes

Name	Abbreviation	Chemical structure
Ceramide	CE	
Sphingomyelin	SM	
Sphingosine	SP	

1.1.4 Glycerolipids

The glycerolipid category (Table 1-4) is dominated by a category of lipids having a glycerol scaffold in which one, two, or three substituted fatty acids are esterified, with fatty acids differing in chain length and number of double bonds. Accordingly, the most prominent glycerolipids include monoglycerides (MGs), diacylglycerols (DGs) and triacylglycerols (TGs), among which TGs account for the highest proportion of total lipids in plasma, being the most abundant dietary lipids. They are distributed between lipoproteins for transportation in the blood stream, and their concentration is dependent on food intake.¹⁶⁻¹⁸ Blood-plasma triglycerides provide a major source of energy, and are secreted from liver. Conversely, adipose tissue has a primary role in the synthesis and storage of triacylglycerol (TG) in periods of energy excess. During periods of energy demand, TG are rapidly hydrolyzed to release free fatty acids, which are then taken up by other organs to meet the energy requirements of the organism.^{19,20}

Table 1-4 Representative chemical structures of glycerolipid family sub-classes

Name	Abbreviation	Chemical structure
Monoglyceride	MG	
Diglyceride	DG	
Triglyceride	TG	

1.2 Lipid Distribution and interaction with proteins

As an insoluble compound, the transportation and delivery of lipids in the blood stream are enforced by complex lipoproteins composed of lipids and proteins that ultimately render the particles soluble in aqueous environments (FFAs bind to albumin and lipoproteins have at most a minor role in their transport). Plasma lipoproteins are spherical particles consisting of a lipophilic core surrounded by an amphipathic monolayer of phospholipids with their hydrophobic tails facing the central core, while their hydrophilic regions face the surrounding aqueous environment. The core of all lipoproteins contains triglycerides (TG) and cholesterol esters, also have small amounts of sphingolipids. The external layer is made of phospholipids and specialized protein components called apolipoproteins or apoproteins. These proteins help to maintain the structural integrity of particles, facilitate lipid solubilisation, and serve as ligands for lipoprotein receptors, while also regulating the activity of their metabolic enzymes. Lipoproteins not only differ in the ratio of protein to lipids; they also vary in terms of type of apoproteins involved. Hence, they are comprised of various attribute densities, sizes, and compositions, ranging from very low-density lipoproteins (VLDL; 2nd highest in triacylglycerols); low density lipoproteins (LDL; highest in cholesteryl esters); and high density lipoproteins (HDL; premier in density due to the high protein to lipid ratio). Chylomicrons are also lipoprotein particles that consist of triglycerides (85–92%), phospholipids (6–12%), cholesterol (1–3%), and proteins (1–2%). They transport dietary lipids from the intestines to other locations in the body. All these plasma lipoproteins encompass low energy of stabilization and constantly lose, acquire, and exchange their lipid and protein constituents during ordinary metabolism.^{13,17,21,22}

1.3 Necessity of lipid analysis and lipidomics

In view of their importance to biologic and pathophysiological processes, lipids share a wide variety of key cellular functions, including compartmentalization, energy storage, cell-signaling, protein trafficking, and membrane anchoring. Such functional diversity is evidently important in maintaining the cellular homeostasis of living organisms; accordingly, any alteration in their critical functionality can induce severe pathophysiological consequences associated to chronic diseases such as diabetes, cancer, arthritis, obesity, as well as neurodegenerative and infectious diseases.^{7,23–30} In order to reveal lipid-related dysfunctions, the biological role of each individual molecular lipid species needs to be identified. Therefore, precise quantification of lipid constituents and apprehension of the origins of their chemical distortion provide important insights to developmental biology, diagnostics, and potential treatments. To this end, lipid analysis will embrace a conclusive explanation of the biochemical mechanism through which lipids interact with each other and with fundamental proteins, and also assist with characterization of their dynamics, kinetics, and alterations. During systematic investigations of entire lipids, it is crucial that their functionality in the physiological and metabolic levels, their signaling pathways and regulation, as well as their correlation with other metabolites be well-understood. Lipidomics is a branch of study that seeks to map the entire spectrum of cellular lipids in any biological system (cell, tissue, organ, or organism). It is an “omics” subdivision that complements proteomics, genomics, and metabolomics so as to provide a more comprehensive perception of system biology in health and disease. Although recent scientific endeavors have been focused on the true power and promises of lipidomics, the true potential of this field is only beginning to be realized.

1.3.1 Trends in lipid analysis

In biological and clinical studies, the development of comprehensive analytical platforms that is capable of providing coverage for a wide variety of lipids continues to be a primary challenge for analytical chemistry. In addition, the diverse chemical structures and large dynamic range of concentrations of lipids complicate their analysis condition. Any successful lipid analysis method is intended to be a flawless workflow of sample preparation and extraction, separation, detection, and straightforward data processing. However, no single methodology or technique is yet in widespread use to screen all lipids. Traditional approaches for determination and quantification of all lipid classes are either not sensitive enough and lack accuracy, or do not provide enough throughput; as such, these methods are inadequate for practical analysis of clinical samples. For the most part, these methods were developed for analyses of specific categories of compounds such as membrane phospholipids or the mitochondrial lipids, and consequently, are unable to cover the whole lipid array.³¹⁻⁴⁰ Although these conventional methods may offer the advantage of simplicity, for instance, by commercializing assay kits for enzymatic methodologies⁴¹⁻⁴⁴ or provide relatively inexpensive approaches, such as thin-layer chromatography (TLC),^{45,46} neither do they provide a full profile of all lipid classes, nor do they evade the necessity of multiple preparative steps, which makes them susceptible to interferences. In this regard, the lipid biology research field is undergoing a cutting-edge technological transformation that involves lipid separation and determination approaches, as well as their further identification and characterization steps. This includes the use of more advanced chromatography techniques, as well as state-of-the-art mass spectrometry (MS), most notably centered on

electrospray ionization (ESI), high-resolution mass analyzer using multiple reaction monitoring (MRM), or selected ion monitoring (SIM).^{47,48}

1.4 Lipid analysis and lipidomics: miscellaneous platforms

In a biological practice, the full lipid content is elucidated by performing high throughput molecular lipidomics on cells or biofluids. Generally, such investigations are conducted with aims to classify and quantify the utmost number of molecular lipids and their feasible systemic interactions, and also to demystify any possible genetic or external perturbations. In this workflow, nuclear magnetic resonance spectroscopy (NMR) and mass spectrometry techniques are most commonly used as analytical tools for detection and determination of lipids. The evolution of lipid analysis and lipidomics has accelerated advancements in new analytic platforms particularly in the area of mass spectrometry. Utilization of this technique allows for streamlining of required procedures, analyses of larger groups of lipid molecules, and collection of more detailed structural information. In this section, the major MS-based platforms used in clinical lipidomics are introduced, and their recent technological developments are reviewed.

1.4.1 Direct infusion and shotgun lipidomics

For lipidomics studies, the MS platform is either supported by separation (chromatographic or electrophoretic) techniques, or alternatively performed solely through direct introduction of lipid extracts to the MS instrument. The latter approach is recognized as direct infusion or shotgun lipidomics, which allows for sample introduction and processing in a high-throughput manner.^{39,49,50} The feasibility of shotgun lipidomics approaches is based on the use of electrospray ionization as an inherent soft-ionization technique. This approach is

mainly practical for lipids with polar head groups (e.g., glycerophospholipids) as readily ionized species with respect to their molecular structure,⁵¹⁻⁵³ although it has also been applied for the characterization of sphingomyelins and ceramides,^{36,54} as well as glycerolipids.⁵⁵ Shotgun lipidomics is typically achievable in MS-only or MS/MS platforms by utilizing high mass accuracy/resolution hybrid instrumentation such as the quadrupole time of flight (Q-TOF), or the linear ion-trap (LTQ) Orbitrap mass spectrometer with an enhanced duty cycle.^{39,49,56-58} The most important advantage of shotgun lipidomics is its ability to provide direct identification and quantification of several hundreds of lipids at the molecular level from total lipid extracts in a relatively short analysis time. On the other hand, a major concern with this approach is the risk of ion suppression encounters, particularly when the sample preparation method generates a crude lipid extract that becomes diluted and infuses directly into the mass spectrometer. However, if accurate measurement of target lipid is prevented by ion suppression, there are a few strategies that may be implemented, one of which is a method proposed and discussed later in this thesis.⁵⁹

1.4.2 GC and GC-MS

Gas chromatography (GC) is often used as a separation technique for volatile and thermally stable analytes where the retention is influenced by the molecular boiling point. Because most lipids are not volatile and some of them are easily degraded in high temperature, GC is not a widely employed technique in lipidomics because analytes must be thermally stable with high vapor pressure to volatilize during injection. Although derivatization can overcome the problems of the analyte in terms of volatility and lability, derivatization may be difficult for the complex biomolecules. Analysis of different categories of lipids by GC involves complex pre-separation steps, due to the complexity of derivatization reagents required for

each lipid class/subclass. These altogether leads to the less frequent application of GC techniques in lipidomics studies.⁶⁰ In fact, gas chromatographic (GC) separation with flame-ionization detection (FID) is suitable for the analysis of fatty acids.⁶¹ Separation of cis/trans isomers of various fatty acid species can be achieved by using conventional GC-FID. The fatty-acid composition of fats and oils is easy to analyze by GC-FID after derivatization to methyl ester fatty acid (FAME) derivatives.⁶²

In lipidomics studies, GC-MS techniques using the electron ionization (EI) or chemical ionization (CI) are most commonly employed for low molecular weight lipids such as fatty acids. A large number of GC-MS studies are focused on free fatty-acid profiling or fatty acyl characterization of phospholipids and TGs. However, while the abovementioned methods provide detailed information about the R-group, they fail to provide lipid-class information because of the need for saponification in the sample preparation step.^{33,62-65} Recent advancements in time-of-flight (TOF) mass analyzer technology, which allows higher scanning speeds (but lower mass resolution), have encouraged wider adoption of EI in comprehensive two-dimensional GC (GC × GC).⁶⁶⁻⁶⁸ These advancements have brought several advantages to the methodology, such as increased separation, higher peak capacity, better reproducibility, and the use of available libraries for matching and compound identification, particularly for EI-based GC/MS analysis. However, several major drawbacks of GC/MS for lipid analysis are related to the critical need of chemical derivatization of lipids in order to reduce their polarity and increase their volatility, which in turn facilitates their separation and ionization in the EI/CI GCMS-based method. While boasting certain advantages, these techniques are restrictive due to the unpleasant derivative steps and their low sensitivity, which have restrained their further application in lipid analysis. Chemical

derivatization may cause molecular decomposition, resulting in complex chromatograms that are hard to interpret.⁶⁹ As a consequence of these challenges, and due to the expansion of soft ionization techniques such as electrospray ionization (ESI), a large majority of lipidomics studies are performed based on LC/ESI-MS, with GC-based techniques being less frequently applied in this area.

1.4.3 LC and LC-MS

The structural diversity of lipids demands for efficient separation approaches that can cover all classes and sub-classes of lipids. As a technique that requires no derivatization, preserves important lipid-class information, and interfaces easily to the soft-ionization techniques of atmospheric pressure mass spectrometers, the liquid chromatography (LC) is the most broadly applicable among all currently available methods. By coupling liquid chromatography to MS, the limitations of direct infusion such as suppression by competing ions, limited sensitivity of detection for low abundant lipid species, and difficulties of detecting isobaric and isomeric lipids could be substantially eliminated. Several LC configurations have been reported for the analysis of complex lipid mixtures, from which reverse phase (RPLC), normal phase (NPLC) and hydrophilic interaction liquid chromatography (HILIC) are the ones which have shown the most potential. Separation of lipids in RPLC (C18 or C8 columns) is based on lipophilicity, where lipid species are retained based on their carbon-chain length and the number of double bonds; as such, this approach provides separation of lipids of a class with excellent retention time reproducibility. On the other hands, NPLC and HILIC typically differentiate lipid species according to their functional group, so that lipids are separated with respect to the polarity of their head group. Depending on the application, RPLC, NPLC, and HILIC offer different advantages for

separation of various lipid categories, where the choice of LC method affects the resolved group of lipids. For comprehensive lipid analysis, normal phase LC can only be used for quick assessments of class-based lipid fractionation, while the use of reversed-phase LC allows for individual lipid fractions to be resolved within a specific class; thus, another layer of molecular information detail can be achieved.⁷⁰⁻⁷⁴ Additionally, off-line and on-line two-dimensional LC-MS approaches have been used for separation of a wide range of complex lipids.⁶⁶ Furthermore, electrospray ionization (ESI), is the most popular interface for coupling LC stream to the mass analyzers and detectors in lipidomics analysis; it can be easily integrated with online databases due to its powerful ability for efficient ionization of compound with different polarities.⁷⁵ The HPLC-ESI-MS is a very appropriate method for targeted and untargeted lipid profiling in biological samples such as blood, plasma, and tissue.^{70,74,76-81} However, one of the restrictions of LC-ESI-MS is that it provides limited information about the fatty acyl constituents of individual lipids; for instance it cannot distinguish the differentiating double-bound positional isomers, cis-/trans-isomers, or regioisomers. For such specific studies, other LC techniques have been used, including silver-ion RPLC, chiral LC, and supercritical fluid chromatography (SFC). In such cases a long chromatographic run of about 1.5–2.5 h is required to determine exact stereo-chemical configurations of lipids, which is a major drawback of these separation approaches.^{60,72,82,83} Conversely, for structure analysis of lipids, more powerful mass analyzers with higher resolving power such as ion mobility,^{84,85} or other soft ionization techniques, such as matrix-assisted laser desorption/ionization (MALDI) combined to Q-TOF, have been reported previously.⁸⁶⁻⁸⁸ MALDI-TOF is a popular technique for lipid analysis, since it can be used to

determine head groups and structural compositions of individual fatty acyl chains when coupled to post-source decay fragmentation.⁴⁷

1.5 Sample preparation and extraction for lipidomics

As a multidisciplinary field, lipidomics necessitates the collaboration of a team of scientists, which may include biologists, analytical chemists, physicians, bioinformaticians, statisticians, etc. The workflow of lipidomics starts with the active contribution of analytical chemists for purification and extraction of lipids from biological samples such as blood, cells, tissues, and subcellular organelles. In addition, choices regarding method development, sample introduction and data acquisition need to be carefully made for optimum results. Different analytical separation techniques and extraction strategies can be designed and developed in accordance with specific lipid components and analyte targets. If the purpose is global lipidomics, the choice of extraction protocol is of great importance, and considerable effort must be put into selecting an approach capable of improving overall lipid coverage. In lipidomics, the lipid extraction procedure must be able to quantitatively extract lipids while avoiding any degradation and possible interferences of non-lipid constituents such as sugars, peptides, and amino acids, which may distress the ionization efficiency. In this section, a detailed critical summary of the most commonly used methods for clinical sample preparation is provided; arguing the pros and cons in detail. This includes various liquid-liquid extraction (LLE) and solid-phase extraction (SPE) protocols that have been previously reported in the literature.

1.5.1 Liquid-Liquid Extraction

Liquid-liquid extraction has been regarded as the technique of choice for lipid extraction; and since its initial debut, many modifications have been applied to this method for different analytical purposes. Due to its relative simplicity, the single organic solvent approach, often using methanol or acetonitrile, has been conventionally applied towards the extraction of polar lipids. This method has in the past been applied to extract glycerophospholipids, lysophospholipids, and other phospholipids from human plasma by adding an excess volume of neat methanol to human plasma or blood, followed by agitation.^{89,90} As the most conventional approach, Folch method,⁹¹ introduced the use of two organic solvents, methanol and chloroform. The ratio of solvents was subsequently modified by Bligh and Dyer⁹² to improve lipid recovery. These methods are based on phase partitioning of lipids into organic and aqueous layers due to their polarity, and have been successfully applied to achieve exhaustive extraction of key lipid classes, ranging from (lyso) phospholipids and glycerolipids, DGs and TGs, to a wide range of bioactive fatty acids.^{47,76,93–100} More recently, alterations in extraction procedures were proposed that use a variety of chloroform/methanol/water ratios, as well as additives such as hydrochloric acid and acetic acid. However, the use of such additives in LLE methods is a matter of concern, since acidic or alkaline conditions induce hydrolysis of endogenous lipids, resulting in artificial generation, and consequently, biased quantification of lipids.¹⁰¹ Other LLE approaches have also been reported with aims to use less toxic organic solvents, such as dichloromethane, butanol, methyl tert-butyl ether, hexane/isopropanol, or ethyl acetate/ethanol mixtures.^{102–104} The Matyash method,¹⁰⁵ uses methyl tert-butyl ether (MTBE), which due to its lower density forms the upper layer during phase separation as the lipid containing organic phase. This

simplifies the final lipid extract collection, and minimizes dripping losses. Other organic solvents such as butanol require an extremely long evaporation process that leads to a very time-consuming extraction procedure. All of these methodologies have aimed to improve the efficiency of extraction with respect to the target matrix; these include biofluids such as serum, plasma, blood, and urine, as well as solid matrices such as microorganisms, tissue, cell lines, etc.^{49,80,106–110} In spite of its advantageous simplicity, the LLE methodology is riddled with disadvantages such as long extraction times, multi-step procedures, relatively high solvent consumption, long reconstitution periods, and poor reproducibility. As described above, lipid molecules containing unsaturated double bonds can be subjected to oxidation in the presence of oxygen.¹¹¹ In this sense, the low sample throughput, time requirements, and high solvent-consumption associated to these classical approaches have been surpassed by other relatively new extraction techniques.

1.5.2 Solid-phase extraction (SPE)

As a common sample preparation technique, SPE utilizes a polymeric stationary phase as a sorbent that captures specific classes of compounds with similar properties. The sorbent is typically embedded in a cartridge format to remove analytes through a differential analyte-sorbent interaction. The analyte is subsequently removed from the sorbent using an organic or a mixture of organic/aqueous eluting solvents. For lipidomics and lipid analysis purposes, SPE is normally employed in conjunction with either LLE or protein precipitation to provide additional sample clean-up and enrich particular classes of target lipids from biological samples.¹¹² Pre-packed SPE cartridges are readily accessible from commercial vendors, with numerous variations in sorbent chemistry. The SPE columns that are most commonly used for extraction of lipids include normal phase silica columns, reversed phase columns (C8 and

C18), and ion-exchange columns (packed with aminopropyl).¹¹³ Aminopropyl columns and silica-based columns are popular for separation and partial extraction of neutral or polar lipid (sub) classes, and can be optimized with proper selection of the eluting solvents.^{37,114} Furthermore, several efforts have been made to apply C8 and C18 pre-packed cartridges for isolation and purification of PC, PE, lysoPC, ceramides, triglycerides, and fatty acids on several clinical samples, including blood plasma,⁸⁹ serum,¹¹⁵ sputum,¹¹⁶ human eye,¹¹⁷ and skin.¹¹⁸ An extra pretreatment step, including either ultracentrifugation, chemical derivatization/pretreatment, or thin-layer chromatography, was required in all cases, while instrumental analysis was mainly carried out with the use of GC or direct infusion MS. In comparison to LLE approaches, SPE presents better sample clean-up and is more convenient. Also major goal of SPE for lipidomics applications involves the reduction of matrix effects, which are the most problematic issue in LLE approaches. Extension of column lifetime and improvements in overall method robustness remain as main challenges of SPE methodologies. Besides the demand of costly cartridges, the main disadvantage of this method lies in the selection of sorbent material to enhance the chemical selectivity of the preparation procedure, which can adversely reduce the lipid class coverage. Moreover, concerns about biosafety issues using eluting solvents have driven the demand for biocompatible and less or non-toxic solvents.

1.5.3 Other emerging extraction techniques

In addition to the described lipid extraction techniques, alternative methods with a focus on specific groups of lipids have been reported. These techniques include microwave-assisted extraction (MAE), supercritical fluid extraction (SFE), and ultrasound-assisted extraction (UAE), which are more commonly used for the extraction of lipids and metabolites from

other biological samples such as plants and foods. SFE is more established for the extraction of lipids from plants and food, and only recently has its application been expanded onto animal tissues,^{119,120} and dried human-plasma spot samples;¹²¹ mainly, it has been applied for the extraction of phospholipids such as PC, LysoPC, PE, and LysoPE. In general, the use of microwave energy during sample extraction, which is applied to increase temperature and pressure, helps in the enhancement of overall extraction efficiencies, with a reduction in the required amount of organic solvents and time of extraction. However, MAE is not commonly used for lipid extraction, as the generated heat could potentially cause the degradation of thermally labile lipids. This method has been mainly used for the extraction of fatty acids.^{95,122–124} Ultrasound-assisted extraction (UAE) utilizes the energy of ultrasonic pulses (frequencies ≥ 20 kHz) to facilitate mass transfer between immiscible phases.¹²⁵ However, this method is normally used in combination with conventional LLE methods to improve the extraction efficiency of lipid species from biological samples.¹²⁶ The application of this method has been recently reported for exhaustive lipid fingerprinting of human plasma with the use of methyl tert-butyl ether (MTBE) and ultrasound (US) energy.¹²⁷ Despite the advantages of the proposed MTBE-US protocol for lipid extraction, it involves long extraction times and a tedious multi-step procedure. In other cases, the application of the ultrasound technique in lipid analysis of biological matrices has been merely restricted to the extraction of fatty acids.^{128,129} For all the above mentioned techniques, in order to achieve an efficient lipid recovery, the operating conditions have to be carefully optimized based on the targeted lipid class of interest; hence, these methods are not adequate for comprehensive coverage of all lipid categories from biological samples.¹³⁰

1.6 Solid-phase microextraction

Solid-phase microextraction (SPME) was first introduced by Pawliszyn and coworkers as a non-exhaustive, equilibrium-based sample preparation technique that provides rapid sample clean-up and pre-concentration in a single step. This method was initially designed for the extraction of volatile and semi-volatile organic compounds for subsequent separation by gas chromatography.¹³¹⁻¹³³ However, over the past twenty years, the technique has evolved significantly due to enormous advancements in its geometry, configurations, sorbent specificity and coating biocompatibility. Consequently, SPME has become a powerful tool in the pharmaceutical, environmental, food, forensic, and clinical fields for the extraction of various classes of compounds.¹³⁴⁻¹⁴³ In terms of format, SPME has endured several transformations to fulfill the compatibility with LC-MS analysis, and thus improved SPME bio-applications.^{138,144,145} In this regard, features such as biocompatible thin-film coating and the use of 12-blade configuration have been introduced to enable automated high throughput extraction in a 96-well plate format.^{136,146} Figure 1-1 schematically illustrates the typical SPME workflow from a given biological sample to LC-MS. Here, the coating is exposed directly to the sample where the target analytes are extracted; subsequently, the coating is removed from the analytical sample and exposed to a desorption solvent for desorption of analytes from the coating and into a solvent solution. An adequate proportion of the obtained solution is eventually introduced to the analytical instrumentation (LC-MS here), and data are acquired and further processed.

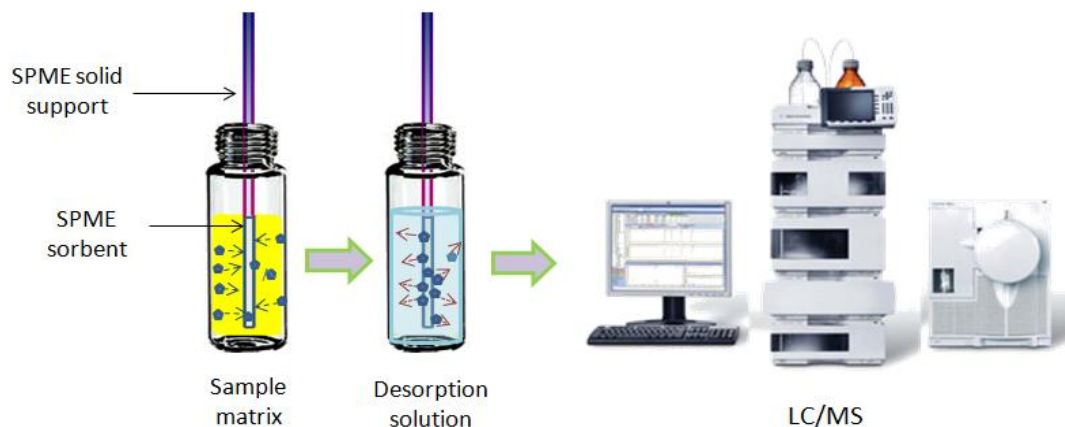


Figure 1-1 Schematic representation of a typical SPME workflow from a given biological sample to LC-MS. Small arrows indicate the direction of mass transfer.

Depending on the type of sorbent, the analyte extraction occurs through either through absorption or adsorption of the analyte to the extraction phase.¹⁴⁷ Therefore, careful selection of appropriate coatings and desorption solvents is required during method development, as different coatings functionalities establish different extraction mechanisms. The extraction of analytes can occur either through the direct immersion of the coating into the sample matrix for capturing semi volatile to non volatile compounds, or by exposing the sorbent to the headspace above the sample for extraction of volatile compounds. Subsequently, desorption of the analytes could be carried out either thermally by direct insertion of fibers into the GC injector, or with the use of an appropriate desorption solvent. The research presented in this thesis deals with the analysis of lipids as non-volatile, semi-polar, and non-polar species from biological fluids; consequently, direct immersion mode and solvent desorption were required throughout this work.

Typically, the SPME device consists of a sorptive extraction coating immobilized on a solid support; the coating is directly exposed to the analytical sample for a sufficient period of time until equilibrium is reached between the sample and SPME coating. In principle, extraction is

performed based on the partitioning diffusion of the analyte from the sample matrix towards a boundary layer and to the sorbent coating. According to the principal theory of SPME, the amount of analyte extracted by SPME in equilibrium conditions is proportional to the volume of the extraction phase and the partition coefficient of analyte between coating and matrix, as calculated by Equation 1-1

Equation 1-1

$$n_e = \frac{Kf_s V_f V_s C_0}{Kf_s V_f + V_s}$$

where n_e is the amount of analyte extracted at equilibrium; V_f and V_s are the volume of sample and coating, respectively; and C_0 is the initial analyte concentration in the sample. Kf_s is the partition coefficient between the extraction phase and sample matrix, and is dependent on the nature of the selected coating and the analyte properties. Kf_s will also vary with temperature, pH, and ionic strength of the sample matrix; therefore, these parameters must be constant during extraction. Another interesting features of SPME is that when the volume of the sample is much larger than the partition coefficient ($V_s \geq Kf_s V_f$), extraction is performed under the conditions of negligible depletion; as such, Depending on the type of sorbent, the mechanism of analyte extraction is enforced either through absorption or adsorption of the analyte to the extraction phase. Therefore, careful selection of appropriate coatings and desorption solvents is required during method development, as different coatings functionalities establish different extraction mechanisms. It is noteworthy to mention that no further extraction supposedly occurs at equilibrium, and thus, probability for local depletion of the analyte under study from the matrix is low. This important feature makes the SPME technique suitable for in vivo applications, since it does not interrupt the internal equilibrium of the living system.

In this regard, it can be concluded that at the optimum extraction time, the analyte is in equilibrium with the coating and other binding components of the sample matrix (such as proteins, for example), and consequently, the amount of extracted analyte is linearly proportional to the unbound concentration and the initial sample concentration. This distinction is considered an important advantage of SPME over traditional methods, as it determines the application of SPME for measurement of free (unbound) or total (bound + unbound) concentrations of analyte through the performance of appropriate calibration.¹⁴⁸⁻¹⁵¹ This is the most important differentiated advantage of SPME from other traditional methods such as SPE, as the SPME procedure is non-exhaustive in nature, and only a small portion of analyte in their unbound format being removed from the sample. In contrast, SPE utilizes large volumes of sorbents to ensure exhaustive removal of analytes from samples.¹⁵² The extraction of analytes can occur either through the direct immersion of the coating into the sample matrix for capturing semi volatile to non volatile compounds, or by exposing the sorbent to the headspace above the sample for extraction of volatile compounds. Subsequently, desorption of the analytes could be carried out either thermally by direct insertion of fibers into the GC injector, or with the use of an appropriate desorption solvent. The represented research in this thesis deals with lipids as non-volatile and non-polar endogenous species in biological fluids; thereby, direct immersion SPME mode was required throughout this work.

Typically, the SPME device consists of a sorptive extraction coating immobilized on a solid support; the coating is directly exposed to the analytical sample for a well-defined period of time until equilibrium is reached between the sample and SPME coating. Principally, extraction is performed based on the partitioning diffusion of the analyte from the sample

matrix towards a boundary layer and to the sorbent coating. According to the principal theory of SPME, the amount of analyte extracted by SPME in equilibrium conditions is proportional to the volume of the extraction phase and the partition coefficient of analyte between coating and matrix, as calculated Equation 1-1 can be simplified, and the amount of analyte extracted at equilibrium can be calculated by Equation 1-2

Equation 1-2

$$n_e = K f_s V_f C_0$$

Due to the growing interest for integration of multi-step sampling and sample preparation, this equation is of great importance, as it determines the insignificant role of sample volume in quantitative analysis. In such cases, sampling can be performed directly on-site or in vivo within a tissue or in circulating blood of a living organism.^{139,153,154,154,155} From the perspective of sample preparation technology, the feasibility of in vivo sampling is considered a very significant competence that makes SPME an outstanding choice for metabolomic studies.

1.6.1 **Thin-film microextraction**

Rod fiber geometry as the original SPME configuration has to date been the most commonly used SPME format in various applications. However, changes in the configuration of the device by enlargement of the surface area of the coating have been shown to improve extraction recovery and result in higher amounts of analyte extraction. Accordingly, the traditional geometry has been recently transfigured to thin-film geometry by immobilization of the coating onto a blade-shaped stainless steel base.¹⁵⁶ Although the fundamental theory of extraction and the requirements for method optimization remain the same regardless of coating configuration, the use of thin-film geometry offers other important advantages over

conventional fibers. First of all, it improves extraction efficiency by increasing the amount of analyte extraction, consequently enhancing the overall sensitivity of method. Secondly, the thinner coating design improves the overall convection and facilitates the mass transfer of analytes, which results in a faster equilibrium rate and ultimately, a higher sample throughput.¹⁴⁶

The demonstration of thin-film SPME and its related theoretical concept for the LC-MS application was reported by the Pawliszyn group, where a layer of octadecyl silica/polyacrylonitrile (C18-PAN) coating was sprayed and immobilized on a 2 cm tip of a flattened metal blade.¹³⁶ The new geometry was represented in the state-of-the-art 96-blade SPME format, and ever since, various bio-applications of this configuration have been reported through direct immersion of the coating into complex sample matrices, without any need for sample pre-treatment. These applications involve high throughput sample preparation and extraction of drugs and metabolites from various biological samples such as whole blood, plasma, urine, cells, and tissue.^{141,156-160}

1.6.2 SPME for metabolomic studies

Metabolomics and lipidomics are powerful approaches in the study of systems biology, aiming to elucidate the metabolic origins and pathways of small molecules such as sugars, amino acids, and lipids present in living systems. As a result, the development of reliable analytical methodologies has been gaining growing interest in these areas of research; in this context, the selection of appropriate sample preparation methods is an important consideration in the metabolomic workflow. In this regard, several SPME approaches have been introduced, using a variety of coatings and configurations. Various headspace (HS) SPME platforms in combination with GC-MS and GC \times GC systems have been used for

extraction and enrichment of volatile metabolites in plant and food metabolomics.^{161–168} In addition, headspace SPME was also successfully applied for the determination of metabolic changes and potential biomarkers from the volatile emissions of breath, skin, cancer tissue, and cell line. However, due to the non-volatile and highly lipophilic nature of lipids, headspace SPME cannot be considered as an option when it comes to comprehensive lipidomic studies.^{169–173}

Biological fluids such as serum, plasma, blood, urine, and saliva consist of several endogenous and exogenous metabolites with a wide range of polarities that exist in abundant to trace concentrations. The selection of potential SPME coatings is therefore critical to guarantee metabolite coverage and metabolomics data quality. To this purpose, different coating chemistries were evaluated by Vuckovic in terms of metabolite coverage¹⁷⁴ by inspecting a variety of SPE particles coated in the SPME platform for a broad range of metabolites polarities. The obtained results indicated that mix-mode (C8 or C18-benzenesulfonic acid), polystyrene divinylbenzene (PS-DVB) and phenyl boronic acid (PBA) coatings provide the best coverage of hydrophilic and hydrophobic metabolites. Subsequently, biocompatible SPME probes were represented by Mirnaghi et al., who included detailed information regarding coating preparation and their evaluation process for in vivo studies of biological fluids;¹³⁶ today, some of these biocompatible SPME fibers are commercially available. Subsequent researches were also reported by the same authors, aiming to establish the optimum extraction phase for a Thin-Film 96-well plate format for high-throughput metabolomics.¹⁴⁰ Additionally, another untargeted metabolomics study was reported for analysis of blood using the needle-based in vivo SPME device. In this research, metabolites with fast turn-over that had not to date been found by traditional methods such as

ultrafiltration and protein precipitation were successfully captured directly from circulating blood.^{174,175} Moreover, a study was recently reported detailing the applicability of mixed-mode SPME coatings for brain tissue bioanalysis, where multiple endogenous neurotransmitters such as glutamic acid, serotonin, and dopamine in the striatum of the rat brain were monitored and quantified.¹⁴²

1.7 Research objectives

Over the last several years, our laboratory has developed different analytical methods for extraction of small molecules such as drugs and metabolites by making various fundamental modifications to different SPME techniques. However, attention has never been focused on the development of a unique SPME approach for comprehensive analysis of the large family of lipids, aiming to cover the entire spectrum of various lipid categories and sub-categories. The main research objective of this thesis is to demonstrate for the first time the adaptability of direct extraction SPME for lipidomics studies using LC-MS platforms.

With this perspective, Chapter 2 focuses on the analysis of fatty acids, which are the major building block of other complex lipids. Biocompatible SPME fibers were utilized for development of a simple, robust and effective extraction protocol for determination of polyunsaturated fatty acids from pooled plasma. Analytical performance and characterization of the final optimized method were assessed for quantification of fatty acids in human and fish plasma individually. In addition, the method was successfully applied for monitoring PUFA changes during an operation procedure with the utilization of a set of plasma samples obtained from patients undergoing cardiac surgery with the use of cardiopulmonary bypass (CPB). Conventional sample preparation techniques for lipid analysis consist of a tedious multi-step sample handling which suffer from lack of efficiency in covering broad range of

endogenous lipids. In addition, failure in sample clean-up as a key issue in traditional methods leads to undesired ionization suppression/enhancement, and the proliferation of significant errors in quantitative data. In Chapter 3, the analytical approach is expanded to the whole lipid spectrum in order to address the requirement for comprehensive analysis of all lipid species from different classes and polarities, while enhancing the sensitivity and throughput by direct immersion of the thin-film 96-blade SPME system. This chapter details the successful application of the lipid quantification technique for measurement of target lipids from human blood plasma. Chapter 4 describes research undertaken on the effect of omega-3 polyunsaturated fatty acid as a treatment agent on the hepatocellular carcinoma HUH7 cell line. lipid profiling was performed on two groups of cells (control and treated cells) with the use of the optimized SPME technique; further, results were compared to concurrent findings obtained by use of the conventional Bligh & Dyer extraction technique as a preliminary proof-of-concept study. Up-regulation and down-regulation of lipids in treated cells were monitored, and important lipid species extracted by each technique are listed and compared. This comparison was useful to place SPME within the context of commonly employed LLE methods, and to investigate whether the offered SPME protocol was competitive in terms of analytical parameters such as sensitivity, precision, and lipid coverage. Finally, Chapter 5 summarizes the main research findings of the current work and proposes future directions and challenges for this type of studies.

Chapter 2

Application of Solid Phase Microextraction for Quantitation of Polyunsaturated Fatty Acids in Biological Fluids

2.1 Preamble and introduction

2.1.1 Preamble

This chapter has been published as a paper: Afsoon Pajand Birjandi, Fatemeh S. Mirnaghi, Barbara Bojko, Marcin Wąsowicz, and Janusz. Pawliszyn, “Application of solid phase microextraction for quantitation of polyunsaturated Fatty acids in biological fluids” *Anal. Chem.*, vol. 86, no. 24, pp. 12022–9, Dec. 2014. The materials of the current chapter are reprinted from this publication with the permission of the American Chemical Society (Copyright American Chemical Society 2012). The contribution of co-author Fatemeh Mirnaghi, Barbara Bojko and Marcin Wasowicz to the work described within this chapter was technical and scientific advice. Provision of biological material, patient’s recruitment and obtaining REB approval for collection of plasma samples from patients undergoing heart surgery was performed at Toronto General Hospital. All of the experimental results and data reported within this chapter have been performed solely by the author.

2.1.2 Introduction

Fatty acids (FA) are essential components of living cells and important substrates that play a critical role in mammalian energy metabolism. They can either be saturated, monounsaturated or polyunsaturated depending on the number of double bonds. They differ

in length as well, majorly having a 4–28 carbons in their chain. Long-chain fatty acids (LCFA) are fatty acids with aliphatic tails of 16 or more carbons. Among the different fats, some fatty acids can be used as functional ingredients such as α -linolenic acid (ALA), arachidonic acid (AA), eicosapentaenoic acid (EPA), docosahexaenoic acid (DHA), stearidonic acid (STA) among others. Fatty acids are combined as the building blocks of more complex lipids through ester or amide bonds and form glycerolipids or phospholipids. Esterified fatty acids serve as primary components of lipid bilayer membrane, lipoproteins and liposomes; act as suppliers of chemically stored energy; or are involved in signal transducers pathways, thereby a small proportion of total fatty acids in the biological systems are present as nonesterified fatty acids (NEFA) also called free fatty acids (FFAs).¹⁷⁶ They are continuously produced, integrated into lipids, and degraded in the β -oxidation pathway and citric acid cycle.¹⁷⁷ Alterations in the metabolism of this portion is of specific interest since it is established to be associated with pathological conditions and observed with numerous disorders, such as obesity,¹⁷⁸ insulin resistance,¹⁷⁹ diabetes mellitus,¹⁸⁰ or metabolic syndrome.¹⁸¹

Accurate determination of the composition of free fatty acids (FFA) in different biological matrices is a predominant problem in total fat extraction. The most common procedures used to measure FFA concentration consist of multiple-step methods, including (a) an extraction procedure to isolate lipids from the sample bulk, (b) separation of FFA from the rest of the lipids using conventional methods such as thin-layer chromatography (TLC) and/or solid phase extraction (SPE),^{182,23} (c) derivatization of FFA to fatty acid methyl esters (FAMES),^{183,62} and (d) a final chromatographic method for differentiation of individual fatty acid species.³³ The chromatographic determination of FAMES is by far mostly done using

capillary gas chromatography (GC,) ¹⁸⁴⁻¹⁸⁶ and less frequently by high performance liquid chromatography (HPLC). ^{183,187,188}

Lipid analysis deals with enormous sample complexity. In order to obtain satisfactory results, the extraction of lipids from complex biological matrices, which aims at removal and isolation from interfering agents such as proteins, saccharides, or other small molecules, is usually indispensable before the analysis. Therefore, a broad range of extraction techniques are currently used for this purpose. ¹⁸⁹ However, the most common extraction approaches have been mainly based on solvent extraction so far. The most popular extraction methods for lipids include the traditional Folch method, ⁹¹ or a modified Folch method ¹⁸⁵ that employs a solution of chloroform/methanol (2:1, v/v), or the commonly called Bligh and Dyer method, in which a chloroform/ methanol/water mixture is used to extract the lipids. ¹⁹⁰ Moreover, exhaustive Soxhlet extraction is probably the most commonly used technique for the extraction of fats and oils from food matrices. ¹⁹¹ More modern methodologies take advantage of solid-phase extraction (SPE) for fatty acid extraction, ¹⁹² typically by using amino-bonded phase and C18 bonded-phase columns. ¹²⁹ In comparison to liquid-liquid extraction (LLE) methods, these procedures minimize the volumes of organic solvents which lead to good recovery and higher reproducibility. However, most of the proposed SPE protocols offer the application of derivatization or solvent extraction followed by evaporation and reconstitution procedure. ¹⁹³ In addition, the limitations may include clogging of cartridges when handling complex matrixes such as plasma or tissue. Considering the exhaustive nature of SPE, the recovery is significantly increased when the volume of the sample is larger but when dealing with a large volume of samples, limitations of breakthrough volume and low peak capacity of SPE cartridges may affect the quantitative results. ^{149,194,195}

In contrast, among all extraction techniques, solid phase microextraction (SPME) is sampling and sample preparation technique characterized by simplicity, reproducibility and non-exhaustive nature of the extraction process when very small sorbent volume is used. The benefits of SPME for highly complex matrices such as biological samples have been already discussed elsewhere.^{143,154,196-199} Headspace SPME (HS-SPME) has been previously reported for determination of short chain volatile fatty acids, including the C₂-C₇ carbon chain or their ethyl esters from waste water.^{200,201} However, extraction of long chain fatty acids in biological and nutrition analysis is a very challenging goal due to their hydrophobicity, perceived abundance as plasticizers, ubiquity in the environment, great tendency to bioconcentrate, vast distribution in conjugated forms in cellular structure, very high affinity to biological proteins such as albumin, and a high risk of matrix effect encounters. The main goal of this study is to address the above mentioned challenges for unbiased high throughput quantification of “total” and “free” concentration of nonesterified fatty acids in the complex biological media via optimization and validation of a SPME assay followed by HPLC-ESI-MS. The method involves a simple SPME protocol with no necessity of using halogenated solvents or chemical derivatization approaches that use highly reactive reagents. In the proposed method, entire procedure is simplified to immersion of SPME fiber into the biological fluids which allows for extraction of the NEFA without interrupting the lipoproteins or cell membrane lipids (Figure 2-1). This is in contrast to the commonly used liquid based methods which only provide estimation of total concentration of fatty acids due to the disruption of protein-bound fractions and complex lipid structures such as lipoproteins by organic solvents. Therefore, as the SPME extraction is non-exhaustive, the natural balance

in the investigated system is not disturbed and the obtained results provide information about the actual equilibrium in the sample.

The possibility of encountering matrix effect in HPLC-ESI-MS analysis of human and fish plasma was evaluated using different experimental approaches. The proposed method was fully validated according to the bioanalytical method validation guidelines. The final protocol was applied to monitor PUFA changes in plasma obtained from a group of patients during cardiac surgery with the use of cardiopulmonary bypass (CPB) and to quantify level of the PUFAs in fish plasma.

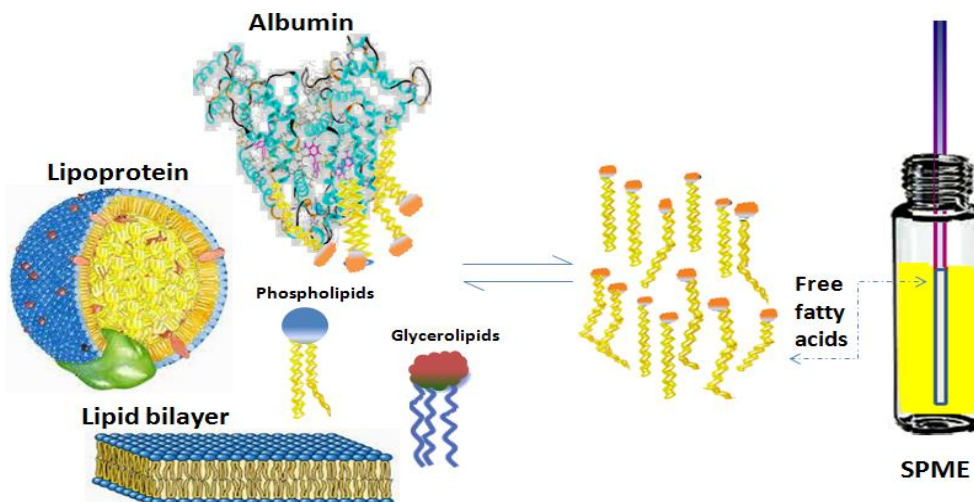


Figure 2-1 schematic of the experimental model for the equilibrium extraction of free fatty acids from plasma using the SPME fiber. Figure reprinted from reference with the permission of the publisher.⁵⁹

2.2 Experimental

2.2.1 Chemical and Materials

Methanol, acetonitrile, 2-propanol (all HPLC grade) were purchased from Caledon Labs (Georgetown, ON). LC-MS grade formic acid was obtained from Fisher Scientific (Ottawa, ON). Biocompatible SPME C18 probes (C18, 45 μm thickness, 15 mm coating length) were

provided by Supelco (Bellefonte, PA). Human serum Albumin, essentially fatty acid free was obtained from Fluka (Sigma-Aldrich Oakville, ON). Fatty acids were selected based on (i) their hydrocarbon chain length and (ii) number and position of double bonds. Docosahexaenoic acid (DHA), Docosapentaenoic acid (DPA), Adrenic acid, Docosatrienoic acid (DTA), Eicosapentaenoic acid (EPA), Arachidonic acid, Eicosatrienoic acid (ETA), Stearidonic and α -Linolenic acid were purchased from Cayman Chemical (Ann Arbor, MI) and stored at -20°C . Individual stock solutions containing 1 mg/mL of each standard were prepared by dissolving the analytes in HPLC-grade methanol. For instrument calibration, working standard solutions with known concentrations of standard fatty acids were prepared by mixing adequate volumes of diluted stock solutions and adding acetonitrile as needed. All stocks and working standards were stored at -20°C . A phosphate-buffered saline (PBS) solution was prepared by dissolving 8.0 g of sodium chloride, 0.2 g of potassium chloride, 0.24 g of potassium phosphate monobasic, and 1.44 g of sodium phosphate dibasic in 1 L of purified water (pH = 7.4). Extraction standards also were prepared daily by dilution to 1 $\mu\text{g/mL}$ with PBS buffer solutions at pH 7.4 to mimic the physiological conditions, while keeping the organic solvent content of all extraction standards at $\leq 1\%$ (v/v). PBS buffer solutions have been used for this study to mimic the physiological conditions for the initial SPME method optimization as a matrix-free environment.

2.2.2 Plasma Sample Preparation

Plasma samples were obtained from seven patients during cardiac surgery involving the use of cardiopulmonary bypass (CPB). Blood samples were taken on a sampling schedule order at 5, 10 and 15 minutes before initiation of the infusion; 5 minutes after chest opening and 5 minutes before commencing CPB, following by frequent sampling every 30 minutes during

CPB; and 5, 60 and 120 minutes after chest closure.^{135,158,202,203} Perioperative care has been provided to all the patients as described previously.²⁰⁴ The study approval was obtained from Toronto General Hospital/University Health Network and University of Waterloo Research Ethics Boards. All the patients signed the consent to participate in the study. Fish plasma samples were also collected from White Sucker (*Catostomus commersoni*) at Lake Superior (Provincial Park, ON) due to their widespread availability in the watershed. Blood was collected by caudal puncture with a heparin-coated needle and syringe (5cc) and centrifuged at 10000 rpm for 4 min to separate plasma. All plasma samples was transferred to a cryovial, snap-frozen in liquid nitrogen and stored at -80C until analysis. Animal care and all investigative procedures adhered to the guidelines of the Office of Research Ethics, University of Waterloo (AUPP:10-17) and the Canadian Council of Animal Care.

2.2.3 Optimization of SPME Procedure

C18 and mix-mode fibers (Supelco, Bellefonte PA) were compared during the preliminary stage of extraction phase selection. In order to determine the extraction efficiency and reproducibility of the SPME coatings, a phosphate buffered saline (PBS) at pH 7.4 was spiked with authentic standards of fatty acids for a concentration of 0.1 µg/ml. Prior to use, all fibers were preconditioned by 30 minutes agitation in a methanol: water solution (1:1, v/v) in order to activate the silanol groups of the stationary phase. The analytes spiked in plasma were pre-incubated in room temperature for 60 min prior extraction to allow establishment of protein binding, knowing that the binding rate of fatty acid to albumin is rapid.²⁰⁵ The SPME experiment was performed by immersing the fibers into 1 mL of sample aliquots for 60 min extraction time with 800 rpm orbital shaking (model DVX-2500, VWR International, Mississauga, ON). Immediately after extraction, fibers were rinsed in purified

water for 10 s to remove any remains of biological material from the coating surface, followed by 60 minutes desorption in 1 ml acetonitrile with agitation (1000 rpm) . Extracts were further injected to HPLC–ESI-MS system for analysis. Percentage of extraction efficiency (or percent absolute recovery) was calculated as the ratio of the amount extracted versus total amount of fatty acid spiked $\times 100\%$.

2.2.4 LC-ESI-MS Operating Conditions

All samples were analyzed using an HPLC-ESI-MS system consisting of two Varian 212-LC pumps (Walnut Creek, CA), a Prostar 430 autosampler, and a 500-MS ion trap mass spectrometer (Varian, Palo Alto, CA). Data acquisition and processing were performed using Varian MS Workstation software (Version 6.6). Chromatographic separation was performed on an Ascentis® Express C18 RP-LC column (2.1 x 150 mm, 2.7 μm). The binary gradient run consisted of eluent A (90% water, 10% Methanol) and B (80% methanol, 20% acetonitrile) at room temperature with a flow rate of 0.3 mL/min and 10 μl injection volume. Optimal separation was achieved using the following solvent gradient elution: Mobile B starts with 60% holding for 1 min (min 0–1), increasing to 95% (min 1–2), increasing to 100% (min 2–5), held for one minute (min 5–6), then ramped back to 60% over thirty seconds, followed by two more minutes of re-equilibration resulting in a total run time of eight minutes. All fatty acids were analyzed at negative ionization mode (forming $[\text{M}-\text{H}]^-$) and were monitored in full scan mode. The optimum MS parameters were as follow: capillary voltage: 90–110 V, RF loading of 80-90, ion spray voltage -4500 V and drying gas temperature 400 °C.

2.2.5 Determination of Matrix Effect and Ionization Suppression

Measurements of matrix effect were evaluated by using two different approaches including the “post-extraction spiked method”²⁰⁶ and the “sample extract dilution” method in triplicates (n = 3). For the post-extraction spiked method, neat solvent of acetonitrile was used (because it was indicated as the optimized desorption solution) at two different concentration level (50 and 500 ng/mL). The extracts from plasma samples were spiked with fatty acid standards at the same concentration as the neat solvent, and samples were individually injected into the LC/MS/MS system for quantification. In addition, matrix effect was also evaluated using the “sample extract dilution”. In this technique, the final sample extract from spiked human plasma is diluted by different dilution factors (1:0, 1:1, 1:2, 1:4 and 1:9). The evaluation of matrix effect using this method was studied for the final extract of SPME for spiked human plasma at a concentration of 2µg/ml of standard PUFAs; results were then compared with that of the absolute matrix effect method.

2.2.6 Determination of Protein Affinity Constant

(K_a) The extraction recovery of NEFAs was measured at different human serum albumin (HSA) concentrations to determine if variations in HSA level affect the free concentration and consequently the extraction recovery of studied fatty acids. Human serum albumin (essentially fatty acid and globulin free) was dissolved in PBS buffer solution (pH 7.4) to reach protein concentrations of 0, 5, 10, 20, 30, 40, 50, 60, 70 and 100 g/L, These solutions were then spiked with fatty acids standards to reach the concentration of 3 µg/mL in all solutions. The study was conducted in duplicate.

2.2.7 Determination of plasma protein binding: investigation of free and total concentrations

The determination of plasma protein binding by SPME is based on the quantification of the free concentration of ligand in the presence of plasma proteins.^{136,146,150,151,153,207,208} In order to have a better understanding of plasma protein binding, the calibration curves were not only constructed in PBS and plasma, they were also constructed in standard human serum albumin solution (essentially fatty acid free) to mimic the plasma with only albumin as binding agent. Linearity was verified by analyzing spiked plasma samples at the concentrations of 0, 1, 2, 3, 4, 5, and 7 $\mu\text{g/mL}$, with three replicates in each point. After incubation allowing for protein binding equilibrium (60 min), extractions from PBS, serum albumin and plasma samples were performed under the same conditions using SPME fibers. Batch-to-batch precision was determined according to Matuszewski et al.²⁰⁹ Five different sources of human plasma at all concentrations (n=3 for each point) were utilized for the construction of standard addition calibration curves.

2.3 Results and Discussions

2.3.1 HPLC-ESI-MS

Electrospray ionization in negative mode was chosen because fatty acids form $[\text{M}-\text{H}]^-$ quasimolecular ions due to their carboxylic acid moiety. Disregard of the applied collision energy level, the product ion spectrum of $[\text{M}-\text{H}]^-$ in MRM mode was also dominated by the unfragmented deprotonated molecular ions of a low sensitivity. The lack of production of detectable fragments in ESI-MS/MS has been already described for underivatized FAs.³² A series of experiments were performed to identify the optimal HPLC method for separation of

nine long chain polyunsaturated fatty acids. A set of different HPLC columns including C8 and C18, as well as different mobile phase compositions were examined. Although, most of fatty acids of interest were different in only one number of double bond or two carbons in the hydrocarbon chain, the column and gradient method were carefully optimized to enable thorough fatty acid differentiation, so that less abundant fatty acids would not be interfered by other abundant species. For chromatographic separation of PUFAs a C18 column with 2.7 μm core-shell particles was chosen. As the main advantage of core-shell compared to UHPLC columns with the fused-core small diameter ($<2 \mu\text{m}$), is to have a major benefit of the small diffusion path (0.5 μm) compared to conventional fully porous particles and are able to achieve high speed and high efficiencies but at much lower backpressures.^{80,210}

Several HPLC additives were also tested with further adjusting pH in the eluent solution. Preparation of mobile phase using tributylamine (pH 9.2) provided less or equal resolution compared to ammonium acetate (pH 8.1) or formic acid (pH 3.2); not only all these additives provide no improvement in sufficient resolution they also established the relevant buffer-induced ion suppression resulting in significant decrease in signal intensity for all fatty acids. Moreover, having data acquired in full scan mode, a background signal of m/z 255 and 283 was always detected in blank which has been previously reported as the mass spectrometric ubiquities contaminations due to the abundant presence of palmitate and stearate as plasticizers in environment and on plasticware.^{188,211} To overcome this problem, replacement of the stainless steel tubing and injection loop by inert PEEK material for chromatographic connections and tubing was done. Additionally, fresh solutions were prepared daily and careful examination of the blanks for these compounds was performed in every experiment.

Based on the chromatographic method, a two-carbon increase in fatty acid chain length increases the retention time by ~1.8 min, whereas introduction of a double bond, decreases retention time by ~0.7 min. Peak widths of 4–6 s were found and chromatographic resolution could be achieved in a total run time of 8 min. A typical SPME-LC-MS/MS chromatographic data set for equilibrium extraction of fatty acids from human plasma is illustrated in Figure 2-2

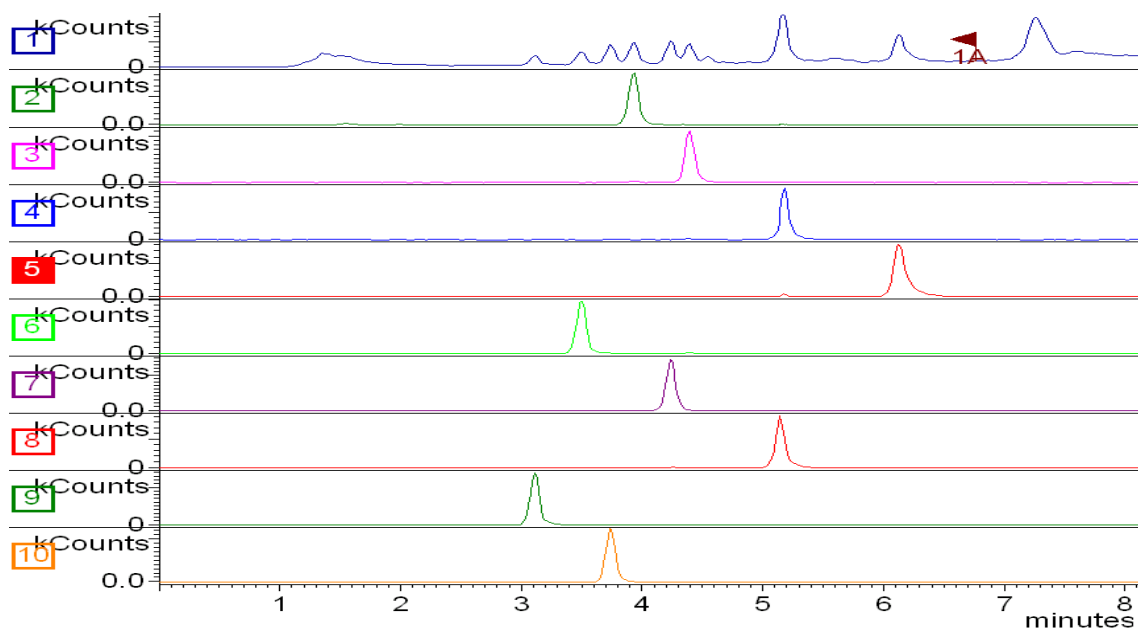


Figure 2-2 Examples of XIC chromatograms for SPME-LC-MS analysis of 2 μ g/mL of fatty acids from human plasma; DHA: 327.3, DPA: 329.3, ADR: 332.3, DTA: 333.3, EPA: 301.3, ARA: 303.3, EPA: 305.3, SDA: 275.2 and 10-ALA: 277.2 respectively)

2.3.2 SPME method development

The experimental standard procedure was followed based on previously published SPME protocol for method validation.¹⁴⁸ The properties of the C18 biocompatible fibers was described in details elsewhere.^{138,144}

Extraction: The extraction time profile was obtained in both PBS and plasma. The initial stages of extraction time profile for all fatty acids under study were similar in both PBS and plasma meaning that the equilibrium was achieved in both media within first two hours.

However, after four hours of extraction in plasma, the extracted amount started to increase reaching second plateau after 10 hours and remaining constant for up to more than 18 hours extraction Figure 2-3. Checking the physical appearance of the fiber, a jelly-like attachment around the fiber was observed after 4 hours extraction with vortex agitation. The initiation of protein attachment was observed around the metal part of the rod fibre which is in contact with plasma during long time aggressive agitation. This effect could be explained as a result of protein attachment to the surface of metal. The coating biocompatibility was tested several times and has been reported previously;^{138,144} hence it is anticipated that this effect is only visible for longer contact of fibre with aggressively agitated sample. Therefore, extraction time must be long enough to meet sensitivity requirement, and short and gentle to avoid the initiation of protein aggregation around the fiber. Therefore, the use of 800 rpm orbital shaking, which is a less aggressive agitation approach compared to vortex agitation, prevent the protein aggregation occurrence. The required time to reach equilibrium extraction in plasma for all nine compounds was less than 120 minutes; therefore, 2 hours was chosen as the optimum extraction time for the entire study.

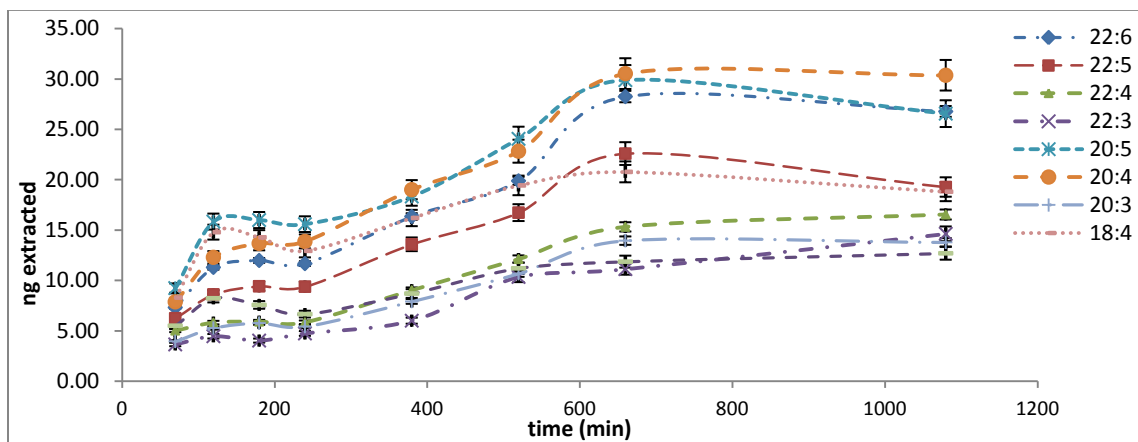


Figure 2-3 Extraction time profile for extraction of (3000 ng/mL) fatty acids spiked in plasma, the second plateau is an unusual observation due to the initiation of protein aggregation around the fiber after 4 hours extraction with aggressive vortex

Wash: Exposure of the coatings to complex biofluidic matrices provides the risk of attachment of particulates and macromolecules into the coating surface. Therefore, optimization of a fast washing step after extraction is crucial for efficient cleaning of the coating surface with minimum loss of analytes. This also helps to minimize the contamination of the final extract and avoid possible ion suppression/enhancement caused by interfering components in electrospray ionization source. Figure 2-4 illustrates the effect of different washing approaches on percentage recovery. The evaluation of the wash step in this study indicated that a 10 s immersion of fibers in nanopure water was found to be optimal for efficient cleaning of the coatings after extraction from plasma samples. Extending the washing step or application of any mechanical agitation in this study resulted in a loss of precision and reproducibility due to an inconsistent loss of analytes and observation of higher variation in the results.

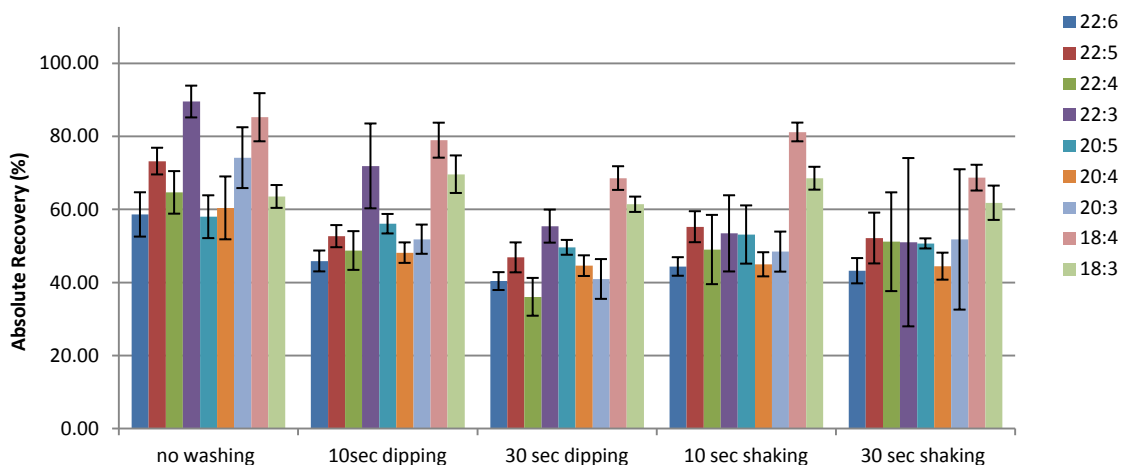


Figure 2-4 Evaluation of analyte loss using different washing strategies, extraction from spiked PBS (30ng/ml)

Desorption: In order to achieve the most efficient desorption of compounds from the coating and to minimize any remaining trace of compounds, desorption conditions should be optimized. Different compositions and ratios of organic:water phases were compared to find

the best desorption solvent. The comparison of the absolute recovery of the five desorption solvents for equilibrium extraction is demonstrated in Figure 2-5. Results indicated that the 100% acetonitrile solvent resulted in the best recovery and the lowest carryover. According to desorption time profile, the most efficient desorption of the analytes with the lowest carryover was found at a minimum 60 min desorption time at 1500 rpm agitation speed (1 mm amplitude).

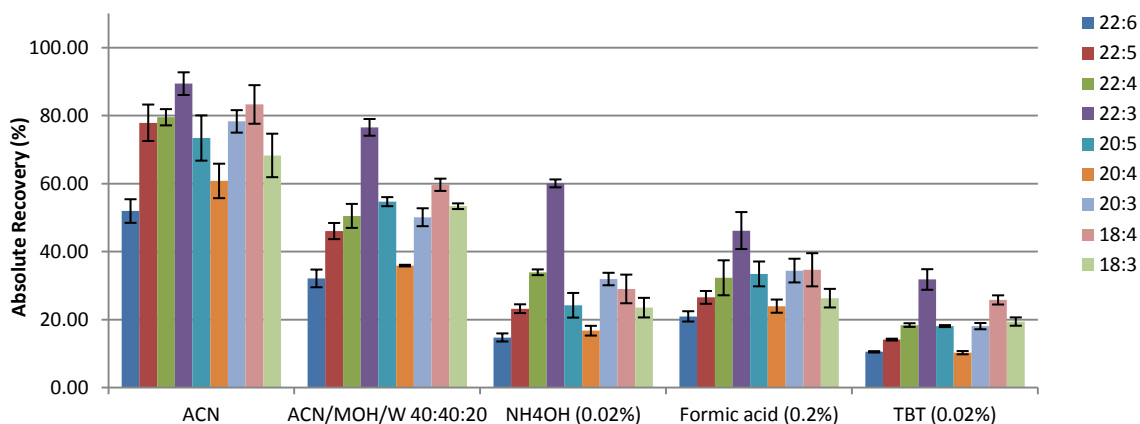


Figure 2-5 Desorption solution composition containing acetonitrile, ACN/MOH/W (40:40:20) plain or with additives of NH₄OH (pH 7.8), Formic acid (pH 3.2) or tributylamin (pH 9.2), extraction from spiked PBS (30ng/ml)

Carry over: Efficiency of desorption should also be determined by evaluation of possible carryover. However, considering that it is impossible to evaluate the potential carryover of all macromolecules and metabolites present in a typical biological sample, these biocompatible SPME devices are recommended for single use for both *in vivo* and *in vitro* applications. This is recommended in order to prevent accidental cross contamination of subsequent samples by any coeluting traces from previous extractions. The amount of carryover of analytes in the coating was evaluated through a second desorption of the same set of fibers used for evaluation of desorption time. Results concluded that a 90 min single step desorption was sufficient to eliminate fatty acids from the fiber, and an analysis of the second desorption did

not result in any detectable signals. A desorption efficiency greater than 95% is acceptable for quantitative analysis. Due to the desorption efficiency of the analytes, percentages of carryover were found negligible regardless of type of extraction biological matrix being sampled.

2.3.3 Extraction efficiency of the SPME method in PBS

The absolute recovery of FAs from a physiological buffer solution (pH 7.4) using biocompatible fibers was higher than 44% for all cases, which resulted in a significant depletion conditions during the binding study. Coatings with such high fiber constants are preferred for the study of FAs in order to ensure that the amount of ligand extracted by the coating is sufficiently high so that instrumental sensitivity is adequate to determine the extracted amount accurately. The results obtained in the PBS buffer solution as a matrix-free media are shown in Table 2-1. The precision of the proposed system was studied as inter- and intra-day relative standard deviations (RSD) for $n = 6$ coatings over four experiments. The assay showed good precision (5–12% intra- and 1–6% inter-day RSDs) for the analysis of all nine fatty acids. The matrix match calibration curve was also constructed in plasma in order to determine the linear regression equation and the correlation coefficient (r^2) of the standard calibration line using the least squares method. The linearity of the standard calibration curve was confirmed by plotting the extracted amount (ng) versus spiked amount in plasma. Limit of quantification (LOQ) was determined by analyzing fatty acids in five replicates and verifying the RSD%, which should be smaller than 15%. Data are presented in Table 2-1.

Table 2-1 Evaluation of SPME method efficiency for extraction of FAs from physiological buffer solution (pH=7.4)

FA	Absolute Recovery (n=5)	Inter-day RSD (4 trials)	Intra- day RSD (n = 6)	LOD ng/mL	LOQ ng/mL	R ²	Linearity ng/mL
DHA	44±7	8	1	1.5	10	0.9986	10-1500
DPA	76±1	7	1	1	7	0.9958	7-1000
ADR	68±1	5	3	1	7	0.9997	7-1500
DTA	90±6	11	2	1.5	2	0.9973	2-500
EPA	61±10	9	4	3	10	0.9984	10-1500
ARA	55±8	8	6	1.5	10	0.9931	10-1500
ETA	74±3	7	2	1.5	7	0.9999	7-1000
STD	81±8	12	3	5	5	0.9981	5-1000
ALA	63±3	6	2	1	10	0.9970	10-1500

2.3.4 Evaluation of matrix effect and ionization suppression

Matrix effect can be considered as the Achilles heel of quantitative mass spectrometric analysis. Matrix effect occurs when matrix molecules coelute with the analyte of interest thus altering the ionization efficiency of the electrospray interface.²⁰⁹ Therefore, it is essential to employ appropriate strategies to minimize the ionization suppression or enhancement phenomenon associated with matrix effect. SPME, however, is a clean extraction method, where the biocompatibility of the polymer coating prevents extraction of macromolecules and other matrix components. Moreover, non-exhaustive extraction by SPME fiber applies not only to the analyte of interest, but also possible interfering compounds, thus eliminating or significantly minimizing competition in ionization process. In this study, the matrix effect was assessed using two different approaches including i) absolute matrix effect evaluation using the post-extraction spiked method described by Matuszewski et al.²⁰⁶ and ii) the sample extract dilution method.²¹² Calculation of absolute matrix effect involved relating the peak area obtained from a neat solvent spike with a known concentration (S2) to the peak area of

the blank extract, which is spiked with the same concentration of analyte standard after extraction (S1)

Equation 2-1

$$ME \% = \left(\frac{areaS2}{areaS1} \right) \times 100$$

ME values larger than 120% and smaller than 80% represent significant ionization enhancement or suppression for a given analyte. For this study, matrix effect (ME) values are reported in Table 2-2. Utilizing the proposed SPME method, no absolute matrix effect was observed. Additional proof is provided by evaluation of matrix effect using the Sample Extract Dilution Method.

2.3.5 Evaluation of matrix effect using Sample Extract Dilution Method

The Sample Extract Dilution method was applied as an additional quantitative method in order to confirm the absence of an absolute matrix effect by proposed SPME method. Therefore, a plot was constructed for each analyte; the x axis reports the dilution factor, and the y axis represents the normalized peak area (peak area of the chromatographic peak multiplied by dilution factor). In the electrospray ionization (ESI) source, the total number of ions per time unit formed is approximately constant; at higher concentrations a competition occurs between all ions to escape from the final droplet surface. Once the compound concentration decreases as a result of sample dilution, this competition decreases concurrently. As a result, the matrix effect on analyte response originated by coeluting compounds can be reduced significantly.²¹³ When there is no absolute matrix effect, the y axis response remains constant for the entire applied dilution factors, within the experimental error Figure 2-6. The results of this evaluation indicated that in spite of the complexity of the plasma matrix, the final extract obtained from the SPME method required no dilution in all

cases. The SPME method resulted in clean final extracts of biological samples due to the isolation of analytes from any interfering matrices. In addition, the application of the biocompatible coatings and washing step aided to prevent transfer of macromolecules (including polysaccharide, proteins, and particulates) and in reducing the possibility of suppression/enhancement of analytes signals during ionization.

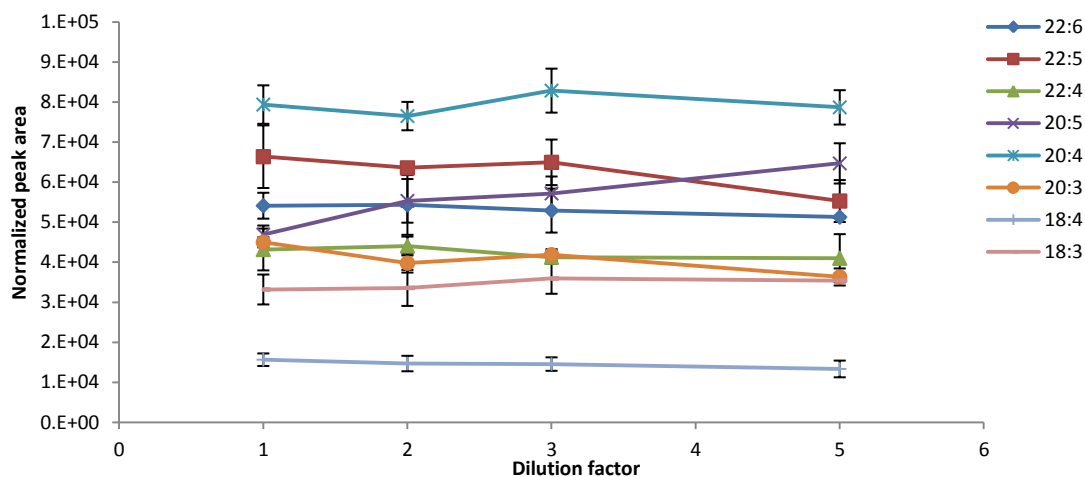


Figure 2-6 Plasma sample dilution effect on normalized ion current intensity for fatty acids extracted from spiked plasma at a concentration of 2 μ g/ml of standard fatty acids

2.3.6 Determination of albumin affinity constant by SPME

In plasma, fatty acids are soluble in concentrations up to about 1 μ M. Owing their low solubility in plasma, FAs require a transporter to increase their concentration in vascular and interstitial compartments. Human serum albumin (HSA) is the transport vehicle for free fatty acids and the main FA-binding protein in extracellular fluids²¹⁴ which binds with approximately 0.1-2 mol per mole protein, under normal physiological condition.²¹⁵ Further increase of NEFA concentration increases the bound NEFA proportion, accordingly.²⁰⁵ Because SPME extraction occurs via free concentration, the study of plasma protein binding (PPB%) and the effect of albumin concentration on fatty acid recovery by SPME seemed

crucial for this study. To ensure accurate quantification of fatty acids independent of albumin concentration, the recovery profile of NEFAs was measured at different HSA concentrations. Amount of FAs extracted from spiked standard human albumin solutions were plotted against the protein concentrations (C_p), and the K_a was determined by fitting Equation 2-2 through the data points.²¹⁶

Equation 2-2

$$C_{free} = \frac{C_0}{1 + K_a f_{up} C_p}$$

Where, C_0 is the amount extracted at a protein concentration of 0, and f_{up} is the unoccupied fraction of protein. In this experiment, f_{up} is approximately equal to 1 because the total protein concentration (5-100 g/L) was much higher than the spiked fatty acid concentration (3 μ g/L). Figure 2-7 shows the absolute recovery calculated for each individual protein concentration. The reference range for albumin concentrations in human blood plasma is 34 to 54 g/L. In the exaggerated range of HSA (<20 and >70 g/L), protein concentration affects the recovery of fatty acids by changing its free concentration equilibrating with the SPME coating. However, these extreme values are not expected in plasma samples except of hyper- or hypoalbuminemia and in this study they are only considered in order to evaluate fiber performance. As the results show in Figure 2-7, absolute recovery is constant within the physiological range of HSA concentration (30-60 g/L). Accordingly, the mean calculated K_a values from this experiment were in the range 9.2×10^4 to $4.3 \times 10^5 \text{ M}^{-1}$ Table 2-2. Affinity constant (K_a) was reported to be dependent on the fatty acids carbon chain length; it increases with an increase in length and decrease of the number of double bounds in studied fatty acids.²⁰⁵ The obtained results for the affinity constant using the SPME method follow the same pattern and correspond very well with literature values,^{214,217} which proves the validity

of the proposed SPME method for the study of free concentration and protein binding of nonesterified fatty acids in biological systems.

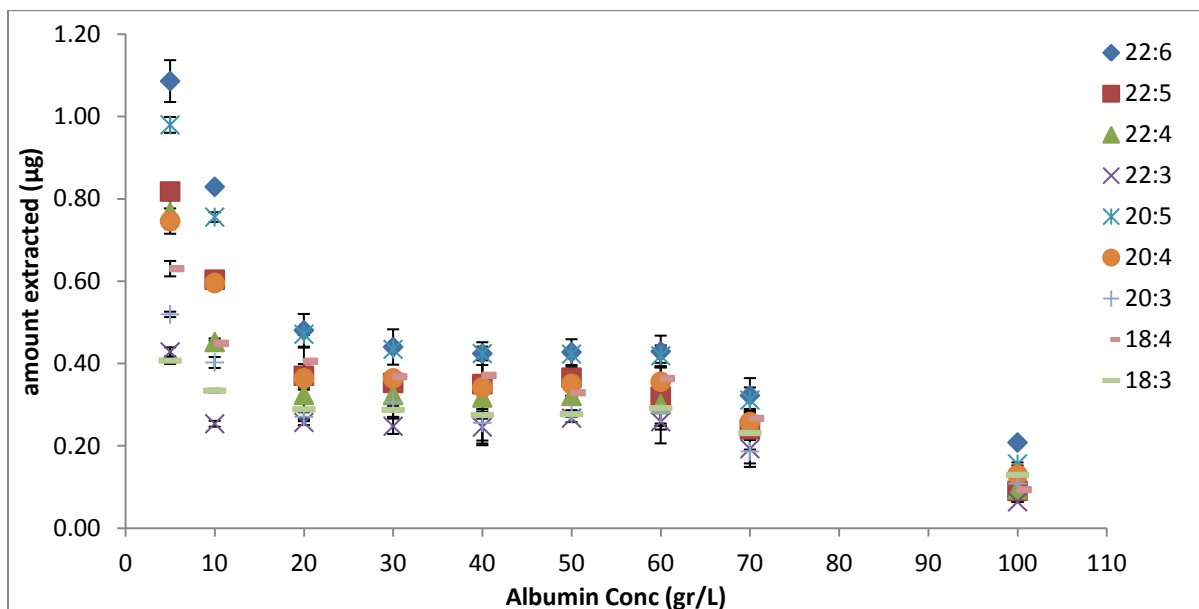


Figure 2-7 Albumin concentration-dependent NEFA recovery; y-axis represents the extraction recovery percentage of fatty acids vs albumin concentrations after 2 hr of extraction. Figure reprinted from reference with the permission of the publisher.

2.3.7 Plasma protein binding (PPB %)

Binding equilibrium studies for long-chain fatty acids to serum albumin are complicated because of the low ligand solubility. The aim of this part of the study was to investigate binding equilibria of long-chain fatty acids in human blood plasma under varying conditions and to compare the results with observations on the affinity constant to serum albumin, which were discussed in the previous section. Plasma protein binding determination by SPME method has been reported based on the measurement of bioactive unbound concentrations of the ligand, which is often referred as the free concentration in presence of plasma protein.²¹⁸ Briefly, the percentage of binding to plasma proteins (PPB) is calculated from the total and free concentrations of analyte using Equation 2-3

Equation 2-3

$$PPB\% = \left[\frac{C_{total} - C_{free}}{C_{free}} \right] \times 100$$

Where C_{total} is the total concentration of ligand and C_{free} is the free concentration of ligand in plasma. Considering that the total ligand concentration is directly proportional to the slope of the matrix-free calibration curve in PBS, and the free concentration is directly proportional to the slope of matrix match calibration;²¹⁸ Equation 2-3 becomes:

Equation 2-4

$$PPB\% = \left[1 - \left(\frac{\text{Slope calibration plasma}}{\text{Slope calibration PBS}} \right) \right] \times 100$$

In order to better understand the FA binding mechanism, the matrix match calibration curve was not only constructed in plasma, it was also constructed in HSA standard buffered solutions (35 g/L). Using the standard slopes obtained from these experiments, Equation 2-4 was applied for determination of PPB values of nine PUFAs under study in both media; results are presented in Table 2-2. The present observations demonstrate that there are no significant variations in PPB values determined by SPME method using different approaches, and it correlates well with average literature values.^{205,217,219}

Table 2-2 Evaluation of albumin affinity constant and % plasma protein binding

	DHA	EPA	ADR	DTA	EPA	ARA	ETA	SDA	ALA
Matrix Effect (%)	103%	96%	88%	91%	116%	110%	93%	112%	116%
Albumin affinity constant (M⁻¹)	9.2×10 ⁴	2.1×10 ⁵	2.2×10 ⁵	4.3×10 ⁵	1.2×10 ⁵	1.5×10 ⁵	2.9×10 ⁵	2.0×10 ⁵	2.2×10 ⁵
Human serum albumin PPB (%)*	97.9	98.6	99.1	99.4	98.0	98.6	99.2	99.5	99.6
Plasma PPB (%)	98.3	99.3	99.5	99.7	98.7	98.8	99.6	99.5	99.6
Intra-batch reproducibility (%)	6	10	6	9	5	5	6	6	10
Inter-batch reproducibility (%)	9	14	8	9	11	8	7	7	12

*PPB values are found with (± 0-0.2) standard deviation and the correlation coefficient (CV) lower than 15%.

2.3.8 Fatty acids quantification in plasma samples

One of the most important elements of assay validation is the evaluation of the effect of matrix on the results of quantitative determination of metabolites in biological fluids.²²⁰ This goal could be achieved by comparison of the assay precision and accuracy of a typical validation experiments performed in a single lot of plasma versus the same validation experiment performed in five different plasma lots according to Matuszewski et. al.²⁰⁹ For this purpose, the standard addition method is used as the most suitable calibration method that recompenses any variation related to complexity of the matrix. For quantification of fatty acids of interest in this study, seven concentration points in three replicates were used to construct the standard addition calibration curves. In order to avoid disturbing the matrix and dilution of the sample, the volume of organic content of added standard solution was kept <1%. The concentration of investigated FAs was kept within the linear range. The limit of detection (LOD) and limit of quantification (LOQ) obtained in the range of 0.5–2 and 5–12 ng/mL, respectively, with a linear dynamic range of 100 fold for each compound. The stability of standard fatty acids was investigated in the stock solutions, PBS and incubated plasma. Storage stability of FAs in human plasma and the influence of freeze-thaw cycles were also examined and convinced by processing a set of QC samples. On the other hands, due to the limited availability of plasma samples obtained from patients, it was essential to compare the reproducibility of standard addition calibration in different plasma lots under the same extraction and chromatographic conditions. Therefore, not only the five calibration curves were built separately in the same single plasma lot to compare the precision and accuracy, they were also built in five different plasma batches to evaluate the relative matrix effect due to the lot-to-lot variation.

The precision and accuracy values obtained in a single plasma lot using the proposed SPME method ranged from 5 to 10%, and 95 to 110%, respectively. The inter-lot and intra-lot reproducibility is reported in Table 2-2. Moreover, when the same validation was attempted in five different plasma lots, the precision values were persuasive (7-14%) under identical conditions; likewise the correlation variance (CV) of standard line slopes did not exceed 4–5% for the method. The very small variability of slopes of calibration curves obtained from five different plasma sources is a direct indicator of assay reproducibility and serves as a good quantitative indicator of the absence of a relative matrix effect in the proposed SPME method. The unknown sample concentrations were calculated from the equation, $y = mx + b$, as determined by weighted ($1/x$) linear regression of the standard line. Eventually, for quantification, the mean calibration equation obtained from five different pooled plasma lots was employed to extrapolate and quantify the unknown amount of PUFAs under study in the patients undergone cardiac surgery. However, due to the limited availability of fish plasma, the standard addition method was performed in an individual lot of pooled fish plasma (three replicates for each concentration point). Data are summarized in Table 2-3.

2.3.9 Comparison of NEFA composition in fish and human plasma

In general, the mean of standard calibration line slopes determined in human control plasma and fish plasma are similar for all fatty acids, which serves as another excellent measure for the absence of a relative matrix effect not only within the same individual, but also between individuals. The observed differences of the Y-axis intercept of the calibration equations clearly indicate that the initial level of fatty acids is considerably higher in fish. Total plasma NEFA in the study of White Sucker species ranged 0.76-11.13 $\mu\text{g/mL}$, whereas for control human plasma only arachidonic acid was detectable in the quantification range. The amounts

of DHA and EPA were significantly higher in fish plasma with a *p* value of 0.002 and 0.007, respectively, though the concentration level of arachidonic acid was not statistically different between these two subjects with a nearly non-significant *p* value (0.78). These results are consistent with the erstwhile work done on the White Sucker fish, which indicated higher DHA and EPA, and lower AA.^{221–223} Our results confirm the well known fact that fish is an omega-3 rich food choice because of its primary source of essential fatty acids and demonstrate that presented analytical protocol can be used for assessing the nutritional value of fish products in simple and relatively fast manner.

Table 2-3 Linear dynamic range of fatty acid concentration in human and fish plasma samples

	Human plasma calibration(n=5) ¹	Lot-to-lot CV (%) ²	Fish plasma calibration ⁴	Human plasma conc.(μg) ³	Fish plasma conc.(μg) ⁵
DHA	y = 0.0041x + 0.67	5%	y = 0.0044x + 26.9	LOD	11.1 ± 0.2
DPA	y = 0.0037x + 10.5	4%	y = 0.0039x + 16.6	ND	6.6 ± 0.1
ADR	y = 0.0019x + 1.6	5%	y = 0.0019x - 0.5	ND	LOD
DTA	y = 0.0018x + 3.3	3%	y = 0.0022x + 4.3	ND	3.0 ± 0.1
EPA	y = 0.0041x + 4.7	3%	y = 0.0041x + 13.1	LOD	9.0 ± 0.1
ARA	y = 0.0036x + 1.7	3%	y = 0.0027x + 1.04	2.9± 0.1	2.7 ± 0.1
ETA	y = 0.0026x + 0.8	4%	y = 0.0025x + 0.4	1.2± 0.1	1.1 ± 0.01
STD	y = 0.0034x + 1.26	4%	y = 0.0044x + 1.1	ND	0.76 ± 0.01
ALA	y = 0.0012x + 1.5	5%	y = 0.0011x + 5.2	2.8± 0.2	1.6 ± 0.1

¹Mean of calibration equation of five different human plasma lots, three replicates each.

²Lot-to-lot variation of slope of calibration equations from five different sources of plasma

³Primary concentration of fatty acids in human plasma extraction, total μg

⁴Mean of calibration equation obtained from single human plasma lot, three replicates.

⁵Primary concentration of fatty acids in fish plasma extraction, total μg

2.3.10 Clinical data analysis

Using the validated SPME method, PUFA changes were monitored in seven patients. The scheme in Figure 2-8 shows the order of sample collection during the cardiac surgery

performed with the use of extracorporeal circulation (CPB). As the results indicate in Figure 2-9, the major changes in concentration of unsaturated fatty acids during the surgery refer to the period when the patient is placed on CPB and the most significant increase is related to the level of ALA (18:3). Pre-operative or intra-operative metabolic changes in cardiac surgical patients are widely discussed in the literature.^{7,224,225} From a metabolic point of view, the cardiovascular response to increased metabolic demands after cardiac surgery may lead to enhanced glucose and down regulated free fatty acid (FFA) metabolism; yet the heart can use several substrates, among which free fatty acids (FFAs) and glucose are the major sources.²²⁴ Having known this fact, the reason behind fatty acid elevation right after commencing bypass could be clearly explained. Hence, the reason for specific amplification of ALA in all patients needs deeper clinical controversy, which is beyond the scope of this article. The alteration in metabolic profile of ALA and its metabolites was already reported and discussed in the studied group of patients and current targeted analysis confirms previous findings.¹³⁵

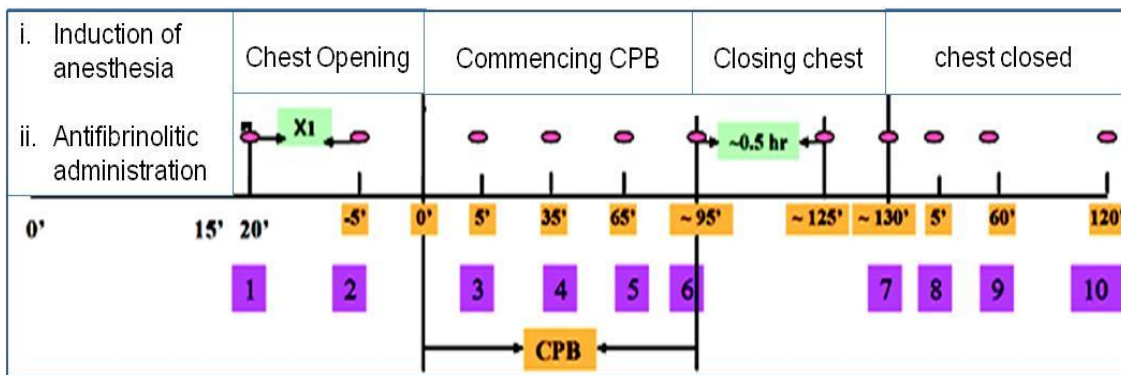
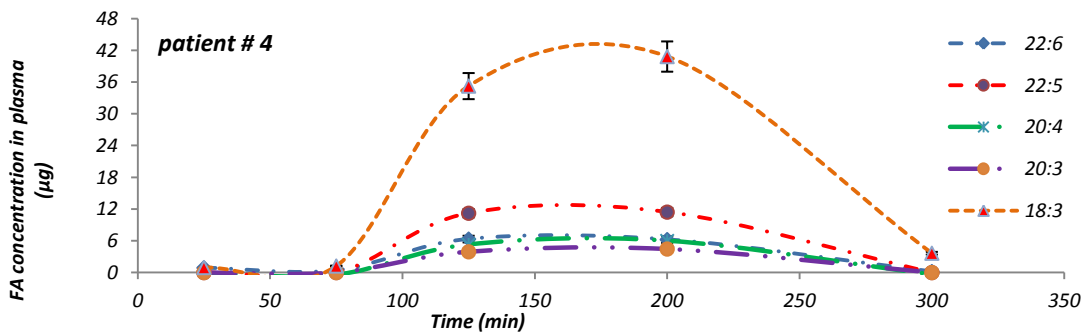
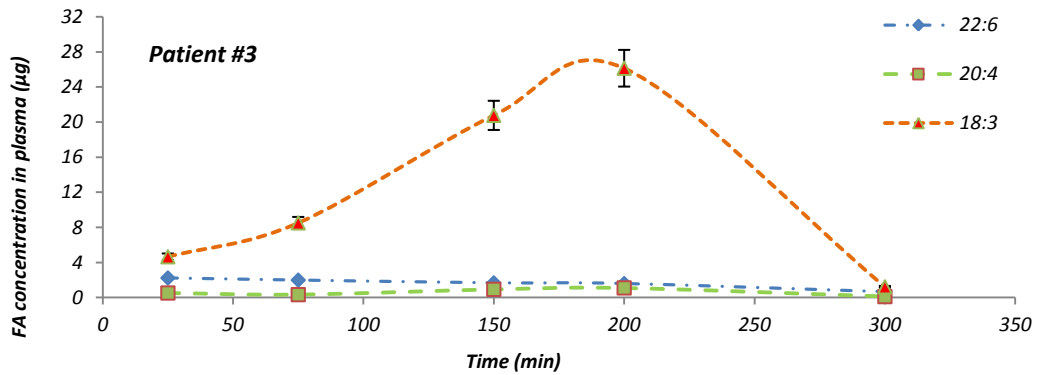
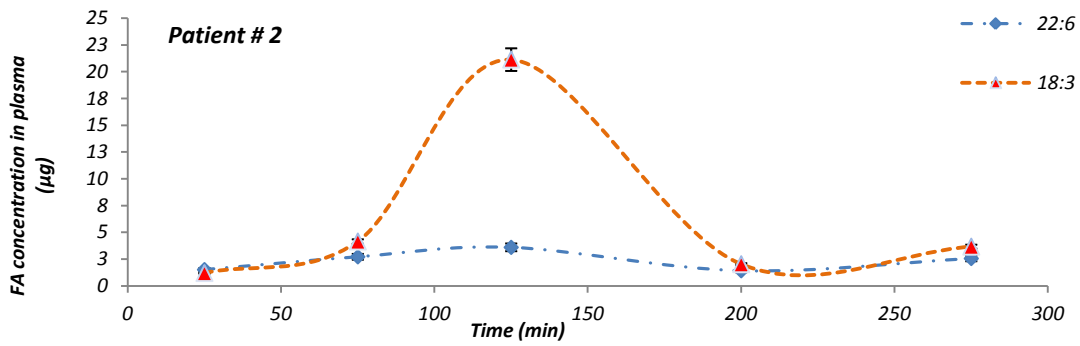
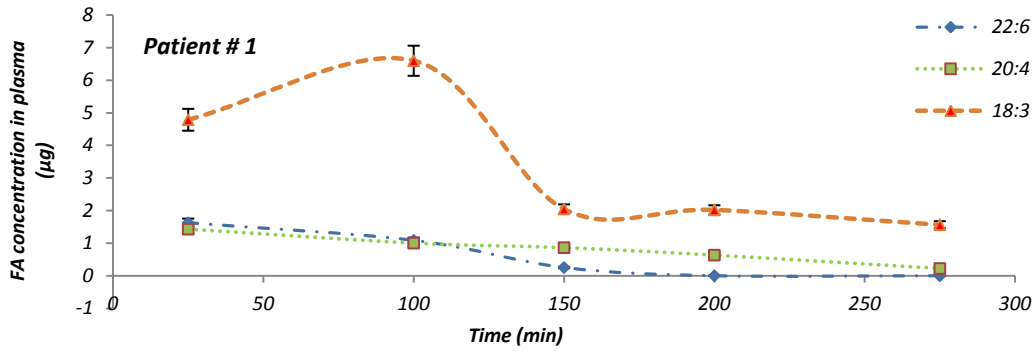


Figure 2-8 Scheme of cardiac surgery with the use of extracorporeal circulation (CPB) indicating the sample collection over the time of surgery. Figure reproduced from reference with the permission of the publisher¹⁵⁸



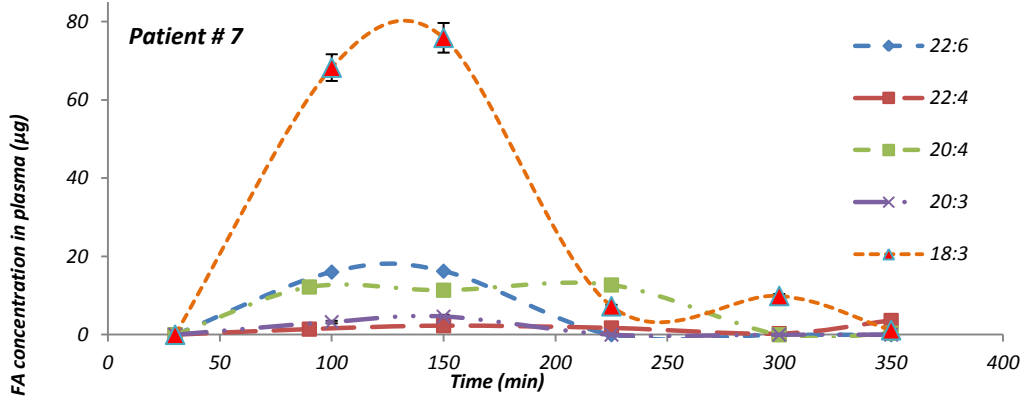
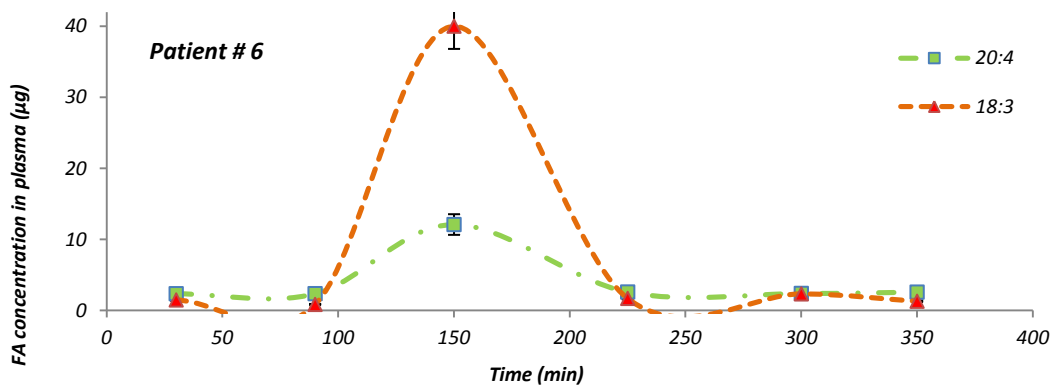
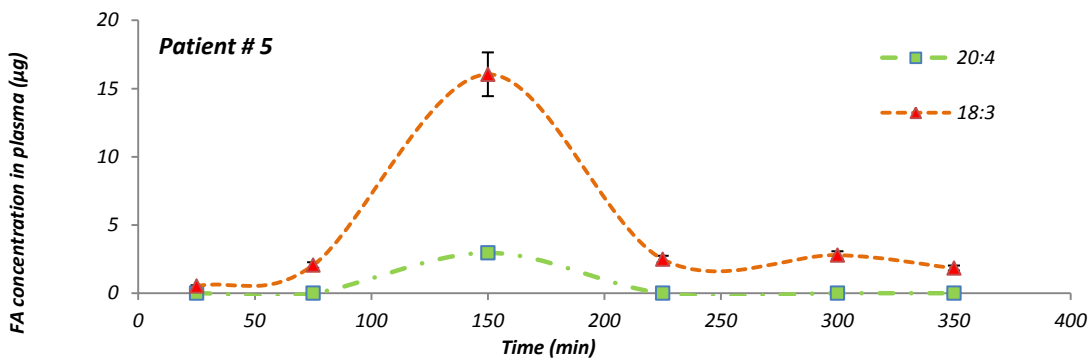


Figure 2-9 Metabolic profile of FAs in patients undergoing cardiac surgery with the use of CPB; the most significant increase of FAs was observed for patient 7, in which the level of ALA reaches to $75 \pm 4 \mu\text{g}$. Based on Table 2-3, concentration of ALA in the normal human plasma is only $2.8 \pm 0.2 \mu\text{g}$. Figure reprinted from reference with the permission of the publisher.

2.4 Conclusions and Future Directions

This research aims to develop a simple unbiased analytical method based on SPME in combination with LC-MS method for the extraction of free fatty acids from human and fish plasma. It was shown that the use of biocompatible C18 SPME fibers could be successfully applied for quantification and qualitative profiling of this group of lipids. This method permits the avoidance of interferences from hydrolysis of esterified fatty acids from other lipid sub-classes. Moreover, the protein affinity constant of polyunsaturated fatty acids has been determined and compared to the literature values. Indeed, the obtained results indicate the selectivity of the proposed method for the determination of fatty acid species despite their slight structural differences in carbon chain length and double bond number and localization. The extensive validation of the method demonstrates the fulfillment of requirements for the bioanalytical assays. The results of calibration equations obtained from fish and human plasma suggested that this approach could be extended to the plasma samples of other biological species. The application of the protocol allowed for the successful monitoring of the elevation of fatty acids in plasma collected from a group of patients undergone cardiac surgery right after initiation of extracorporeal circulation. The promising outcomes of the study show the potential of the approach for profiling and quantification of fatty acids *in vivo* in low invasive way as it was already demonstrated for other fiber-based SPME applications.^{154,199,226–229} The presented method could be also adopted for high throughput *in vitro* analysis either in its fiber form or using thin-film geometry format using automated 96-SPME device autosampler.¹⁵⁷

2.5 Addendum and Acknowledgment

The text of this chapter was rewritten in comparison to published research article. The SPME study was supported by Natural Sciences and Engineering Research Council of Canada (NSERC). The authors express their sincere gratitude to Professor Mark Servos at the Biology Department of University of Waterloo as well as Environment Canada for providing fish plasma samples. Supelco is gratefully acknowledged for providing biocompatible C18 fibers.

Chapter 3

Methodological modifications on quantitative analysis of plasma lipids using high throughput solid phase microextraction

3.1 Introduction

Lipidomics is a relatively new branch of “omics” science and a quickly progressing discipline that aims to comprehensively determine the lipid composition in living cells and organisms, as well as to characterize their biochemical relations and interactions with other neighboring lipids and proteins. To this end, accurate quantification of individual lipid species, as a first step in lipidomics, remains a very essential, yet challenging task.²³⁰ Lipid quantification generally falls into two categories: i) relative quantification that measures the pattern changes of lipids and ii) absolute quantification that calculates the exact amount of individual lipid species and subsequently, the mass level of particular subclasses and classes.⁵⁰ A quantitative method should strive for the highest degree of accuracy and precision; accordingly, the error propagation in each step, from sampling to experimental analysis and data processing, must be carefully pre-estimated and controlled.

General analytical platforms of lipid analysis and lipidomic studies have been already introduced and discussed in section 1.4 and 1.5 followed by a detail description of the most important conventional sample preparation techniques involved in lipid analysis, represented in section 0 of Chapter 1. To date, sample preparation followed by chromatographic approaches coupled to mass spectrometry remains as the chief technological approach used in lipidomics. This includes various cutting-edge tandem mass spectrometry strategies,^{39,51,75,77,231,232} specialized reagents and calibration standards,^{4,233} and

comprehensive searchable lipid databases,² towards online data analysis.^{3,234,235} Within the whole workflow, the possibility of matrix effect encounters, chances of chemical cross-contamination and co-elution, as well as isobaric interferences of naturally occurring lipids with the same nominal mass are the key analytical challenges of lipid quantification. To correct biased losses of lipid classes, spiking of samples with lipid standards is a necessary step that needs to be taken prior to extraction. As a critical step, appropriate calibration strategies should be employed by performing comparisons of analytes against either external or internal standards with similar molecular structures (e.g. stable isotopologue of analytes). For quantitative analyses of the lipid complex in a biological system, it is certainly impractical to use one isotope-labeled standard per each lipid species. Bearing in mind that the response factor of lipid species in ESI-MS depends primarily on the ionization properties and polarity of the head group of a given lipid, a single species per entire lipid sub-group can be employed as an external standard to allow quantification of individual lipid species within the same class.^{52,236,237}

In clinical and biological applications, sample extraction techniques have not kept pace with the development of analytical technologies such as state-of-the-art mass spectrometry, and thus sample preparation techniques have become the weakest link in modern chemical analytical procedures. Although some of these methods are efficient, most of them are slow, labor/time intensive, and challenging to automate; in addition to requiring high consumption of organic solvents. Within the past years, driving forces such as the need for faster high throughput analyses have encouraged chemists to pursue automated modern sample extraction methods. Lipids are commonly extracted by traditional Bligh & Dyer or Folch protocols that use chloroform, methanol, and aqueous buffer. Nevertheless, the conventional

sample preparation methods relying on manual lipid extraction are labor intensive and prone to error, thereby difficult to fulfill the need for large scale lipidomics studies that require the throughput of numerous samples per day.^{238,239} In this context, automation of the sample preparation and extraction procedures is essential for improving the cost effectiveness of such projects, minimizing sample losses, and decreasing unexpected experimental artifacts. Over the past years, attempts have been made to use the robot-assisted sample preparation and lipid extraction procedure in the 96-well format.⁵⁶ In this regard, a high throughput method termed Matyash¹⁰⁵, which combines methyl-tert-butyl ether (MTBE) extraction with mechanical homogenization and a conventional micropipetting robot, was introduced for the extraction of lipids from human brain²⁴⁰ and blood plasma.¹⁰⁵ In related work, dimethyl sulfoxide (DMSO) was reported for extraction of cellular lipids from microalgae samples using a 96-well plate in conjugation with the fluorescence spectrophotometer.²⁴¹ Another solvent-based extraction method termed BUME, based on a butanol:methanol mixture, was used in conjunction with an automated 96-well robot for the performance of total lipid extractions from plasma or serum.¹⁰³ However, besides the high toxicity of these methodologies, which are all riddled with a high solvent-to-sample ratio, conventional approaches are also challenging for automation in the 96-well format. To bypass these challenges, automated 96-well format solid-phase extraction (SPE) has been widely used for high-throughput determination of phospholipids in nutritional and epidemiological studies.²⁴²⁻²⁴⁴ Various sorbent chemistries, such as aminopropyl silica, mixed mode, C18, etc., were used to analyze lipids, but they either mainly focused on analysis of fatty acids,^{62,210} or were otherwise class-selective depending on the elution conditions used.^{37,112,245,246} The Waters Ostro 96-well Plate was originally intended as a sample clean-up

approach for the capture and removal of highly abundant phospholipids in the analysis of polar metabolites;^{238,239} but was later modified for target lipid extraction during routine bioanalysis.^{247,248} Although this approach promises significant advantages for analysis of large sample numbers in shorter times, it reportedly has several qualitative and quantitative limitations. Several attempts have been made to combine liquid–liquid extraction and solid phase extraction methods (LLE-SPE) for plasma and blood, primarily with the purpose of separating phospholipids from the rest of metabolites; in different studies, the use of this approach was reported to achieve better lipidome coverage.^{238,249} However, the method is tedious and labor intensive, yields unavoidable experimental artifacts, and due to the multiplexed sample preparative steps that need to be taken, impractical to wholly automate.¹³⁰

Thin-film microextraction (TFME), as a newly emerged format of the SPME technique, offers improvement of sensitivity without sacrificing time by increasing the available surface area and volume of coatings. Current thin film configurations are available on a fully automated 96-blades system compatible with standard 96-well plates, and different coating chemistries have been reported for various applications, including the analysis of drugs and metabolites from biofluids, tissue, cells, and food matrices.^{137,141,146,159,204,250–253} In spite of the promise of the method for extraction of hydrophilic and hydrophobic compounds, this technique has never been applied in lipidomics and lipid analysis studies. In the last chapter (Chapter 2) we presented the novel application of disposable rod fiber SPME for analysis of nonesterified fatty acids from biological matrices. The aim of this study was to develop a high throughput automatic 96-blade SPME protocol towards the production of a crude lipid extract for analysis on the LC-ESI-MS/MS system in order to obtain a highly reproducible

methodology that could be used to quantify lipid classes in clinical studies. In this regards standard addition calibration was used based on the one-class/one-standard approach for the determination and quantification of unknown lipids from plasma samples.

3.2 Experimental

3.2.1 Reagents and materials

LC-MS grade Methanol, acetonitrile, 2-propanol (all HPLC gradient grade) were purchased from Fisher Scientific (ON, Canada). LC-MS grade acetic acid and ammonium acetate were obtained from Fluka (Sigma-Aldrich Oakville, ON, Canada). Human Na citrate plasma was purchased from Lampire Biological Laboratories, Inc. (Pipersville, PA, USA). Two groups of lipid standard with even-numbered carbon chains (endogenous lipids), as well as odd-carbon acyl chains (non-endogenous) from each lipid class and subclass species were purchased from Avanti Polar Lipids (Alabaster, AL) for method development: 1-palmitoyl-2-hydroxy-*sn*-glycero-3-phosphocholine, (LPC 16:0); 1-oleoyl-2-hydroxy-*sn*-glycero-3-phosphocholine, (LPC 18:1); 1-myristoyl-2-stearoyl-*sn*-glycero-3-phosphocholine (PC 14:0/18:0); 1-stearoyl-2-arachidonoyl-*sn*-glycero-3-phosphocholine, (PC 18:0/20:4); 1-palmitoyl-2-linoleoyl-*sn*-glycero-3-phosphoethanolamine, (PE 16:0/18:2); N-oleoyl-D-*erythro*-sphingosylphosphorylcholine, (SM d18:1/18:1); 1-(9Z-octadecenoyl)-*rac*-glycerol, (MG 18:1(9Z)/0:0/0:0); 1,2,3-trihexadecanoyl-glycerol, (TG 16:0/16:0/16:0); 1,3-di-(9Z-octadecenoyl)-2-hexadecanoyl-glycerol, (TG 18:1/16:0/18:1); 1,2-distearoyl-*sn*-glycero-3-phospho-(1'-*rac*-glycerol), (PG 18:0/ 18:0); N-lauroyl-D-*erythro*-sphingosylphosphorylcholine, (SM d18:1/16:0); N-heptadecanoyl-D-*erythro*-sphingosine, Ceramide (d17:1/17:0); 1-heptadecanoyl-*rac*-glycerol, (MG 17:0); 1,2-diheptadecanoyl-*sn*-

glycero-3-phospho-(1'-*rac*-glycerol), PG(17:0/17:0); 1,2-diheptadecanoyl-*sn*-glycero-3-phosphocholine, (PC 17:0/17:0); 1,2-diheptadecanoyl-*sn*-glycero-3-phosphoethanolamine, (PE 17:0/17:0); 1-heptadecanoyl-2-hydroxy-*sn*-glycero-3-phosphocholine, (LPC 17:0); 1,2,3-triheptadecanoyl-glycerol, (TG 17:0/17:0/17:0).

3.2.2 Preparation of standard solutions and plasma samples

A standard mixture containing equal amounts of all authentic standard lipids was prepared in chloroform/methanol 1:1 (v/v) to reach a concentration of 0.5 mg/ml for each lipid, and stored at -30°C. Working standard mixtures were prepared freshly every day in IPA/methanol 1:1 (v/v) for immediate use. The working standard solutions at the calibration range were injected in the beginning and the end of sequence, for evaluation of instrumental performance throughout a long sample sequence. The phosphate-buffered saline (PBS) solution (pH 7.4) was prepared by dissolving sodium chloride (8.0 g), potassium chloride (0.2 g), potassium phosphate (0.2 g), and sodium phosphate (1.44 g) in 1 L of purified water. PBS and plasma samples were spiked with working standard solution while stirring at 500 rpm to prepare the required concentrations for the method development experiments. In order to validate the optimized SPME method in plasma, calibration standards and validation samples were prepared by spiking an appropriate amount of each lipid standard in plasma to reach a final concentration range between 500-8000 ng/mL (keeping the organic solvent concentration at approximately 1% methanol). After spiking, plasma samples were incubated at room temperature for one hour to ensure binding equilibrium occurred prior to extraction.

3.2.3 Preparation of C18-PAN 96-Blade coatings

For the high-throughput analysis of lipids, coated thin-film SPME blades were immersed into plasma samples using the manual Concept 96 unit (Professional Analytical System (PAS) Technology, Magdala, Germany). The TF-SPME blades were made in-house. For efficient immobilization of coating particles, the stainless steel surface was conditioned by sonication of blades in strong hydrochloric acid for approximately 60 min prior to the coating process. The blades were then rinsed thoroughly with nanopure water, dried in an oven for 30 min at 150 °C, then left to cool until they reached room temperature. The slurry of C18-PAN mixture was sprayed to immobilize the C18 particles on the surface of the stainless steel blades, followed by immediate thermal curing at 180 °C for 2 min. The identical coating-curing sequence was repeated 10 times in order to ensure uniform exposure and proper thickness of the C18-PAN coating on the surface of the blades. A comprehensive report of this procedure is discussed elsewhere.¹³⁶

3.2.4 Optimization of the SPME procedure

Time is one of the key factors in SPME procedure; the amount of analyte extracted increases as time of extraction elapses, until equilibrium between analyte and SPME coating is established. Therefore, extractions from a 200 ng/mL mixture of lipids in PBS (pH=7.1) were carried out with the use of C18-blades for 5, 10, 20, 30, 45, 60, 75, 90, 120 and 160 minutes to ensure sufficient time coverage for extraction equilibrium under agitation conditions. For plasma samples, extraction times were extended up to 600 min in order to outline the equilibrium profile of lipid species in such a complex matrix. For each time point, two replicates were considered. After the extraction process, desorption time profiles were constructed for 5, 10, 20, 30, 45, 60, 75, 90, 120, and 160 minutes to ensure desorption

equilibrium. Since most of the studied lipid classes are highly hydrophobic, the same SPME blades were desorbed for a second time in 1 mL of desorption solvent in order to evaluate the amount of analyte residue on the coating after the first desorption. Likewise, extraction recoveries were also compared for different desorption solutions using various ratios of water/organic solvents. All SPME coatings were pre-conditioned for 30 min in a mixture of methanol/water (1/1, v/v) prior to use in order to activate the silanol groups of the stationary phase. SPME blades were immersed into 1 mL of sample aliquots for 90 min extraction with 1000 rpm orbital shaking. Immediately after extraction, coatings were rinsed by dipping the blades in purified water for 10 s to remove any residuals of biological material from the coating surface. Afterwards, the coatings were agitated for 60 minutes in 1 ml IPA/methanol for proper desorption of lipids, and the resulting extract solutions were injected to the HPLC–ESI-MS/MS system for analysis.

3.2.5 LC-ESI-MS Operating Conditions

All samples were analyzed using a LC-MS/MS system consisting of a Shimadzu high-pressure liquid chromatography system (Shimadzu, Kyoto, Japan) operated with dual pumps (Shimadzu LC10ADvp), a system controller (SCL10Avp), and SCIEX API 4000 hybrid triple-quadrupole mass spectrometer with a Turbospray liquid interface (Applied Biosystems, CA, U.S.). The chromatographic system was equipped with apolyether ether ketone (PEEK) connection tubing consisting of a non-metallic injector unit and a 10- μ l PEEK sample loop; this was done to avoid systematic carryover due to the undesired interaction of lipids with metallic materials.

Data acquisition and processing were performed with the use of Analyst software (version 1.4.1). The instrument tuning was performed manually by infusion of individual lipid

solutions and scanning the ion mass of each lipid considering the ion adduct with highest intensities. The MS/MS analysis was performed in positive mode under multiple reaction monitoring (MRM) conditions; instrument settings are described in Table 3-1. MS conditions were optimized for curtain gas at 10, collision gas at 8 (arbitrary units), and 25 and 40 for ion source gases 1 and 2, respectively, with 5500V for ion spray voltage and 450°C temperature. A CTC PAL auto-injector from Leap Technologies (CTC Analytics, NC, U.S.) was used for injection of 10µl sample volumes into the LC–MS/MS system. Analytes were separated using an XBridge C18 3.5µm 2.1x150mm Column (Waters Corp, Milford, MA); mobile phase A consisted of water/acetonitrile (10:90) containing 0.1 % Acetic acid, while mobile phase B consisted of 100% isopropyl alcohol, with addition of 0.15 mM ammonium acetate for a flow rate of 300 µl/min. Optimal separation conditions were as follows: mobile B started at 10% and remained constant until minute 6, then increased to 60% until minute 8, followed by isocratic hold at 60% B until minute 18, then ramped back to 10% for one minute, followed by six further minutes of column re-equilibration, for a total run time of 25 minutes.

3.2.6 Data analysis and calculations

After data acquisition, the Quantitation Wizard feature of the Analyst software (version 1.4.1) was used for calibration of individual lipids using 1/x weighted linear regression. The instrument calibration curve was obtained daily from the standard working solution of lipids in desorption solution (single standard per concentration level, minimum of 6 levels to cover the entire linear range of the instrument). Weighted regression was found to perform better than simple linear regression by improving the accuracy of low concentration standards. Extraction efficiency (or absolute recovery) was calculated for each lipid standard by

percentage ratio calculation of the extracted amount (ng) to the total spiked amount of analyte (ng). The instrumental calibration curve was used to determine the extraction efficiency (or absolute recovery) of the SPME method. The experimentally determined concentration was divided by the nominal spiked concentration (ng/mL), and the obtained result was multiplied by 100% in order to calculate the relative recovery percentage (accuracy). The SPME calibration of lipids in plasma was performed for each standard in duplicate for a minimum of six concentration levels across the entire linear range. The unknown sample concentrations were calculated from the equation, $y = mx + b$, as determined by weighted ($1/x$) linear regression of the standard line.

3.3 Results and Discussion

3.3.1 Chromatographic Method Validation

Blood plasma is a complicated biological mixture containing a variety of lipids including phospholipids, sphingolipids, glycerolipids, etc., which vary in fatty acid composition and glycerol backbone occupation. In order to establish an SPME method for sample preparation and clean-up, an integrated LC-MS based analytical platform relying on gradient elution and MS/MS fragmentation in this study.

The LC/MS method was developed and assessed using lipid standards aiming to provide maximum coverage for lipid classes and sub-classes. In this study, the MRM approach allowed absolute quantification of endogenous molecular lipids; for this methodology, method quality assurance by spiking an appropriate representative of each lipid (sub) class is indispensable.²⁵⁴ Systematic studies of instrument response determined that ionization efficiency was predominantly dependent on the polar head group of each lipid category; whilst length and structure of fatty acid moieties played minor roles in ionization efficiency.^{52,74} In order to evaluate such a possibility, two sets of lipid standards, including one set of synthetic lipids with heptadecanoyl (17:0)n FA moieties and another set containing most common endogenous lipid species with even FA moieties, were simultaneously employed throughout the SPME method validation procedure. None of the odd-lipid (those that have odd number of carbon in FA chains) class selective standards were detectable in the total extract of plasma samples. It is also noteworthy that these standards are commercially available, and since they are not isotopically labeled, their precursor and fragment peaks produce natural isotopic profiles, identical to endogenous lipids. A detailed list of all lipid standards including odd and even groups is represented in the Table 3-1. The solutions of

both lipid sets in different concentrations were injected to the LC/MSMS system and the dynamic range of instrumental calibration was determined (data shown in Table 3-2).

Table 3-1 Summary of LC-MS/MS parameters for analysis of lipids

Lipid	Q1	Q3	Ion adduct	DP (V)	EP (V)	CE (V)	CXP (v)	LOD (ng/ml)	LOQ (ng/ml)
LPC 17	510.2	184.1	[M+H]	110	8	37	18	10	10
LPC (16:0)	496.2	184.1							
PE (17:0/17:0)	720.6	579.5	[M+H]	80	10	28	20	5	10
PE (16:0/18:2)	716.6	575.6							
SM (d18:1/17:0)	647.4	184.1	[M+H]	88	10	30	15	1	5
SM (d18:1/16:0)	703.7	184.1							
MG (17:0)	362.4	327.2	[M+H]	100	9	15	10	15	25
MG (18:1)	374.5	339.3	[M+NH ₄]						
TG(17:0/17:0/17:0)	862.4	579.5	[M+NH ₄]	95	10	35	20	10	25
TG(18:1/16:0/18:1)	876.7	577.6							
PC 17:0/17:0)	762.7	184.1	[M+H]	90	10	40	18	5	10
PC (14:0/18:1)	734.9	184.1							
PG (17:0/17:0)	773.5	194.9	[M+H]	100	10	45	20	5	10
PG (18:0/18:0)	801.7	194.9							
CE (d18:1/17:0)	552.6	264.1	[M+H]	70	10	35	10	1	5
CE (d18:1/18:0)	566.6	264.1							

*DP=Declustering potential, FP=Focusing potential, EP=Entrance potential, CE=Collision energy, and CXP=Collision cell exit potential

Choosing an optimal mobile phase composition is one of the most crucial bottlenecks of LC-MS method development for lipid analysis. The optimal elution system must contain proper buffer additives and ionic strength in order to facilitate efficient electrospray ionization, while also providing proper peak shape and retention. A desired scan spectrum presenting only simple adducts of lipids with high intensity was achieved through tuning of the ion source settings in the presence of mobile phase. However, the ionization of different lipid classes was observed to be contrarily dependent on the mobile phase buffer additives. For

example, certain lipid classes, such as glycerolipids, mainly form $[M+NH_4]^+$ adducts; in this sense, the mobile phase must supply sufficient ammonium ion to facilitate formation of this adduct..

Conversely, it was observed that the presence of ammonium salt caused buffer-induced ionization suppression and peak deformation for some phospholipids. As phospholipids contain at least one acidic phosphate group, the mobile phase must be slightly acidic to force them into a protonated state, as this improves chromatographic peak shape; since they mainly form $[M+H]^+$, the acidic mobile phase must also supply the ESI source with sufficient hydrogen ions. In contrast, the acidified solvent works oppositely for glycerolipids, causing peak tailing and mainly peak deformation for most glycerol lipids such as TGs and MGs. In general, PC, PE, and SM species are retained as broad peaks when the standard eluting system of acetonitrile/water (9:1) in the absence of acid (pH 6.7 by ammonia) is used, whilst TG shows a sharp Gaussian peak under such circumstances. On the other hand, when the solvent contained 0.2% formic acid (pH 4.8), the PC, PE and SM tailings were corrected although the peak related to TG was extensively broadened. This contrasting behavior is expected due to the positively charged head group of phospholipid compounds. Therefore, the acidic solvent reduces the undesired interaction between the mobile phase and the positively charged head group of PC, PE, and SM species. Figure 3-1 illustrates the effect of buffer additives on these two major lipid classes.

In order to overcome such a conflict, adopting a proper gradient method and best balance of buffer additives would allow us to find the ionization behavior of lipid classes in formation of ion adducts with highest intensities and meanwhile to produce good resolution for all lipid

species of interest. Figure 3-2 indicates the optimum gradient method as well as the final obtained chromatogram.

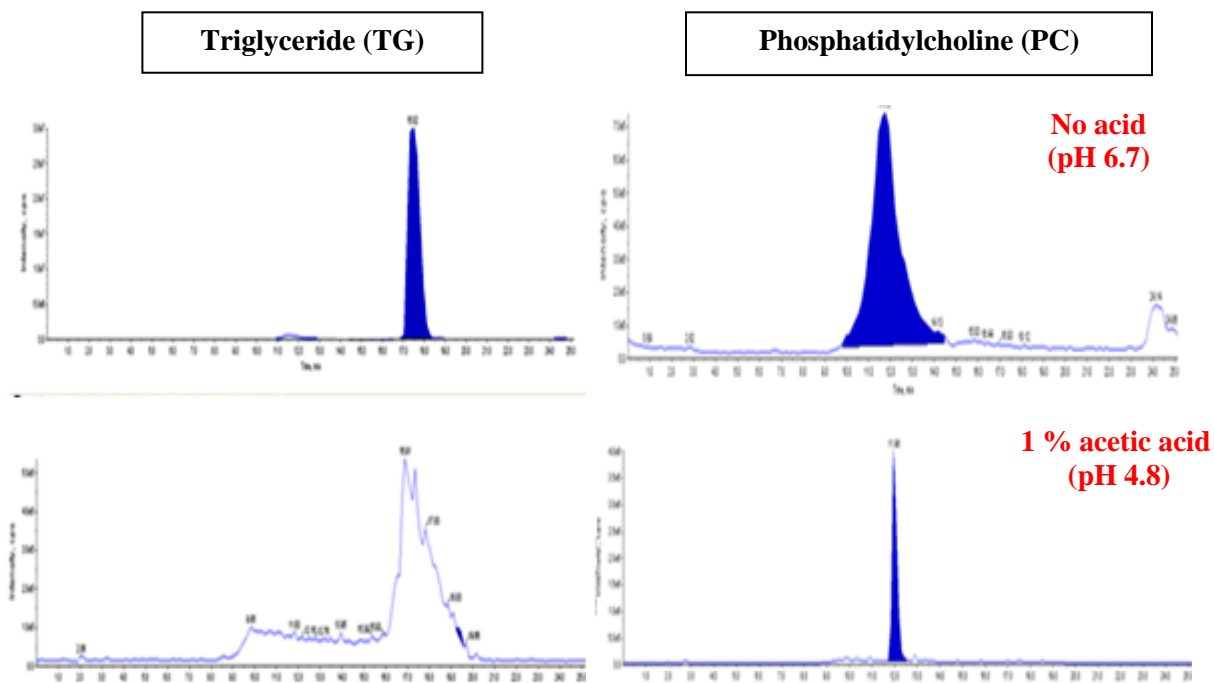


Figure 3-1 Extracted ion chromatograms (XIC) of PC and TG using acidic buffer in elution

As part of this series of adjustments, various LC mobile phases were examined; an ideal elution was established when 10mM ammonium acetate was added to mobile phase A (water/acetonitrile) and 0.1% formic acid added to mobile phase B (IPA). Accordingly, the final gradient method was programmed in a way that mobile phase B reached 70% of total elution (maximum acid) in the region where phospholipids are retained, followed by a ramp back to only 10% (minimum acid) in the region where glycerol lipids such as TGs and MGs are retained.

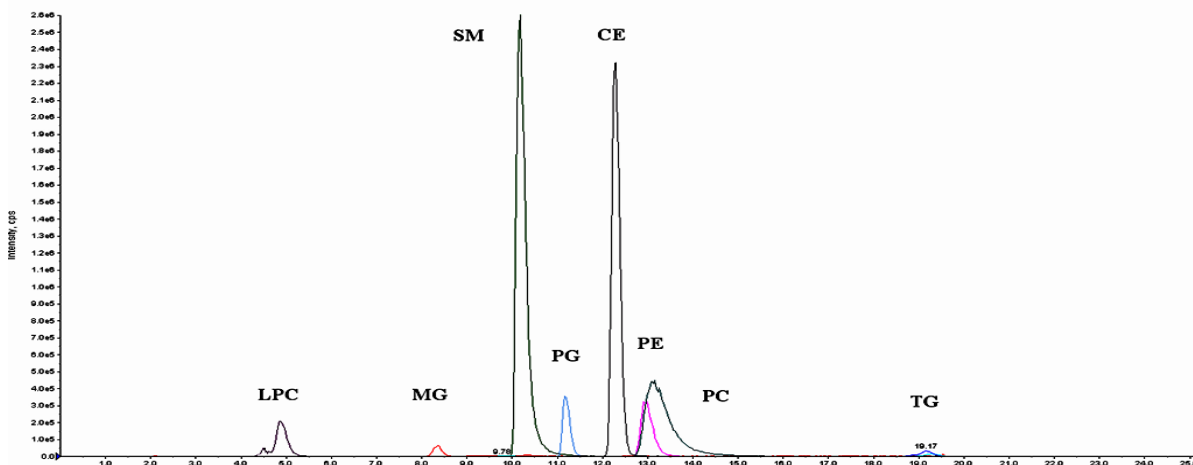


Figure 3-2 Example of extracted ion chromatograms (XIC) for 3 mg/mL odd lipid standard in blood plasma; mobile phase A consist of ACN/ W (90:10) Containing 0.1 % Acetic acid and mobile phase B consist of IPA 100% 0.15 mM amonium acetate

Our final validated LC/MS method provides a complete separation of multiple categories of lipids within a single run and in less than 18 min, while the adduct preference accommodates a high signal intensity. Figure 3-2 represents the optimized MSMS chromatogram of lipid standards in positive ion mode. Table 3-2 represents the instrumental validation of lipid standards in positive ion mode

Table 3-2 Automated LC-MS/MS method validation and instrumental robustness results

Lipid	log p	water solubility (mg/mL)	RT (min)	LOD (ng/ml)	LOQ	Dynamic range	Intra-day precision %	Inter-day precision %
LPC	2.38	2.75e ⁻⁰⁴	4.5	5	10	10-1000	1	7
PE	8.97	8.97e ⁻⁰⁵	13.5	1	10	10-700	1	2
SM	5.41	3.23e ⁻⁰⁵	10	1	5	5-500	1	12
MG	5.32	1.51e ⁻⁰³	8.5	15	25	25-1000	7	11
TG	10.74	7.70e ⁻⁰⁶	18	10	15	15-800	11	8
PC	6.8	2.40e ⁻⁰⁵	11.5	5	10	10-500	4	3
PG	8	1.090E ⁻⁰⁴	11	5	10	10-1000	3	5
CE	9	2.120E ⁻⁰⁵	12.5	1	5	5-1000	4	5

3.3.2 Extraction phase: Comparison of C18 fiber and thin film

For the validated extraction method of fatty acids represented in Chapter 2, commercial rod fibers were selected that are suitable for in-vivo applications. However, in order to extend the analytical method for the whole lipid spectrum, evaluation of an appropriate extraction phase with relatively high affinity is preliminary in the method development procedure. Therefore, due to the hydrophobic nature of most lipid species, polymeric C18 particles were used as a primary extraction phase in two different geometries: the commercial rod fiber (Supelco, Bellefonte PA, USA) and the in-house thin film coated blades. In addition, previous research conducted in our group has indicated that the “hydrophilic lipophilic balanced” (HLB) particles are efficient for the extraction of hydrophobic compounds ^{142,155,159,198,255,256}. Accordingly, HLB particles (60 nm, average particle diameter) were similarly used to prepare the thin-film coated blades. Extraction of a lipid mixture in PBS (300ng) demonstrates the relative affinity of target compounds.

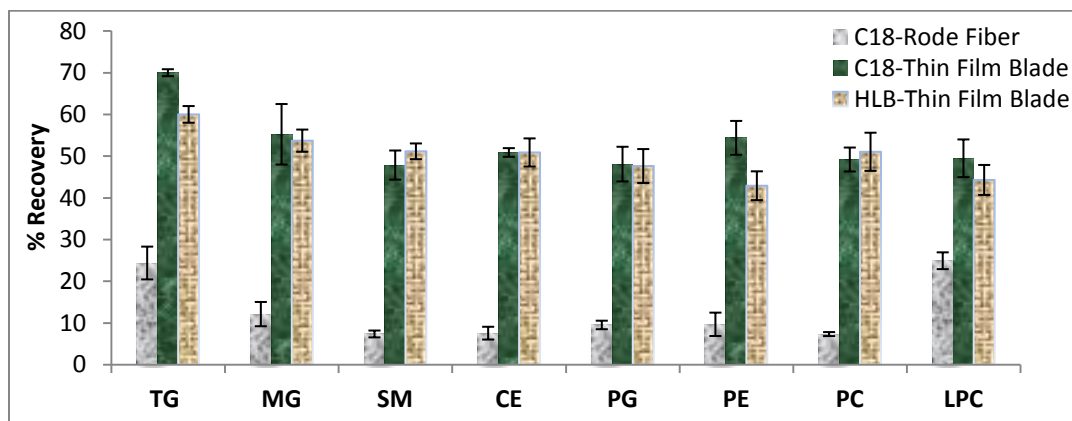


Figure 3-3 Evaluation of different SPME coatings for the extraction of lipids from PBS; comparison of coatings (C18 vs. HLB) and geometries (rod fiber vs. Thin-Film)

Based on the obtained results, although both HLB and C18 extraction phases have shown nearly comparable affinities for all lipids, C18 is a better candidate for some lipid categories such as TGs (logP 10.74) due to their more hydrophobic characteristics. With respect to the

configuration, all analytes were extracted more efficiently with thin film phases than with cylindrical fibers. The likely reason is the difference in surface area and volume, which is about 10 times greater with the films than with the fibers (Figure 3-3). Therefore, changing the geometry of the coatings and using C18 particles could achieve a significant improvement to the method sensitivity. In addition the new thin-film configuration could be applied in a 96-well plate to perform high throughput analysis of lipids from complex biological matrices.

3.3.3 Optimization of extraction and desorption conditions

Desorption: various solvents and solvent mixtures were evaluated in order to optimize desorption with minimum carryover, 1ml of lipid mixture solution in PBS buffer (n=3) was extracted for 90 min and desorbed into 1ml solution.

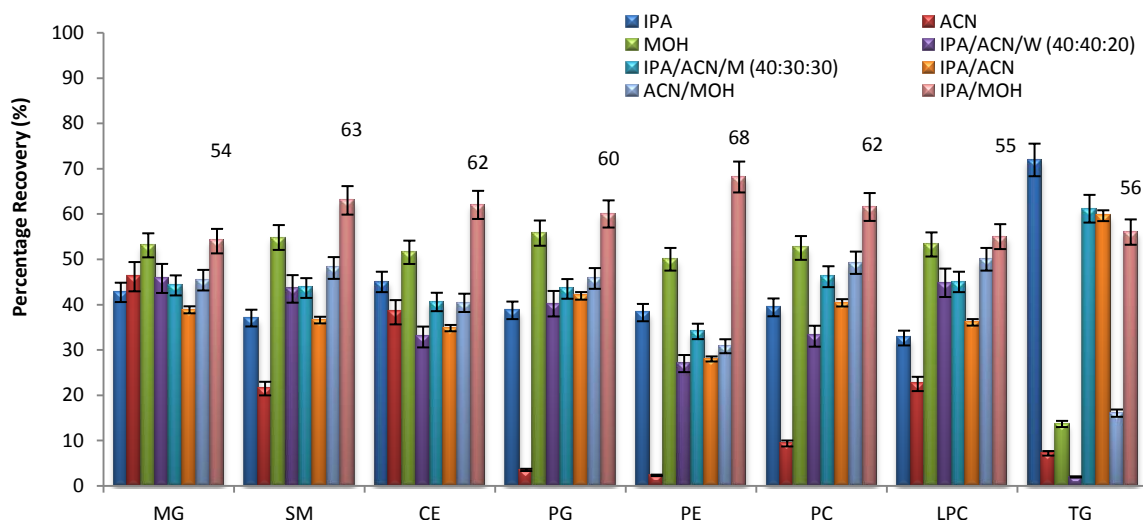


Figure 3-4 Evaluation of desorption solvent for C18-PAN coatings for equilibrium extraction from PBS buffer solutions containing 200 ng/mL lipids

Acetonitrile provided poor efficiency in desorbing of most lipids, while the solution containing water and ACN resulted in incomplete desorption of more hydrophobic lipids such as TG, PC, and PE from SPME coatings, resulting in higher carryover (4-6%) on the

fiber. A 50:50 ratio of MOH/IPA was selected as the desorption solvent, providing efficient desorption of analytes with negligible carryover ($\leq 1\%$). Figure 3-4 summarizes the desorption recovery of individual lipids using various desorption solutions. Desorption time profiles were also prepared by desorbing the coatings into MOH/IPA for different time lengths. As the Figure 3-5 indicates, 60 min is the optimum time for highest desorption recovery with least carryover on the coatings.

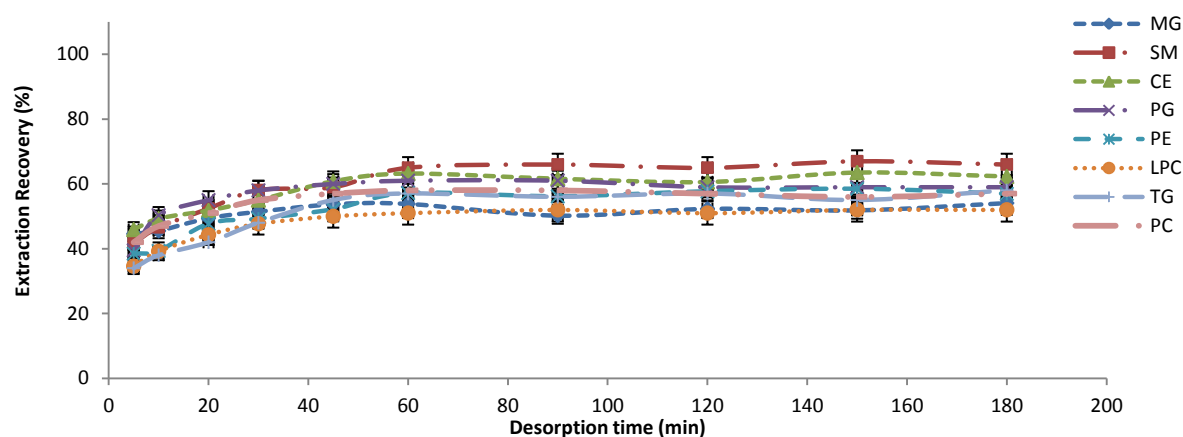


Figure 3-5 Evaluation of the optimized desorption time profile in 1ml MOH/IPA desorption solution

Extraction: An extended extraction time would allow the analytes to reach the equilibrium stage improving of SPME potential sensitivity. Hence, optimization of extraction time is important in the primary stages of SPME method development. Equilibration times were determined by generating a time profile for extraction of each lipid species spiked in PBS and plasma individually. Compared with pre-equilibrium SPME, equilibrium sampling offers better sensitivity and reproducibility, and both free and total concentrations of analytes are easily determined simultaneously. Conversely, increases in sampling time and amount of extracted analytes may result in non-negligible depletion and disturbance to the system under study, particularly when thin film SPME is utilized.

For extraction from plasma, a very long extraction time frame was selected to ensure that equilibrium was achieved for all lipid species. The inset graph obtained from PBS indicates an optimum extraction time of 90 min. Similarly, in plasma, the required time for all analyte lipids to reach the initial equilibration was determined to be also 90 min, in which the extraction recovery remains constant up to 180 min, as shown in Figure 3-6. When the extraction times were extended more than 180 min, a second plateau was observed for all lipid species. Coating biocompatibility was tested several times, and has been reported previously elsewhere;^{138,144} hence, it is anticipated that this effect is only visible for longer lengths of contact between the coating and sample in cases where the analyte is hydrophobic. The excessive extraction time was measured to investigate any possible effects of complexity of plasma matrix on the diffusion of analytes to the fiber. The aforementioned phenomenon can be likely explained by possible changes in lipoprotein composition of plasma as a result of degradation in room temperature, which hypothetically results in constant leakage of lipids to the plasma matrix. However, no study was performed to further investigate the nature of changes, because such a long time span would not be relevant in practice.

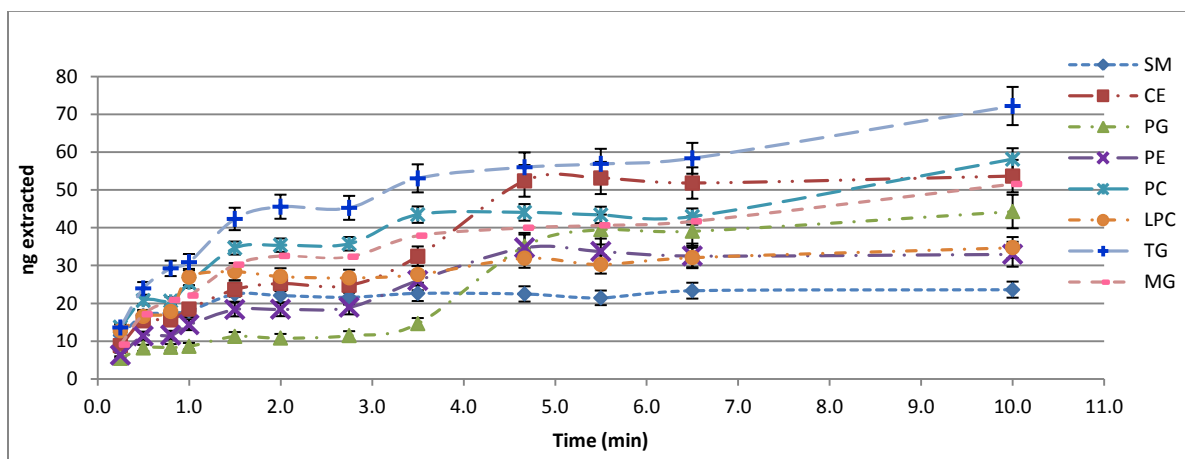


Figure 3-6 Extraction time profile obtained for lipid standards using Thin-Film C18 coating. Extraction conditions: (3500ng/ml) standards of odd lipids spiked in human plasma

It is important to note that at equilibrium, no further extraction of the analyte is expected and thus the initial plateau may reflect the presence of intact plasma proteins, and the delayed extraction increase some uncharacterized degradation process. As a result, 90 min was selected as the optimum extraction time.

3.3.4 Mass balance and distribution; Investigation of suitability of PBS buffer for free concentration determination

Physiological buffer (PBS) is commonly used as a protein-free environment that can provide information about extraction performance. However, for hydrophobic species, PBS might not be desirable due to the lack of solubility and the possibility of nonspecific bindings of these compounds. In order to verify if a single SPME extraction step is sufficient to determine lipid concentration, and to investigate if PBS can serve as an adequate surrogate matrix for such applications, a mass balance experiment was performed. Mass balances were established for the first and second SPME measurements from PBS solution, as well as the residual fractions adsorbed to pipette tips and test vessels due to secondary interactions of lipids with plasticwares.

For less volatile compounds including lipids, the effect of headspace partitioning was shown to be insignificant, since their vapor pressures are typically very low; ²⁵⁷ accordingly, the headspace portion was not considered in further mass balance evaluations. A mixture solution of standard lipids in PBS was prepared to make a 100 ng/ml mixture. Using plastic pipette tips, 1 ml of this solution was placed individually in each 96-well (n=4 replicates) and submitted to the first SPME procedure for 90 min. The used pipette tip was also rinsed using 1ml desorption solution for 5 push-pull cycles. Subsequently, the same extracted PBS solutions were re-extracted with a new set of preconditioned SPME coatings for another 90

min and desorbed in 1ml fresh desorption solution. Finally, the PBS were carefully discarded, and the used wells were rinsed by agitating 1ml fresh desorption solution for 30 min. All the obtained solutions were injected to the LC-MS/MS system individually, and amounts calculated for each fraction. The mass balance recovered percentages are summarized Table 3-3

Partitioning of lipids in PBS solution indicates a total mass balance of 66–82%. The mass balance is obtained when the sum total of analyte amounts distributed in the individual phases is equal to the initial amount of the analyte in the system. When the total extraction recovery is less than 80%, it can be assumed that the mass balance for those lipids is not obtained and thereby the amount of analyte loss is significant enough to potentially affect quantification results.^{153,257–261}

Table 3-3 Evaluation of Mass balance and total absolute recovery (%) from PBS solution containing 200ng lipid mixture using SPME extraction under optimized conditions; the total extraction recovery is compared to the recovery percentage reported in the literature

	1st Ex	2nd Ex	96-well	pipette	Total	Folch ₂₆₂	Folch ₁₀₃	BUME ₁₀₃	Matyash ₂₆₂	SPE-Ostro FT ₂₆₂	SPE-Ostro E ₂₆₂
SM	62±3	8±2	12±3	ND	82 ± 8	101±5	101±5	97±3	-	-	-
CE	63±6	3±1	10±3	ND	76 ±10	91±3	91±3	92±4	98±2	-	-
PG	59±4	4±1	11±3	ND	74 ±8	74±4	84±1	94±6	101±6	82 ± 3	2 ± 4
PE	54±6	4±1	12±3	ND	70 ± 10	134 ± 14	102±4	97±2	91±5	105 ± 3	11 ±1
PC	57±5	6±2	10±3	ND	68 ± 10	76±4	92±3	97±3	92±2	0	105 ± 10
LPC	51±8	7±1	14±3	ND	66 ± 11	85±3	-	88±3	92±2	2 ± 0.4	102±12
MG	53±6	7±2	12±2	ND	72±10	-	-	-	-	-	-
TG	54±10	9±3	14±2	ND	67 ± 10	103±8	-	-	86 ±7	47 ± 8	25 ± 6

It is also presumed that due to the initial “overspiking”, the standard lipids may aggregate upon addition to PBS and rapidly form vesicular structures of concentric lamella that

sediment to the plasticware.²⁶³ In the PBS solution, aggregation happens due to the absence of biologic micellar components such as liposomes and lipoproteins that assist the lipid dispersion throughout the bulk of fluid. Therefore, a secondary interaction may lead to nonspecific binding and adsorption losses of lipids through their attachment onto the surface of plastic wells. This will consequently reduce the available proportion of lipids for SPME and cause lower extraction recoveries from PBS. To prevent the undesirable effect of adsorption loss in our quantitative evaluation process, further calculations and measurements were performed directly from spiked plasma.

Based on the principles of SPME theory, the amount extracted from a matrix-free environment is equal to the total amount due to the absence of binding components. In this regard, the reported extraction recoveries of standard lipids from PBS and plasma by various extraction techniques are collected from the literature and compared against the results of total recoveries by SPME (Table 3-3). All the presented classical techniques including LLE and SPE have been already described in sections 1.5.1 and 1.5.2 and their fundamental differences are discussed in detail. The percent recovery of SPE using the commercial Ostro Flow Through cartridges was reported for zero recovery of PC, while the Ostro Eluate Plate has been shown to work well for this compound. A comparison of extraction recovery values for the Folch method reveals lower percentage recoveries and significant variations in experimental data for some cases. Generally, extraction recoveries for SPME have been found to be lower than those of other techniques because SPME is non-exhaustive by nature, while all others are exhaustive methods. It is noteworthy to mention that in conventional methods, such as LLE, regardless of the secondary interaction, all analytes, including the proportion attached to the labware as well as the bound/free portion, are washed out during

the adsorption step; thus, secondary interaction of analytes with used equipments do not affect the quantitative results. Conversely, in addition to the use of large volumes of toxic organic solvents in these laborious processes, none of the classical techniques provide fundamental information about analyte distribution and bound/free fractions. As an alternative, the SPME approach is sensitive to all changes and points of analyte loss in a sample matrix. But when the method is properly optimized and the experimental conditions are well controlled this shortcoming could be dispelled. In addition, SPME provides detailed information on free and total concentrations of analytes in complex and dynamic systems; in classical approaches, this achievement is not an option.

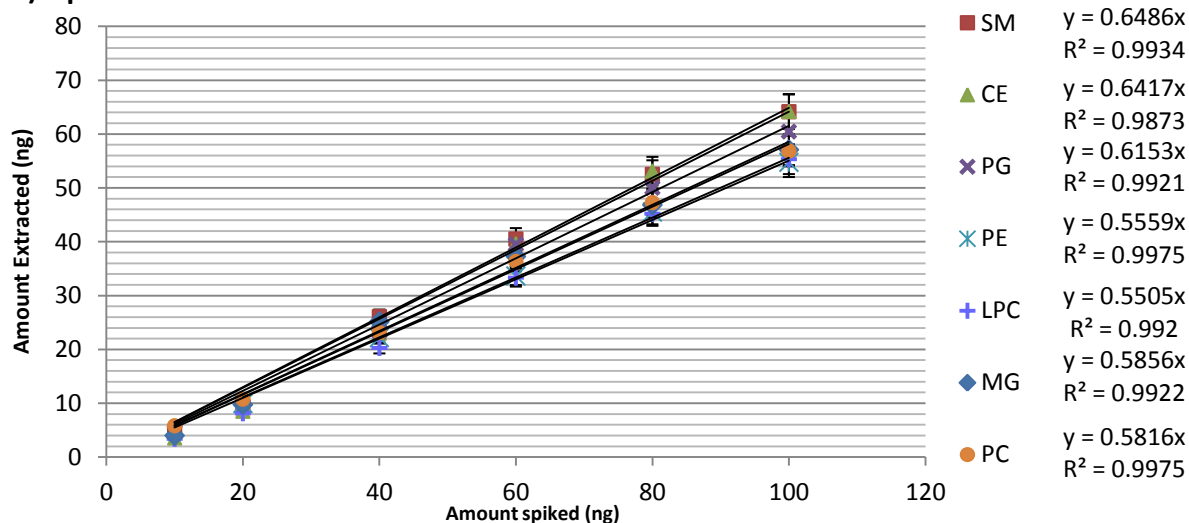
3.3.5 Matrix free calibration

Experimentally, matrix-free calibration is performed in a physiological buffer because it mimics the ionic strength and pH of the biological fluid, while allowing free analyte concentrations to be determined due to free and total concentrations being equal in the absence of binding components. In order to determine if adsorption loss influences the measurement of lipids in PBS, a matrix-free calibration was performed by extracting the lipids at different concentrations from PBS solutions and the obtained linear regression (R^2) and fiber constant ($K_{fs}V_f$) inspected. This procedure is necessary to determine the product of $K_{fs}V_f$ as the slope of the linear regression line by performing equilibrium extractions from a set of standard solutions with known analyte concentrations prepared in an appropriate matrix.

Multiple point matrix-free calibration was obtained by analyzing PBS solutions at both low and high concentration ranges (10-100 and 100-500 ng/mL; n= 3 replicates in each point) with the use of the optimized 96-blades SPME system. For the calibration curves in both low

and high concentration ranges, the linearity was verified by achieving regressions $R^2 \geq 0.98$. This indicates that although nonspecific binding occurs upon addition of lipids to PBS, the amount of adsorption loss is proportional to the analyte concentration.

a) Lipids Matrix Free Calibration-Low Concentrations



b) Lipids Matrix Free Calibration-High Concentrations

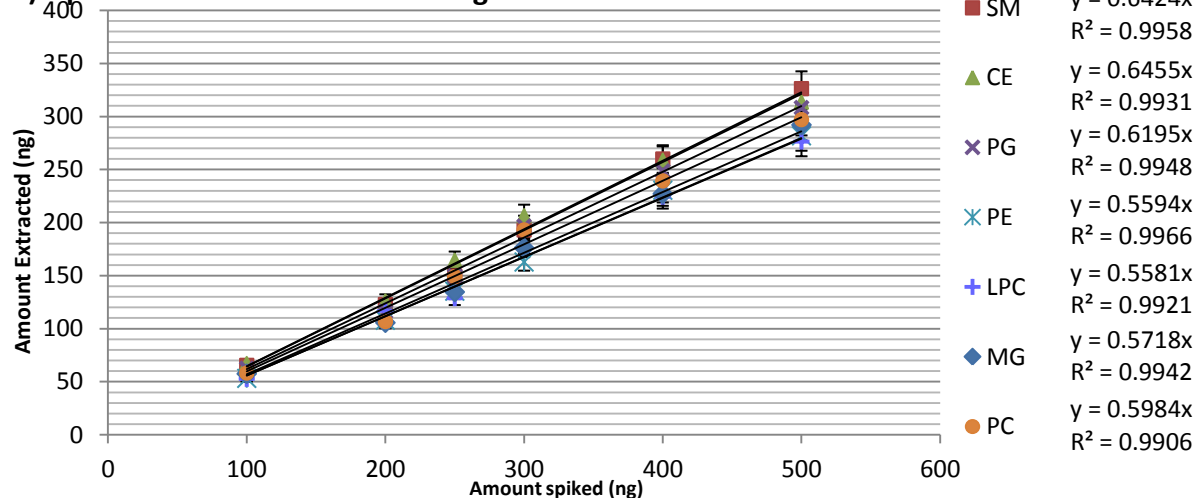


Figure 3-7 Example of matrix-free calibration curves obtained in PBS in a) low and b) high concentration ranges; the slope of calibration as well as linearity regression of each lipid are displayed beside the plots

This result, in turn, determines that adsorption to the plastic wells plays a minor role in our experiment and does not disturb the calculation of partition coefficients between the coating

and aqueous phase. Regardless, the use of correction factor was considered in the calculations when constructing the matrix free calibration plot and acceptable linearity was achieved. However, the adsorption loss of lipids was noted to occur when extractions were performed in unsupported aqueous media such as PBS which does not contain proteins. This phenomenon however is not expected where lipids can be immersed and transported by large biologic assemblies such as liposomes and lipoproteins of plasma and cells. In these biological environments, the availability and interaction of lipids to the bulk fluid and plastic surface will be restricted when the matrix is subjected to extraction.^{263,264} In conclusion, matrix-free calibrations (performed in PBS) were corrected according to the mass balance percentage recovery, and further analytical assessments as well as matrix-matched calibrations were performed directly in plasma to prevent any potential pitfalls and errors. Examples of calibration curves of lipids in low and high concentrations extracted from PBS buffer are shown in Figure 3-7

3.3.6 Evaluation of matrix effects

The quantification of lipids from complex biological environments is challenging due to the possibility of matrix effect encounter, especially for the direct infusion approaches. However, this concept may mislead scientists if the importance of selecting appropriate sample preparation and extraction techniques is overlooked. Therefore, if proper conditions that provide clean extract solution for direct infusion to ESI source are employed, the ionization suppression/enhancement could be minimized or completely avoided. In lipid analysis, matrix effects may be particularly serious, because species (or classes) with minor abundance could be easily masked in the presence of more abundant species (or classes). Conversely, application of appropriate chromatographic approaches may mitigate matrix effects by

providing efficient separation of discrete lipid categories, since they retain in different time domains due to their structural difference. However, chromatography still fails to resolve the lipid species of the same sub-categories when their co-elution causes saturation of ion source. This is particularly significant for phospholipids that belong to discrete sub-categories. For instance, ubiquitous PCs or PEs may co-elute with less abundant isobaric PGs, with competition for ionization causing signal suppression for PGs.^{107,230,239,265,266} Previous research showed that SPME can address such critical concerns in LC–MS approaches for the analysis of drugs and metabolites from biological matrices.^{146,149,158,174,198,203,255,267–270} The detailed procedure for calculation of absolute matrix effect is already discussed in section 2.3.4 and 2.3.5. In this study, blank plasma extracts were spiked with low and high concentrations (50 and 500 ng/mL) and peak areas were compared to those of pure standards at the same concentration. Table 3-4 summarizes the observed absolute matrix effect for both concentration levels for all nine compounds. As the results indicate, no significant matrix effects were determined with the use of C18 coatings for all lipids, both in low and high concentration ranges. This indicates the effectiveness of a selective extraction mechanism and the superiority of the SPME extraction technique in avoiding matrix effects.

A “sample extract dilution” experiment was also performed following the same detail procedure described in section 2.2.5 in order to ensure the absence of matrix effect. Briefly, plots of normalized peak areas (peak area multiplied by dilution factor) were constructed against the corresponding dilution factor for each analyte under study. If no matrix effect were present, the normalized response was similar for all dilution factors (within the experimental error). Figure 3-8 illustrates a comparison of maximum dilutions of sample extracts obtained from SPME; as can be seen, no matrix effect could be observed. This could

be explained firstly as a result of the biocompatibility of the coating, which prevents fouling of the coating with proteins and other macromolecules, consequently decreasing the chance of ion suppression/enhancement of the analytes by matrix interferences. Secondly, due to the non-exhaustive nature of extraction, only a small proportion of whole lipid quantity is extracted by SPME and as such, unlike exhaustive extraction approaches such as LLE and SPE, no extreme concentration is introduced to the ESI source. Lastly, the washing step after extraction is another efficient factor in successful cleaning of interfering compounds from coatings, preventing their transfer to the final extracts.

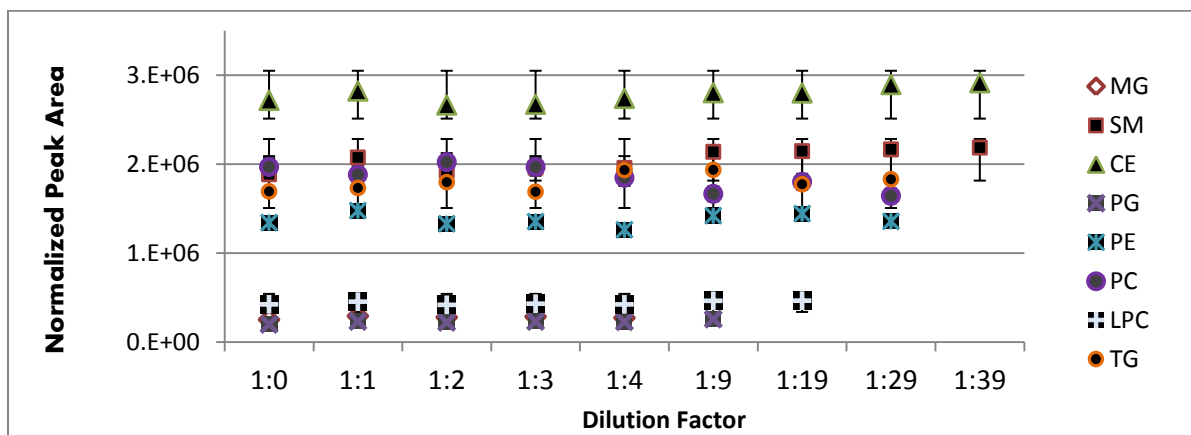


Figure 3-8 Matrix effect of SPME method using the sample extract dilution method; for some lipids signal was not detected in higher dilution levels. No dilution was required for SPME extracts for any of the studied lipids.

In addition, as for all analytical methods, optimizations for effective chromatographic separation as well as performance of standard addition calibration are two auxiliary approaches that can be applied to compensate for any possible matrix effects. No ion suppression/enhancement was observed when extracting lipids by the optimized SPME-LC system. A comparison of the results obtained for the two independent matrix effect experiments confirms the reliability of the obtained quantitative results for all cases.

Table 3-4 Evaluation of matrix effect and ionization suppression in two different concentration levels

		MG	SM	CE	PG	PE	PC	LPC	TG
ME %	low conc (50ng/ml)	102%	85%	86%	89%	87%	98%	94%	112%
	High conc (50ng/ml)	94%	104%	100%	91%	107%	101%	104%	88%
IS %	low conc (50ng/ml)	-2%	15%	14%	11%	13%	2%	6%	-12%
	High conc (50ng/ml)	6%	-4%	0%	9%	-7%	-1%	-4%	12%

3.3.7 Evaluation of non-depletive extraction recovery by sequential SPME extractions

In order to investigate the non-depletive extraction condition with thin-film, and to determine whether a single extraction is suitable to quantify the amount of lipids in biological systems, further investigations were required. Therefore, successive SPME extraction was performed in human plasma to inspect depletion and identify the extraction response in a real sample environment, where all the binding components and complex molecular assemblies exist.

A series of sequential extractions were performed from the same spiked plasma using fresh preconditioned SPME coatings in each step. Spiked plasma samples were prepared at a low quality control (QC) concentration. A row of preconditioned C18 blades were immersed in 1ml spiked plasma (n=5 replicates), and extractions performed for 90 min. After extraction, the blades were transferred to a dry and clean 96-plate containing IPA:MOH (1:1), and desorption was performed for 60 min. A new row of preconditioned C18 blades were then placed in the same plasma and agitated for another 90 min, followed by desorption in a fresh set of solutions for 60 min. This sequence was repeated 6 times (6×90min extraction from the same 1 ml plasma). This way, the measured amounts of lipids in each step must remain constant if the extraction is non-depletive; if extraction concentrations drop, this would reflect a situation in the bio-assay where plasma is depleting the analytes.

For this purpose, extracted amounts in each step were calculated for the spiked lipids as well as natural non-spiked lipids. For instance, for measurements of phosphatidylcholine, an odd non-endogenous lipid, standard PC (17:0, 17:0) was spiked to plasma, and extracted amounts were monitored in each step for 6 time sequential extractions. Meanwhile, PC (14:0/18:0) and PC (18:0/18:0), abundant phospholipids existing naturally in plasma, were simultaneously monitored at each extraction step. This approach was similarly employed for at least one representative of each lipid class and sub-class based on their standard availability. The results are shown in Figure 3-9.

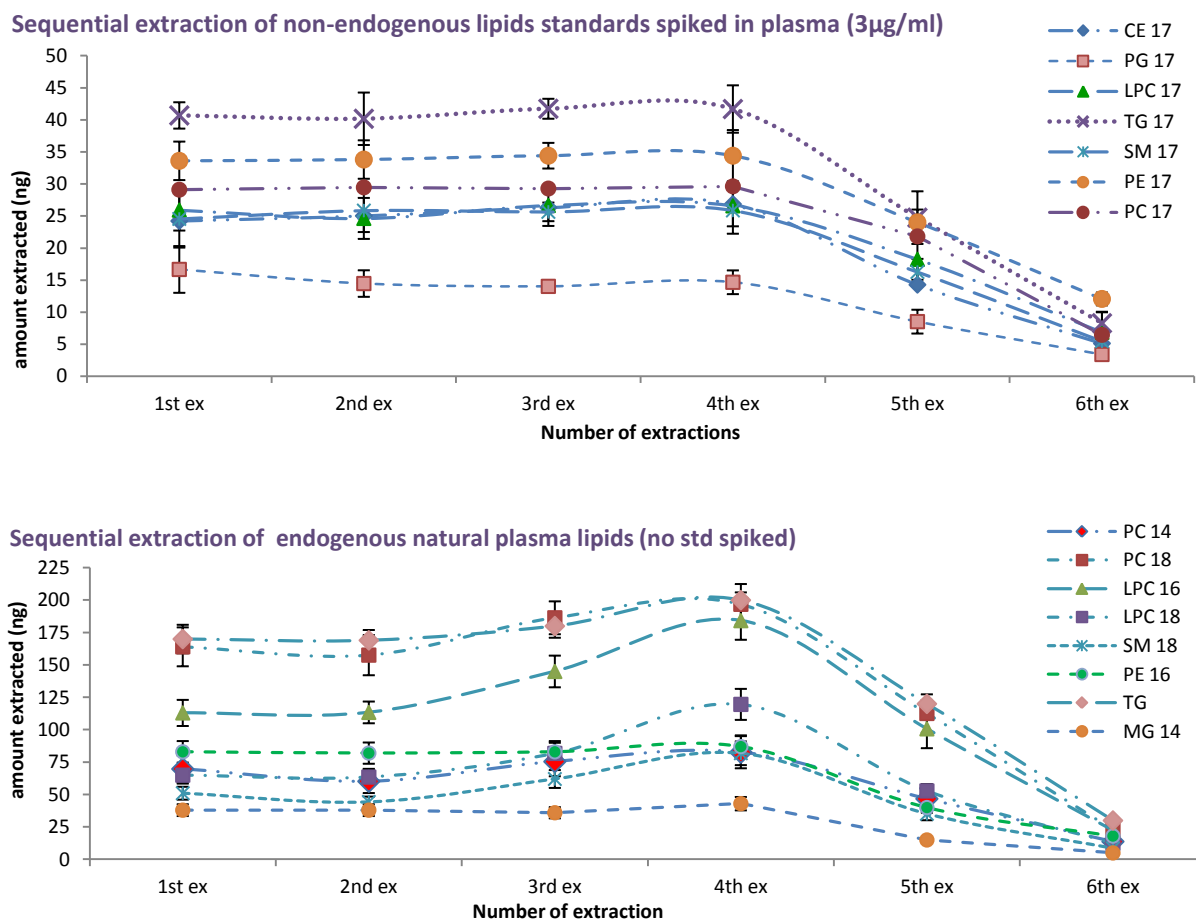


Figure 3-9 Measured concentrations (n = 3) of consecutive SPME measurements for a) spiked odd lipid standards and b) natural non-spiked lipids. The extraction uptake was monitored for the 1st, 2nd, 3rd, 4th, 5th and 6th successive extractions.

Considering the vast distribution of lipids in biological macro-structures, a valid analytical method must provide accurate quantitative measurement of both, total and free concentration of the analytes through a non-depletive extraction condition where the system equilibrium is not disturbed, while the integrity of lipoproteins and liposomes remains intact. The suggested SPME method provides a maximum percentage recovery of 1% for all lipid species from plasma, which is sufficient for sensitive detection while satisfying the non-depletive condition. Based on the obtained graphs (Figure 3-9), depletion of both natural and odd lipids for a single SPME measurement is below 1%, which is considered negligible.

Depletion was only observed after 4 successive extractions for both lipid groups, bearing in mind that each extraction step was performed for 90 minutes. Spiked odd lipids (17:0) demonstrated constant recovery for the first four SPME measurements, followed by a sudden significant drop after the 5th extraction; in the 6th measurement, the extracted amount reached below method sensitivity. It is important to note, that failure to comply with the non-depletive condition after 4 subsequent extractions for natural non-spiked lipids is observed after an increase in measured concentrations. The extraction of lipids by the thin film C18 coating in a single step extraction is too small to cause depletion; accordingly, the conditions of negligible depletion SPME (nd-SPME) are ensured.^{271,272} Therefore, equilibrium SPME coupled to external calibration was chosen for the quantitative analysis of free and total lipid concentrations in plasma. Previous reports prove that multiple extractions from one sample vial may result in statistically significant analyte depletion.¹⁴⁵ However, total extraction recovery less than 1% in a single step implicates that analyte-sorbent partition coefficient is very small and therefore the extraction condition can be considered negligible.

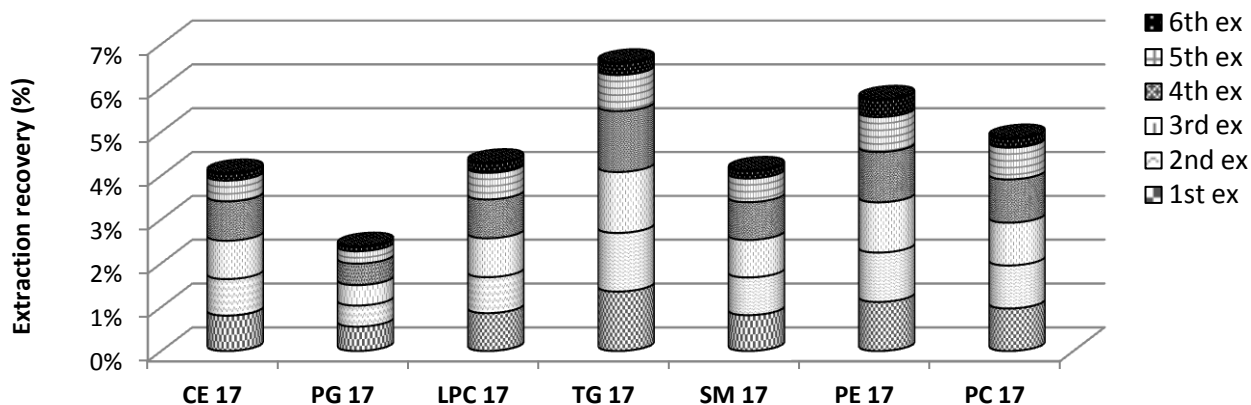


Figure 3-10 Extraction recovery after 6 sequential extractions from spiked plasma (3000ng)

Figure 3-10 illustrates the maximum extraction recovery achieved after six successive extractions from plasma samples, with extraction duration of 90 min at each step. In the highest case, for TG, the extraction recovery reaches no more than 7% after multiple extractions. These results are in line with the results obtained for extraction time profiles in section 3.3.3 where the recovery of lipids from plasma illustrates the appearance of a second plateau after 3 hours of constant extractions from the same plasma and with the use of the same coating. In this experiment, an increase in extraction recovery is observed after 4 extractions of the same plasma (4×90 min), using fresh coatings in each step. Therefore, it seems possible that the increased recovery in repeated extraction steps is again related to certain changes occurring in plasma as a result of exposure to more than three hours experimental conditions (agitation, open vial, prolonged contact with air, etc.).

3.3.8 High throughput 96-blade SPME system for Plasma Protein Binding (PPB %)

Due to the hydrophobic nature and poor water solubility of lipids, transportation of these compounds is severely restricted in aquatic environments. However, lipid transfer proteins (LTP), so-called “lipid chaperones”, are effective transport vehicles that mediate lipid

translocation through their connection to the lipoproteins.²⁷³⁻²⁷⁵ Lipid transfer proteins (LTP) operate both intra- and extracellularly. They deliver lipids to plasma lipoproteins since they are able to reversibly and non-covalently interact with lipids, enhance their solubility, transport them in the blood stream and facilitate their trafficking through membrane. Conversely, apoproteins are distributed among various lipid-protein complex structures and form plasma lipoproteins of different density classes.^{13,17,21,274} The interaction and transportation sufficiency of apoproteins is directly related to the structure of the individual apoprotein and the specific nature of the lipid. As a result of this dynamic exchange and the net transfer of lipids between lipid transfer proteins and apolipoproteins, the content of plasma lipoproteins is continuously modified during their intravascular metabolism. Therefore, availability of lipids is distinctly regulated by the significance of protein affinity in a temporal and spatial manner, and can be varied in the presence of other competing ligands. The dynamic equilibrium of lipids between various binding compartments of blood plasma such as albumin or multiple apoprotein constituents of lipoproteins generates a series of lipid fluxes within the blood stream that can be analyzed by advanced separation techniques.

SPME has been reported as an extraction technique that can precisely determine the percentage of ligand-protein binding by measuring the total and free concentrations of the molecules. The detailed principles and equations of SPME for calculations of free, total, and percent ligand-protein binding for variety of drugs and exogenous compounds are already reported in the literature.^{138,146,151,218,276} Moreover calculation of FA-protein binding has been extensively discussed in section 2.3.6 and 2.3.7 of this thesis. In this section, SPME is assessed for the study of lipids in their natural state, and was applied for evaluation of protein

binding of lipids under negligible depletion conditions of a 96-blade SPME system. For this reason, calibration curves were constructed in spiked PBS at two different concentration levels (5-100 and 100-500 ng/mL), as well as in spiked plasma (0.5-8.0 µg/mL) based on optimized SPME conditions. The detailed description of calculation of protein binding by SPME using the Equation 2-3 and Equation 2-4 is already discussed in section 2.2.7. Briefly, the percentage of lipid binding to plasma proteins (PPB) is calculated from the total and free concentration of lipids. Lipids in plasma are solubilized and dispersed through their association with specific groups of proteins. Most free fatty acids and related structures with carboxyl functional groups associate with albumin, whereas the transport and distribution of more complex lipids are accomplished by means of plasma lipoproteins. Equation 2-4 was applied for the determination of lipid plasma protein binding for the test lipids and results are summarized in the Table 3-5 for each lipid category. However, based on these data the distribution and affinity of each lipid class to individual carrier proteins and apolipoprotein particles of the bloodstream cannot be provided and only total plasma binding is considered. Here, total protein binding is equal to the lipid distribution between HSA, LTPs, and various apoproteins involved in lipoprotein structure, and can be written as:

Equation 3-1

$$\%PPB_{total} = \%PPB_{HSA} + \%PPB_{LTP} + \%PPB_{apoproteins}$$

Considering the variety of apoproteins involved in the structure of different lipoproteins, the PPB% related to apoproteins can be written as:

Equation 3-2

$$\%PPB_{apoproteins} = PPB_{apoA-I} + PPB_{apoA-II} + PPB_{apoB} + PPB_{apoC-I} + PPB_{apoC-II} + PPB_{apoE}$$

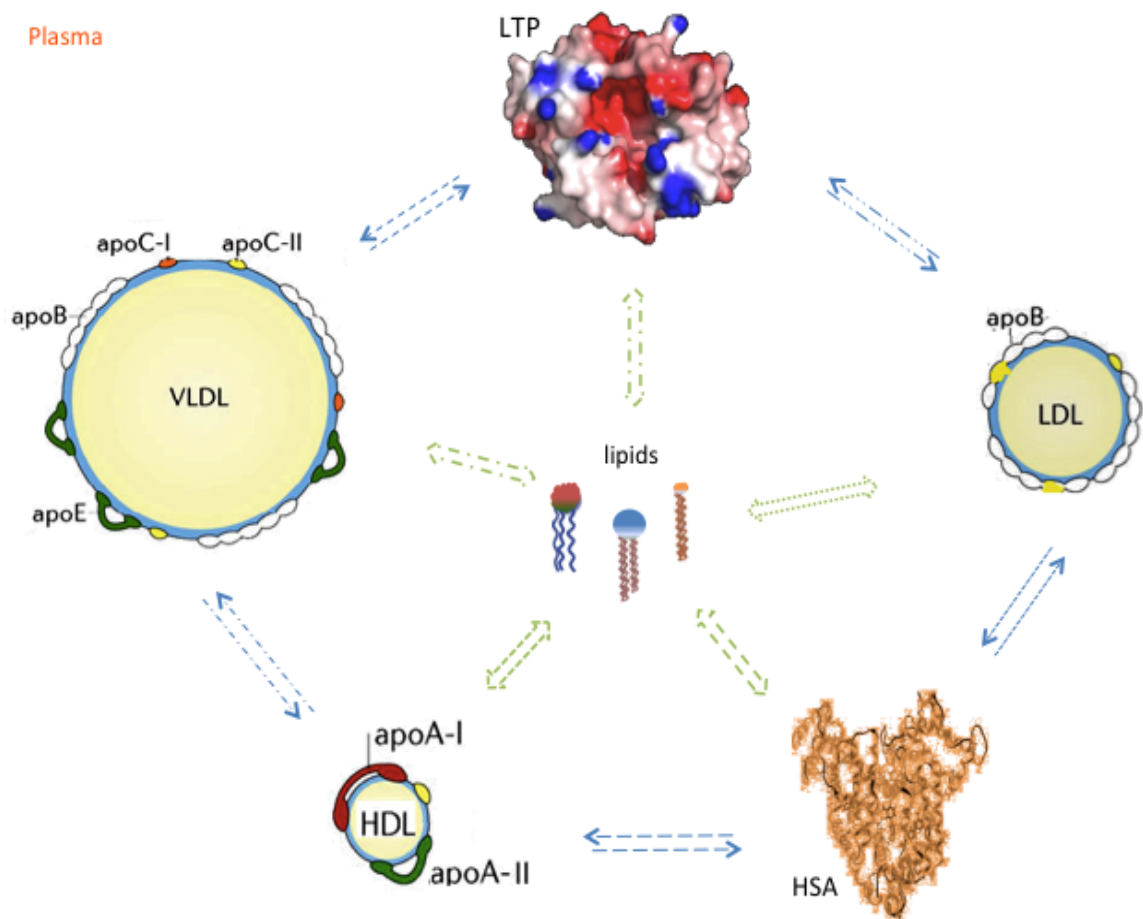


Figure 3-11 Schematic of different lipid-binding proteins in interaction with lipids in plasma. Binding is a complex function of the affinity of proteins to different lipids.

Binding is the complex interplay of protein affinity to various lipids. Therefore, percentage data were converted into an equivalent logarithm of the apparent affinity constant $\log K$ by application of formulation derived from the law of mass.^{277,278}

Equation 3-3

$$\log K_A = \log \left[\left(\frac{\%PPB}{100 - \%PPB} \right) \right]$$

K_A denotes an average of binding affinity to all available lipid transfer proteins under the assumption that binding is not exclusively limited to HSA. $\log K_A$ is then a binding constant that estimates the net complementary properties of the binding adhesions established between all available proteins to a given lipid. This approach is also based on the hydrophobic subtraction model of binding, since the lipophilicity and $\log P$ of lipids play a major role in providing binding affinity to proteins, whilst other factors such as electrostatic, charge, and hydrogen bond may add their contributions to binding. Thus, the binding affinity (K_A) of every lipid species is distinct to specific apoproteins associated in the structure of HDL, LDL, or VLDL. On the other hands, the association of lipids with lipoprotein particles may not follow the law of mass action kinetics since lipids do not occupy well-defined individual binding sites on proteins but they merge into protein-coated lipid droplets. The model described by Equation 3-3 can be served to develop an original approach for comparison of protein selectivity in correlation with lipid attribute. Theoretically, this value could be also determined for each protein involved in lipid transportation when SPME is applied to that specific protein instead of whole plasma. By far, no concrete guideline is reported to generate quantitative information in regards to lipid distribution patterns for specific transfer lipoproteins based on binding affinity. Consequently, if the suggested SPME protocol be applied to isolated and characterized lipoprotein fractions, this method may be applicable as

an optional approach for obtaining such information. Further, the proposed protocol could be a subject of future studies.

Table 3-5 different plasma lots by solid phase microextraction (SPME)

Lipids	SM (17:0)	CE (17:0)	PG (17:0)	LPC (17:0)	PE (17:0)	PC (17:0)	MG (17:0)	TG (17:0)
%PPB	98.0	97.1	98.3	96.6	97.1	96.0	93.6	89.6
Log K	1.68	1.52	1.75	1.46	1.52	1.38	1.17	0.93

3.3.9 Summary of method performance

Reliable quantitative analysis necessitates accurate measurement methods for which either external or internal calibration techniques are mostly employed. Relative extraction recoveries may be significantly influenced by the presence of biological matrix components, which may consequently distort SPME quantitative measurements. Therefore, it is important to understand the relation between deviations in calibration curve linearity associated with measurement errors, and to address them accordingly. Due to the high level of protein binding for all lipids, the use of both matrix-free and matrix-matched calibration curves provide an advantage for determination of both free and total concentrations using a single analytical method. The approaches for calculation of free (unbound) concentrations using matrix-free calibration in PBS, as well as mass balance assessment and its related corrections, have been discussed earlier in this chapter (section 3.3.4). However, when an appropriate blank matrix is unavailable (due to the abundant presence of lipids in plasma), the standard addition calibration is acknowledged as the best applicable quantitative method that can compensate for variation of measurements in such complex matrices. Therefore, the amount of analyte extracted by SPME was individually plotted against known concentrations

of spiked standards in plasma to determine the total and unknown concentrations of lipids. Calibrations were performed for both odd (as nonexistent lipids) and even (naturally existent lipids) lipids in plasma so as to compare the correlation between the data set obtained from each group. The least square linear regression method was used to construct calibration curves. For the even lipids, the calibration curves were extrapolated to quantify the unknown amounts of each lipid analyte in the pure plasma sample (0 added), whilst the calibration curves were forced through the origin for odd lipid standards, since they are not endogenously present in plasma. The linear dynamic range was calculated using a non-weighted linear least square regression fit for both calibrations. As shown in Figure 3-12 a good linear relationship was obtained for seven-point calibration ($n = 3$ each point) for all lipids. In the present study, the thin-film constant ($K_{fs}V_f$ obtained from SPME main equation¹⁴⁷) as the slope of matrix-free and matrix-matched plots was calculated for PBS and plasma individually. These values were used for determination of free and total concentrations of lipids in plasma. Moreover, the linear regression coefficient (R^2), sensitivity (curve slope), reproducibility, LOD, LOQ, and dynamic range of the SPME-LC-MS/MS method were studied as described in section 2.3.8. For each lipid class/subclass, comparisons were carried out between extracted amounts of spiked odd standards and those of spiked standards with even carbon numbers. For instance, the calibration curves of two different molecular phosphatidylcholines, *PC (17:0/17:0)* and *PC (14:0/18:1)*, were monitored at equimolar concentrations with the use of SPME-LC-MS/MS. The linear regression and correlation coefficient (R^2) were subsequently obtained by plotting spiked versus extracted amounts at each concentration level, the results of which can be found in Table 3-6.

Linearity was evaluated by constructing three independent calibration curves in three different plasma batches, using independent sets of blades to investigate if the acquired calibration equation was reproducible for quantitative analysis of lipids. The results showed excellent agreement. For instance, the average slope of three calibration curves in three different plasma lots of blood plasma was found to be 0.022833 for *PC (14:0/18:1)*, and 0.0234 for *PC (17:0/17:0)*, while the linear regression coefficients (r^2) ranged from 0.987-0.999, as shown in Figure 3-12. Using this approach, a comparison could be carried out between the measured amounts of extracted odd versus even lipid standards of the same category. In a similar fashion, for other lipid standards, measurements of odd and even species showed a correlation higher than 0.8 ($R^2 \geq 0.8$) for lipids of the same class/subclass. The good agreement between odd and even lipid quantification (in the range of experimental error) demonstrates that fatty acid chain length and degree of saturation within the same lipid subclass do not create variations in calibration measurements. Accordingly, one universal calibration equation per each lipid subclass could be applied for calculation of all lipids of the same sub-category, regardless of the differences in their fatty acyl moieties. This is illustrated in the example calibration curve obtained for PC from three different plasma lots. The linearity data further confirms good overall performance of the SPME method to compensate properly for inter- and intra-lot variations by elimination matrix effect issues.

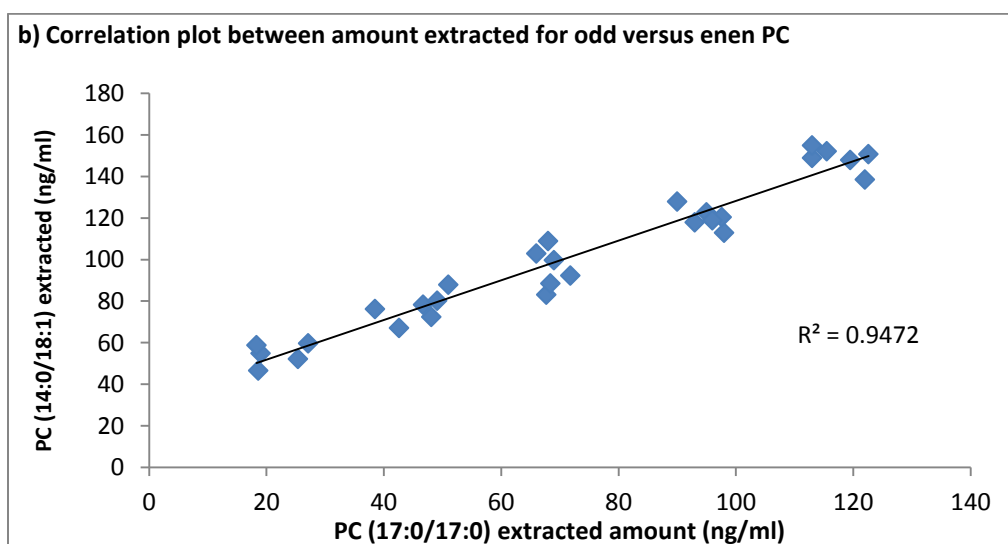
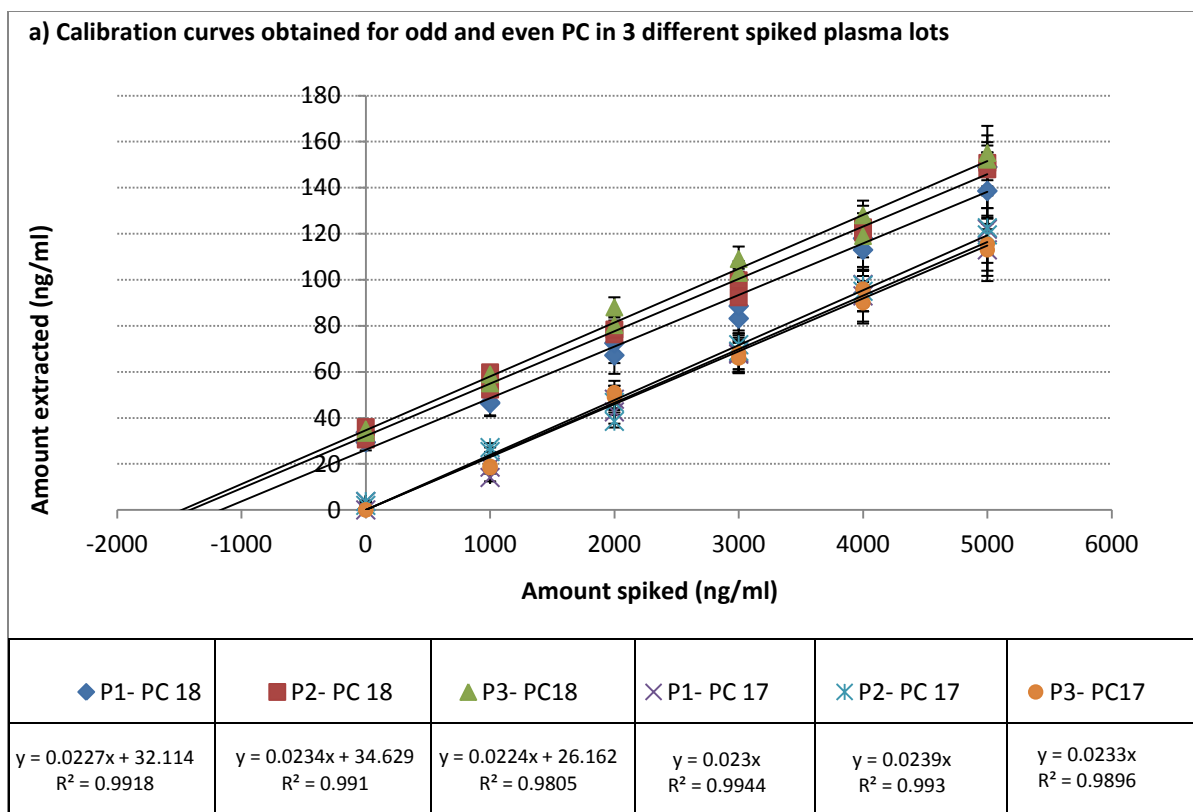


Figure 3-12 Human plasma samples ($n = 3$ lots) were analyzed by SPME-LC-MS/MS; a) example calibration curve of class-specific lipid standards for PC (17:0/17:0) and PC (14:0/18:1) at equimolar concentration range (500-5000 ng/mL; $n=3$ each point). Linear regression and correlation coefficient (R^2) are compared; b) Correlation between data obtained for measurement of PCs of different aliphatic chains.

Table 3-6 Summary of linearity results obtained for C18 coatings in 3 different pooled plasma lots. Each point of each calibration set was obtained using different sets of coatings (n=3 determination for each concentration level).

Lipids	Unweighted linear regression equation	Lot-to-lot CV %	Correlation coefficient, R ²	LOQ (ng/ml)	linearity range (ng/ml)
LPC (16:0)	y=0.3026 (±0.0090)x	5 %	0.9862 (±0.0068)	0.5	10-500
LPC (17:0)	y=0.0193 (±0.0002)x	1 %	0.9934 (±0.0027)		
MG (18:1)	y=0.0369 (±0.0014)x	4%	0.9951 (±0.0010)	2	20-1000
MG (17:0)	y=0.0377 (±0.0003)x	1%	0.9900 (±0.0080)		
CE (d18:1/18:0)	y=0.0226 (±0.0004)x	3 %	0.9797 (±0.0042)	0.3	5-800
CE (d18:1/17:0)	y=0.0200 (±0.0009)x	5 %	0.9945 (±0.0034)		
SM (d18:1/16:0)	y=0.0137 (±0.0007)x	5 %	0.9881 (±0.0020)	0.5	5-1000
SM (d18:1/17:0)	y=0.0131 (±0.0006)x	5 %	0.9881 (±0.0020)		
PE (16:0/18:2)	y=0.0143 (±0.0005)x	1 %	0.9916 (±0.0034)	0.5	7-1000
PE (17:0/17:0)	y=0.0192 (±0.0001)x	1 %	0.9956 (±0.0015)		
PC (14:0/18:1)	y=0.0228 (±0.0005)x	2 %	0.9877(±0.0063)	1.5	10-1000
PC (17:0/17:0)	y=0.0235 (±0.0003)x	1 %	0.9910(±0.0008)		
PG (18:0/18:0)	y=0.0151 (±0.0001)x	1 %	0.9908 (±0.0033)	1	8-1000
PG (17:0/17:0))	y=0.0113 (±0.0002)x	2%	0.9884 (±0.0034)		
TG(18:1/16:0/18:1)	y=0.3105 (±0.011)x	4 %	0.9955 (±0.0011)	0.8	12-1500
TG(17:0/17:0/17:0)	y=0.1451 (±0.0026)x	2 %	0.9925 (±0.0022)		

The method was linear in the range of 500-8000 ng/mL obtained by extraction of lipids from plasma, making it amenable for quantitative monitoring of these lipids. Summary of obtained data and calculations are represented in Table 3-6. It should be noted that the upper bound of the linear dynamic range reported here is due to limitations of MS detection (detector saturation or ESI droplet surface saturation) and not by the SPME procedure itself. This means that samples exceeding the upper limit can still be successfully analyzed after

appropriate dilution. In addition, the reproducibility of the assay was studied through an evaluation of inter- and intra-day RSD, and excellent reproducibility was found for all lots with all RSD values ranging from 2-7% for all analytes tested. Meanwhile, the inter- and intra-day method precision ranged from 1-12% RSD, both of which meet acceptance criteria for quantitative bioanalysis. The obtained results for all compounds (n = 5 coatings) indicate proper sensitivity and reproducibility of the SPME-LC–MS/MS method for determination of lipids from the complex matrix under study.

3.3.10 **Conclusions and future directions**

In this study, the SPME-LC-MS/MS method was developed for simultaneous quantification of the most abundant lipid classes present in plasma and whole blood. The quantitative procedure relied upon the use of a set of seven diheptadecanoyl (17:0/17:0) synthetic standards based on one-class/one-standard approach for common phospholipids, sphingolipids, and glycerolipids classes and their subclasses. Another important approach was the use of additives in the aqueous chromatographic elution to improve phospholipid and triglyceride peak shapes and retention time stabilities. The SPME methodology produced a comprehensive and quantitative description of the complex ensemble of lipid species by the direct analysis of total lipid extracts of human plasma. In addition, the developed method provided a good degree of recovery, reproducibility, and quantitation for the analysis of the compounds under study. The performance of the proposed SPME-LC-MS/MS method was found satisfactory for the analysis of lipids in human blood plasma, meeting all regulatory requirements codified by the ICH²⁷⁹ and IUPAC²⁸⁰ guidelines. The obtained results show that the LOQ (5 ng/mL) achieved in the current work is satisfactory, while the achieved sample throughput is considerably improved due to the parallel nature of extraction. In principle, the

fact that SPME extracts via free concentration makes it on one hand a limitation because of the low recoveries which can lead to sensitivity issues, while it is compensated in cases of compounds with high concentrations and high affinities to the extraction phase. Considering the high natural concentration of all lipids as one of the most abundant metabolites of plasma, this approach is still suitable to meet minimum quantitative requirements. Meanwhile, the lower extraction recoveries could be considered as an advantage when considering the results of the matrix effect evaluation, which indicates the suitability of this technique for analysis of lipids, keeping in mind that lipids have a bad reputation for ion suppression/enhancement in ESI approaches. By optimizing the geometry of coatings, the disadvantages of low extraction recoveries could be successfully overcome for the SPME approach, which requires no evaporation/reconstitution step, unlike other conventional techniques employed for lipid analysis. Furthermore, the absence of matrix interferences indicates that the proposed biocompatible SPME system can be used for quantitative analysis of lipids in other types of biological matrices such as cell lines and tissue through direct immersion extraction without the need for any additional pre-treatment of the sample. The method developed here should be useful in both research applications and diagnostic routine, taking to account that lipids are implicated in multiple biological and pathophysiological processes.

Chapter 4

Discovery Lipidomic of Hepatic Cancer Cells in Response to Treatment by a Polyunsaturated Fatty Acid: Eicosapentaenoic Acid

4.1 Introduction

Hepatocellular carcinoma (HCC) is one of the common types of human cancer with high morbidity and mortality; the threat of HCC is expected to continue to grow in the coming years. One of the major causative factors in the development of hepatocellular carcinoma is the persistent infection of liver with the hepatitis C virus (HCV).^{281,282} Chronic liver infections subsequently lead to the accumulation of intracellular lipids (mostly TGs) in the liver known as steatosis. The abnormal retention of lipids can lead to more advanced and severe disease state called hepatic cirrhosis, which can potentially designate the progression of liver carcinogenesis. Thus, developing effective and efficient care for patients with end-stage liver disease and HCC must become a significant focus. Changes in lipid constituents alter the functionality of cell membrane by changing its fluidity and polarization which leads to alteration of their metabolic activity and cell signaling.²⁸³ For the past few years, lipids, and in particular omega-3 and omega-6 polyunsaturated fatty acids (PUFAs), have received considerable attention in human health. Epidemiological studies are trying to find evidences for possible correlation between PUFA-rich diets and a reduced incidence of cancer. There are numerous experimental findings that indicate the effect of ω -3 PUFAs such as docosahexaenoic acid (DHA) and eicosapentaenoic acid (EPA) in preventing cancer.²⁸⁴⁻²⁸⁷ These findings could be further examined and validated through “discovery lipidomics”. This

new subdivision of lipidomic studies aims to reveal the lipid treasury of a biological system in an untargeted fashion. Additionally, it aims to investigate the statistically significant variations between control and test group data sets, and finally, to explore disease-related molecular markers by determining their chemical structure and biosynthesis pathways.^{288,289}

In order to obtain reliable and meaningful answers in lipid discovery experiments, not only specialized mass spectrometric techniques are required to facilitate lipid characterization and identification, sample preparation strategies are also needed before implementation of the instrumental procedure.

In the previous chapter (Chapter 3) we described the development and validation of quantitative analytical method by employing the Thin Film Microextraction in the 96-well plate format for the extraction of lipids. The present study was designed to investigate the effect of ω -3 PUFAs on the lipidome profile of HCC cell lines by performing a “discovery lipidomics” experiment. Within this project, we aimed to evaluate the strengths and weaknesses of our validated SPME protocol in providing a comprehensive profile of lipidome changes by comparing the obtained results to that of classical liquid-liquid extraction based on Bligh & Dyer approach.

4.2 Experimental

4.2.1 Cell culture

Human HCC cell line Huh7 was seeded in six 75cm² flasks (n=3) in DMEM supplemented with 10% fetal bovine serum, 2 mM L-glutamine, and penicillin/streptomycin, then incubated at 37°C in a humidified CO₂ incubator. Twenty four hours after seeding, media was changed to serum-free medium for 6hrs; three flasks containing HUH7 cells were then treated with

eicosapentanoic acid (EPA) at 0.4mM for 4hrs, while the control set (n=3) was kept untreated. Cells were then washed with 1ml of cold phosphate-buffered saline (PBS) twice, and scraped off the surface of the flask using a cell scraper in PBS. The cell suspension was then spun at 5000×g for 20 min, the supernatant discarded, and the cell pellet flash-frozen in liquid nitrogen. The pellets were stored at -80 °C until use. Each cell pellet of biological replicates (n=3 control and n=3 treated) contained approximately 8.4×10^6 HUH7 cells. Upon analysis, samples were thawed at room temperature, and 6ml of cold PBS were added to each sample tube, which were gently swirled until complete suspension was achieved. The content of each tube was divided into six aliquots of 1ml, from which 2×1ml portions were subjected to the lipid extraction based on Bligh & Dyer procedure, and 4×1ml portions were subjected to SPME analysis.

4.2.2 Lipid extraction by Bligh & Dyer protocol

This study employs two different extraction methods for lipid analysis on HCC cell lines, aiming to assess the potential impact of different extractions on current cancer lipid research. The standard procedure of lipid extraction was performed according to the Bligh & Dyer method, and results were compared against the data obtained from the optimized TF-SPME method. For each method, preparation and extraction of cell samples were carried out separately. In order to avoid bias, sample preparation was carried in a randomized order for biological replicates. For the Bligh & Dyer method, the total lipid fraction was extracted from 1ml cell suspension (1.70×10^6 cells/ml) with the addition of 3.75 ml chloroform/MeOH mixture (2:1, v/v), followed by vigorous shaking. Then, 1.25 ml extra chloroform was added to the mixture solution, which was subsequently vortexed for 20 s, followed by addition of 1.25 ml nanopure water, and swirling for another 1min to form a two-phase system. The

lower organic phase contained almost all of the lipids, while the upper aqueous phase contained many of the non-lipid compounds as well as polar lipid species. The mixture then was settled at room temperature for 10 min to reach equilibration, and centrifuged at 2000 RPM and 5 °C for 5 min. The organic bottom phase was recovered and transferred to a new tube. Subsequently, the chloroform was evaporated under N₂ gas to dryness and the sample re-suspended in 1 ml IPA/methanol (1:1) for injection to LCMS.

4.2.3 Preparation of C18-PAN 96-Blade coatings

For the high-throughput analysis of lipids, coated thin-film SPME blades were exposed to the plasma with the use of the manual Concept 96 (Professional Analytical System (PAS) Technology, Magdala, Germany). The thin-film SPME blades were prepared in house following the same procedure as discussed in section 3.2.3 and a comprehensive description of this method is given elsewhere.¹³⁶ In this study, the commercial mixed-mode SPME fibers were enclosed beside each pin in the 12 thin-film blade set. This assembly was designed to capture other polar metabolites from the same sample on the mixed-mode coatings, while lipids are captured by the C18 thin-film coatings. As the mix-mode coating has been previously reported as the most effective sorbent for the extraction of a range of highly polar to semi-nonpolar metabolites in metabolomic studies,^{154,174,290} this enables any potential biomarkers to be tracked and related to probable metabolic pathways, if particular biomarkers were to be found. Figure 4-1 shows the arrangement of the 12-thin film set and mixed-mode fibers.

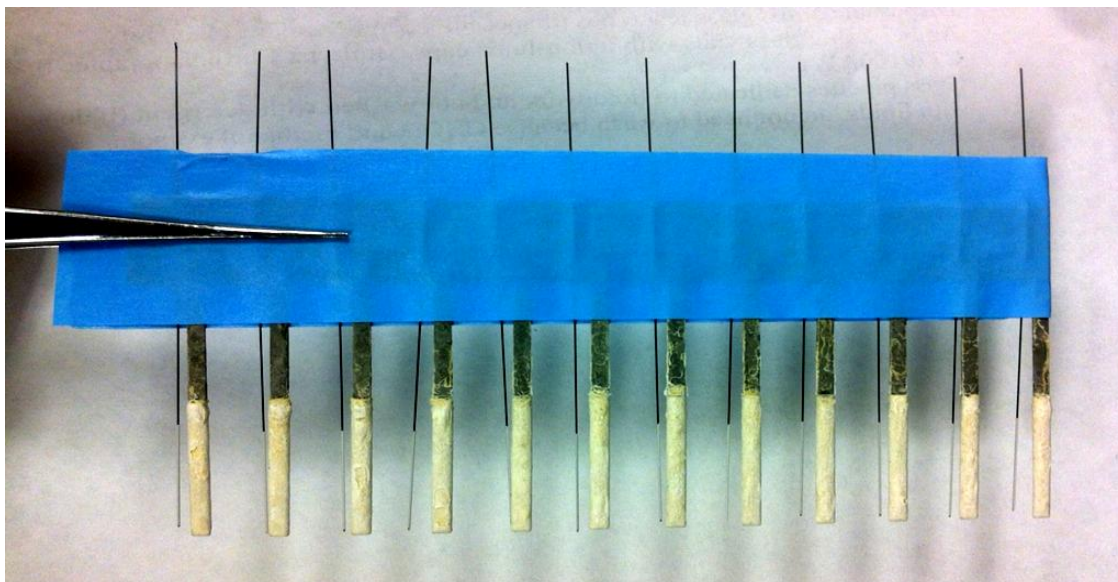


Figure 4-1 Thin-film C18 blade set/ MixMode SPME fiber assembly for simultaneous extraction of lipids and polar metabolites of HuH7 cell sample placed in the same well

4.2.4 SPME procedure

All SPME coatings were pre-conditioned for 30 min in a mixture of methanol/water (1/1, v/v) prior to use in order to activate the silanol groups of the stationary phase. For the SPME approach, cells were homogenized by vigorous agitation using the VWR DVX-2500 digital vortex (Mississauga, ON, Canada) and incubated for 30 min at 37°C prior to analysis with SPME. The SPME experiment was performed by immersing the fiber-blade assembly directly into 1 mL sample aliquots, which were then randomly placed in each well of the 96-well plate and agitated with 2400 rpm vortex agitation for a total extraction time of 90 min. Immediately after extraction, coatings were rinsed by dipping the set in purified water for 10 s to remove any residuals of biological material from the coating surface. Afterwards, blades and fibers were disassembled, and rod fibers were placed in individually labelled glass vials and preserved in a -80 °C freezer for further investigations if necessary. Subsequently, thin-film coatings were agitated for 60 minutes in 1 ml IPA/methanol (1:1 v/v) for proper

desorption of lipids, and the resulting final extract solutions injected to the HPLC–ESI-MS/MS system for analysis. The total workflow from sampling to sample preparation is presented in Figure 4-2 Schematic of sampling order for SPME and B&D procedure for the cell suspension of HuH7; Each replicate tube contained approximately 8.4×10^6 cells.

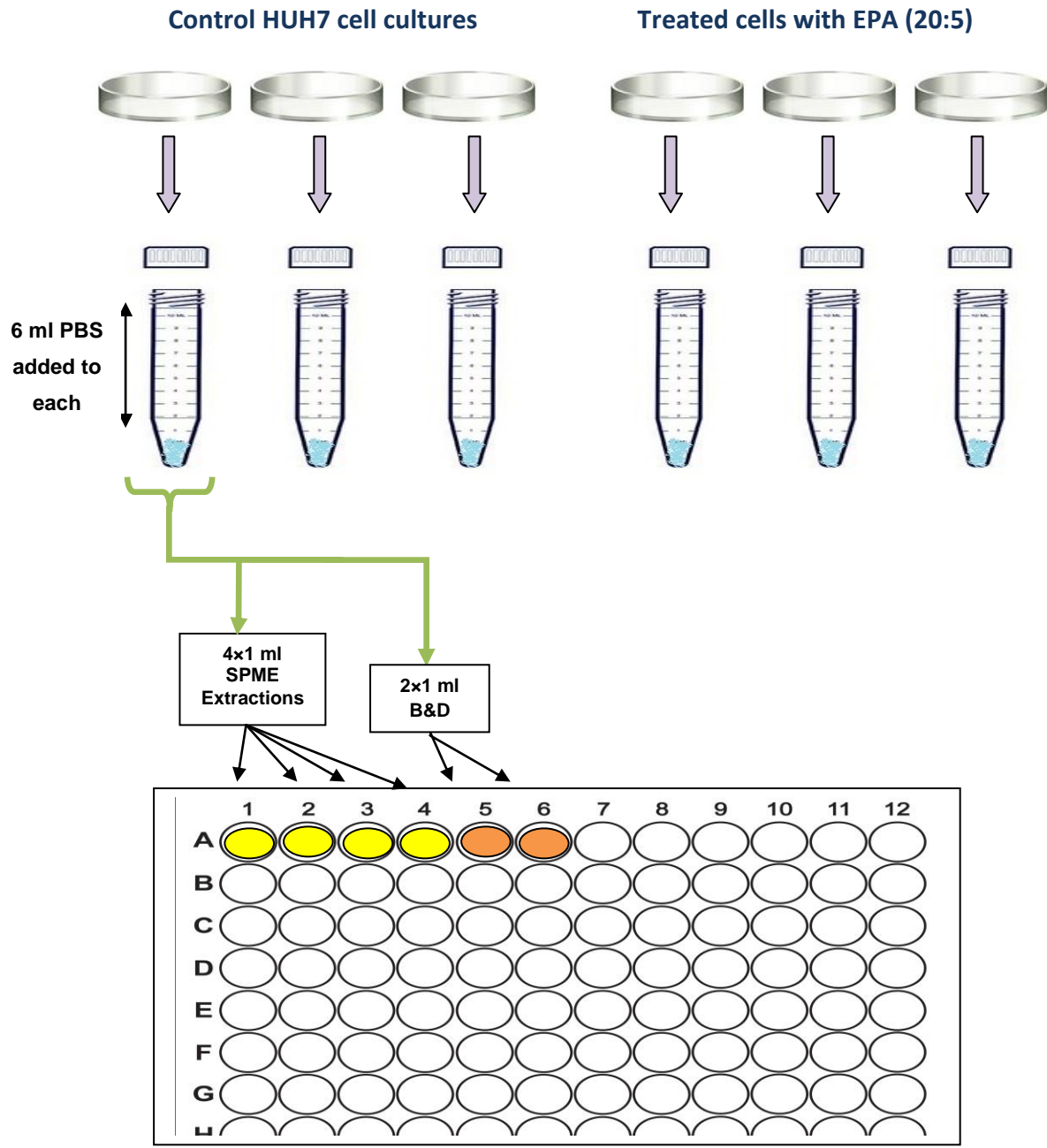


Figure 4-2 Schematic of sampling order for SPME and B&D procedure for the cell suspension of HuH7; Each replicate tube contained approximately 8.4×10^6 cells

4.2.5 LC-ESI-MS operating conditions

Analyses of cell extractions were performed on a LC–MS system consisting of the Accela autosampler with a cooled system tray, Accela LC Pumps, and the Exactive Orbitrap mass spectrometer (Thermo, San Jose, CA, USA) equipped with a heated electrospray ionization (HESI) probe. Sheath gas and auxiliary gas (arbitrary units), spray voltage (V), capillary temperature (°C), capillary voltage (V), tube lens voltage (V) and skimmer voltage (V) were set to 30, 10, 4000, 350, 50, 100, and 25 for positive ion mode and 55, 30, 3500, 275, -67, -85 and -24 for negative ion mode, respectively. To maintain a mass accuracy better than 5 ppm, the Exactive Benchtop Orbitrap was calibrated every 24 hr with a Thermo Scientific ESI Calibration Solution consisting of Caffeine (20µg/mL), MRFA (1µg/mL), and Ultramark 1621 (0.001%) for positive ion mode and a sodium dodecyl sulfate (2.9µg/mL), sodium taurocholate (5.4µg/mL), and Ultramark 1621 (0.001%) solution for negative ion mode.

Samples were analyzed with the use of an XBridge BEH C18, 2.5 µm, 150 mm × 2.1 mm column XP (Waters Corp, Milford, MA). A binary solvent system was used for gradient elution that consisted of water/acetonitrile (10:90), with 0.1 % acetic acid as mobile phase A and isopropyl alcohol as mobile phase B, and 0.15 mM ammonium acetate, for a flow rate of 200 µl/min. Optimal separation was achieved using the following solvent gradient elution: Mobile B starts at 10%, remaining constant until minute 6, then increasing to 60% until minute 8, followed by a gradual increase to 70% B until minute 18, then ramping back to 10% for one minute, followed by four further minutes of column re-equilibration, for a total run time of 22 minutes. Quality control (QC) samples were prepared by pooling 10 µL aliquots of all sample extracts. Initially, 5 injections of blank and 10 injections of pooled QC were run for “system conditioning”. The cell lipidome was profiled by injecting each sample

once, in a well-considered randomized order, with periodic injection of blanks, QC, and standard lipid mixture throughout the sequence to evaluate system performance. This sample sequence yielded a total of 67 injections, each of which was run separately in positive and negative modes.

4.2.6 Data processing

The msConvertGUI.exe program from ProteoWizard was used to convert raw data output to the open .mzXML format.²⁹¹ Data were then further processed with the open source XCMS R-package (Scripps Center for Metabolomics, CA, USA) for automated retention time correction, peak alignment, and peak integration. Following data processing, ion annotation was conducted with the use of the CAMERA R-package (Bioconductor Version 2.10) to identify adducts and isotopes through application of optimal parameter settings suggested by Patti et al.²⁹² After data processing, an exported csv file was generated and converted to a Microsoft Excel spreadsheet containing accurate mass and retention time, m/z, and signal intensity for each generated molecular feature.

4.2.7 Data analysis

The produced datasheet was submitted into the SIMCA-P software 11.0 (Umetrics, Umea, Sweden), where statistical data analysis and data visualization were carried out. Unsupervised principal component analysis (PCA) was employed to demonstrate general clusters and trends among the observations. For validated models, Orthogonal Partial Least Squares-Discriminant analysis (OPLS-DA) was performed to establish which variables drive the separation. Prior to analysis, Pareto scaling was used on the acquired datasets and accurate masses were used as variables. Score plots derived from OPLS-DA and discriminant

compounds with absolute VIP (Variable Importance in Projection) values higher than 1.0 were selected for identification. Feature identification was obtained through a mass-based search against three databases: Human Metabolome Database (HMDB), METLIN, and LIPID MAPS, with a mass tolerance window of 5 ppm. In order to avoid the possibility of false identification, the retention time of the related peak was compared with the partition coefficient ($\log P$) of the matching features.

4.2.8 **Data Quality Assurance**

The stability of the chromatographic system throughout the data acquisition phase was first examined through the PCA of datasets (biological and QC samples) and confirmed by overlapping batches; clear spatial separation was found among different sample classes, regardless of the batch injection order and randomization. No instrument failure, indicating a decline in sensitivity, RT shifts, or changes in mass accuracy, was observed. The mass accuracy was assured by tracking the MS standard calibration every 24 hours.

4.3 Results and discussion

4.3.1 LC-MS method assessment

Lipids are found in a broad range of physical and chemical diversity, which create variation in their physical and chemical characterizations such as logP, charge, and functional group structure complexity. This diversity is a result of head group polarity between lipid categories, acyl side chain lengths, as well as degree of unsaturation within sub-categories. Due to the diverse nature of cell lipidome, both positive and negative ionization modes must be employed in the LC/MS profiling methods to achieve comprehensive coverage. Although some phospholipid species are ionized in both polarities, they all exhibit a significantly higher sensitivity in positive ion mode. In contrast, PI and PS are the only phospholipids that solely ionize in negative ion mode. This matter was considered as one of the determinant criteria during feature identification when searching the obtained m/z ions against online databases. The LC/MS method was assessed on the Orbitrap system using lipid standards following the same procedure described in section 2.3.1. Our final validated LC/MS method is capable of analysing multiple categories of lipids in a single run with improved signal intensity and peak shape, while known ionization polarities and adduct preferences accommodate to confine the multiple hints for each identified ion.

Figure 4-3 represents the XIC chromatogram of lipid standards in positive and negative ion modes. The same set of odd lipid standards were employed for evaluation of retention time and mass intensity. As could be observed, lipids involved in the same sub-category could show different retention times due to differences in their fatty acyl chains. Lipid standard solution and QC samples were frequently injected during the 24 hour sequence for each ion polarity. By placing these QC samples at regular intervals throughout the analytical run, LC-

MS stability could be assessed, and any variation monitored in terms of relevant analytical parameters such as retention time, peak shape, peak intensity, and mass accuracy. Meanwhile, randomization of different biological replicates alternated with QCs allowed for the detection of systematic variability throughout the LC-MS measurement.

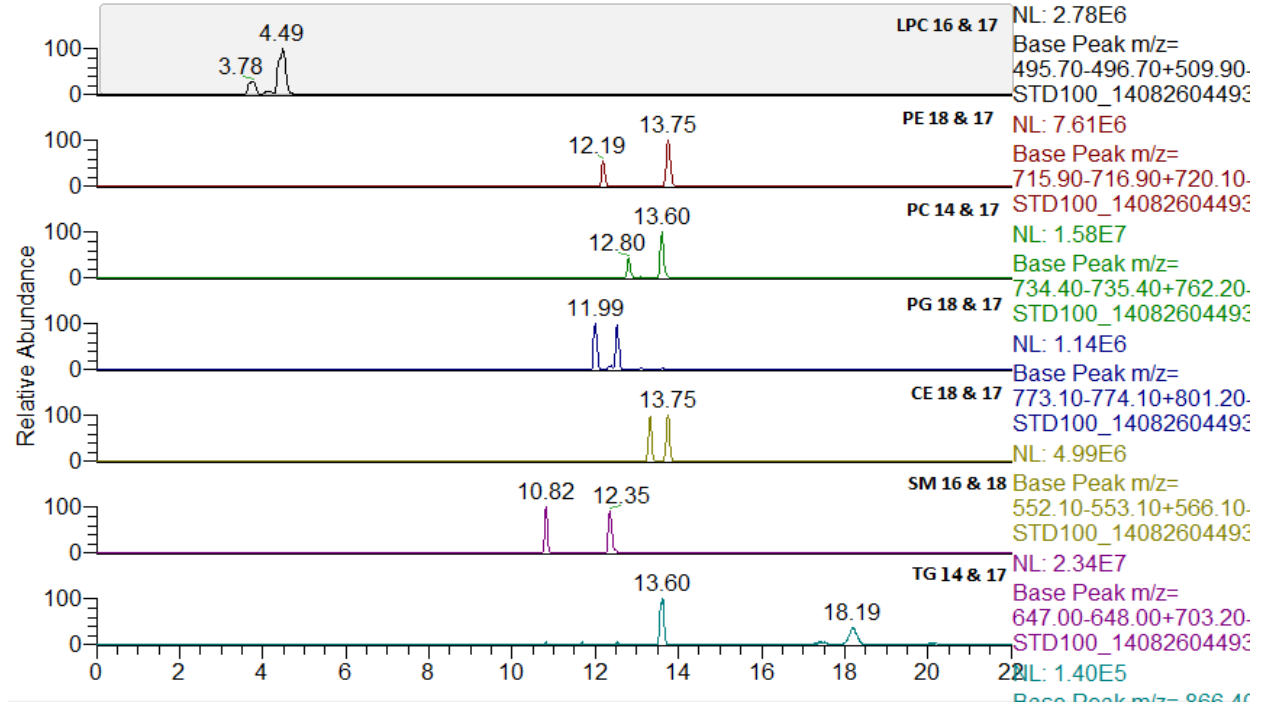
Table 4-1 A breakdown of the lipid classes surveyed in the BIODTD using the LC-MS system developed on orbitrap mass spectrometry

Lipid class	Ionization polarity		Retention time region (min)
	Positive	Negative	
Lysophospholipids (Lyso-)	[M+H] ⁺	-	2-4
Phosphoethanolamine (PE)	[M+H] ⁺	-	10-12
phosphocholine (PC)	[M+H] ⁺	-	11-13
phosphoglycerol (PG)	[M+H] ⁺	[M-H] ⁻	9-11
Ceramide (CE)	[M+H] ⁺	-	12-14
Sphingomyelin (SM)	[M+H] ⁺	-	9-12
Monoacylglycerol (MG)	[M+NH ₄] ⁺	-	7-9
Diacylglycerol (DG)	[M+NH ₄] ⁺	-	9-12
Triacylglycerol (TG)	[M+NH ₄] ⁺	-	13-18
Cardiolipin (CL)	[M+NH ₄] ⁺	-	15-20
phosphoserine (PS)	-	[M-H] ⁻	11-13
phosphoinositol (PI)	-	[M-H] ⁻	9-11
Fatty acyls (FA)	-	[M-H] ⁻	5-8

Upon analysis of standards of each lipid class and subclass, the “major adduct preference” with higher ionization intensity was determined and represented.

➤ **A) Standard Lipids in POSITIVE ion mode**

RT: 0.00 - 22.03



➤ **B) Standard Lipids in NEGATIVE ion mode**

RT: 0.0 - 22.0

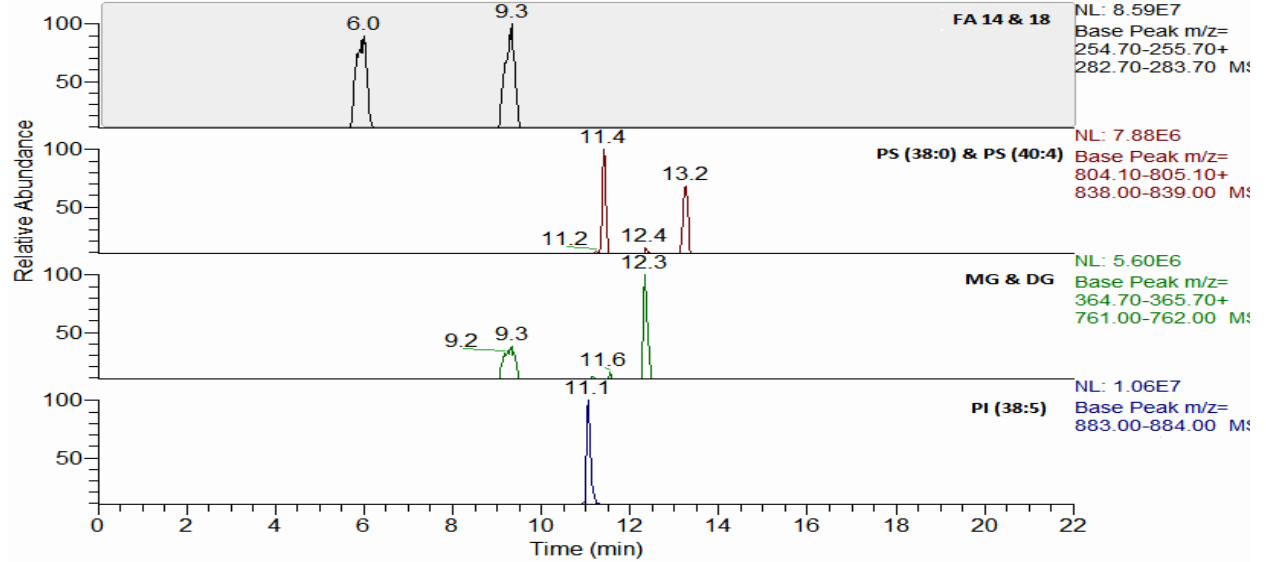


Figure 4-3 XIC chromatogram of lipid standards in A) positive and B) negative ion mode. Variations in retention time are expected for lipids of the same class and sub-class dependent on their structural orientation and acyl chain length

Figure 4-4 shows the total ion chromatograms (TICs) obtained from control samples using BD and SPME methods individually in positive and negative ion modes. Evaluation of total

ion chromatograms (TICs) highlighted the dramatic changes in the overall chromatogram signal intensity when comparing BD versus SPME extraction methods. The TIC intensity for Bligh & Dyer (panel B and D) was 2.99×10^8 and 2.31×10^8 in positive and negative ion modes respectively; whereas the TIC intensity for SPME (panel A and C) was nearly one order of magnitude lower at 7.88×10^7 and 6.81×10^7 in positive and negative ion modes. In this regard, for XIC specimens, the signal to noise ratio was 30-50 times higher for Bligh & Dyer. For instance, the calculated S/N of PE (35:0) with m/z ratio of 720.59000 is 1682:1 for SPME, while this value for Bligh & Dyer is 58180:1. The observed discrepancy in signal intensity is related to the different nature of the two extraction methods. Bligh & Dyer is a Liquid-Liquid extraction method that exhaustively extracts all lipid components of cells, including bound and free lipid species, whilst SPME is a non-exhaustive extraction method that purely extracts lipids in their free (unbound) format. Therefore, as opposed to the Bligh & Dyer technique, lipids involved in complex cell structures which are bound to proteins or particles of cell membrane remain intact in SPME. On the other hand, higher extraction recoveries in Bligh & Dyer when dealing with biological samples for analysis of lipids is not necessarily an advantage, as high concentrations of abundant phospholipids may saturate the ESI source and cause ionization suppression or enhancement (this is thoroughly discussed later in this report in the matrix effect section). It should be noted that higher signal intensities are indeed necessary and considered an advantage when the instrumental performance is average. However, the higher signal intensity in Bligh & Dyer is attributed to higher concentrations of extracted lipids that may saturate the ESI source and reduce the chance of ionization for less competitive species. In the LCMS method used for this research, all phospholipids were noted to elute between min 8-13, with retention times of various

phospholipid subclasses varying based on their acyl moieties; in such cases, the possibility of co-elution, and consequently, saturation of ESI source is still significant.

All detected lipid species for both SPME and Bligh & Dyer methods demonstrate an S/N ratio of at least 26 or greater, well above the assigned limit of detection (LOD) at S/N=3. The relative LOD range for extraction of different lipid classes using the proposed SPME method was 0.5-1 ng/ml (5-17% RSD, n=5), while for Bligh & Dyer, LOD values were found to be between 0.05-0.1 ng/ml. It is important to note that although SPME extracts smaller proportions of lipids, it does not substantially compromise the signal-to-noise and dynamic range for the detection of low-abundance lipid species. However, application of this method may potentially limit the identification of lipids present at trace levels due to its lower extraction recovery in comparison to Bligh & Dyer. During analysis, lipid standards showed RT coefficients of variance (CV) of less than 0.03% when compared within single ionization mode. The integration of XIC peak areas had CVs of less than 2.1% in either ionization modes.

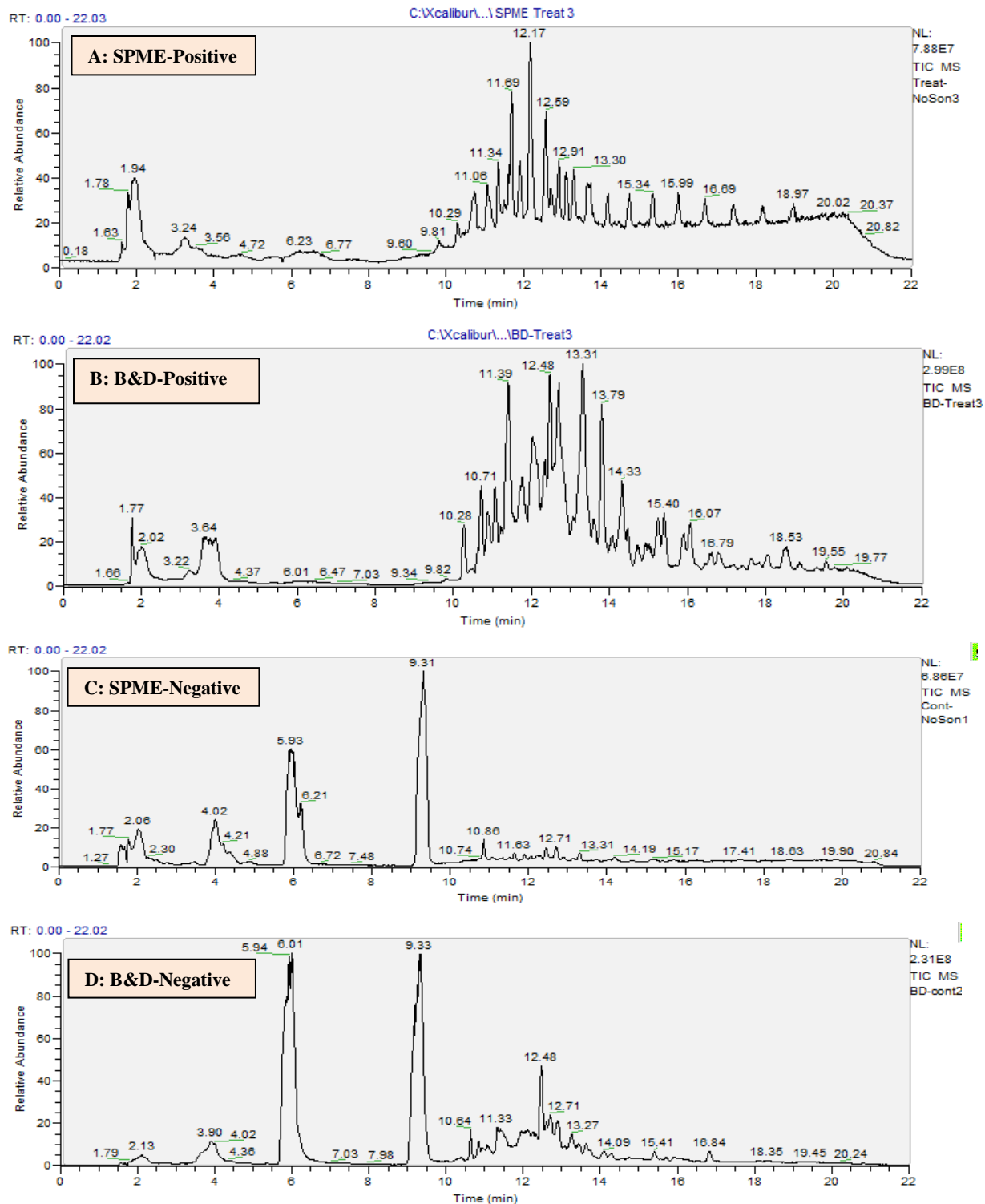


Figure 4-4 Total ion count (TIC) chromatograms from control HUH7 cell lines obtained by: panels A and C) SPME and panels B and D) Bligh & Dyer extraction methods in positive and negative ion modes respectively

4.3.2 Comparison of sample preparation methods for known identified lipids

Extracted Ion Chromatogram (XIC) of cell samples were compared to the XIC of injected authentic lipid standards and both accurate mass and retention time were used to assign the identity of these species in unspiked cell samples. Method precision for each sample preparation procedure was determined on the basis of five independent extractions of the same pooled cell samples. Example results are shown in Figure 4-5. The overall variability of SPME was below 18%, which is considered satisfactory for analytical method validation criteria. Contrarily, the results obtained for Bligh & Dyer demonstrate poor precision for SM, MG and LPCs. For Bligh & Dyer, an interesting trend was observed, where less hydrophobic lipid species with lower LogP values, such as LPC, MG, and SM, not only presented higher %RSDs, but were also detected in low signal intensities compared to those for SPME. This trend is unexpected, since in general, signal intensities for Bligh & Dyer are expected to be much higher than those of SPME due to the exhaustive nature of this method. Therefore, not only does the obtained higher deviation demonstrate slightly poor precision of the traditional technique for extraction of such compounds, the lower signal intensity could be related to the possibility of ionization suppression associated with this technique. This issue was investigated further under matrix effect studies. This issue is further examined in section 4.3.10.

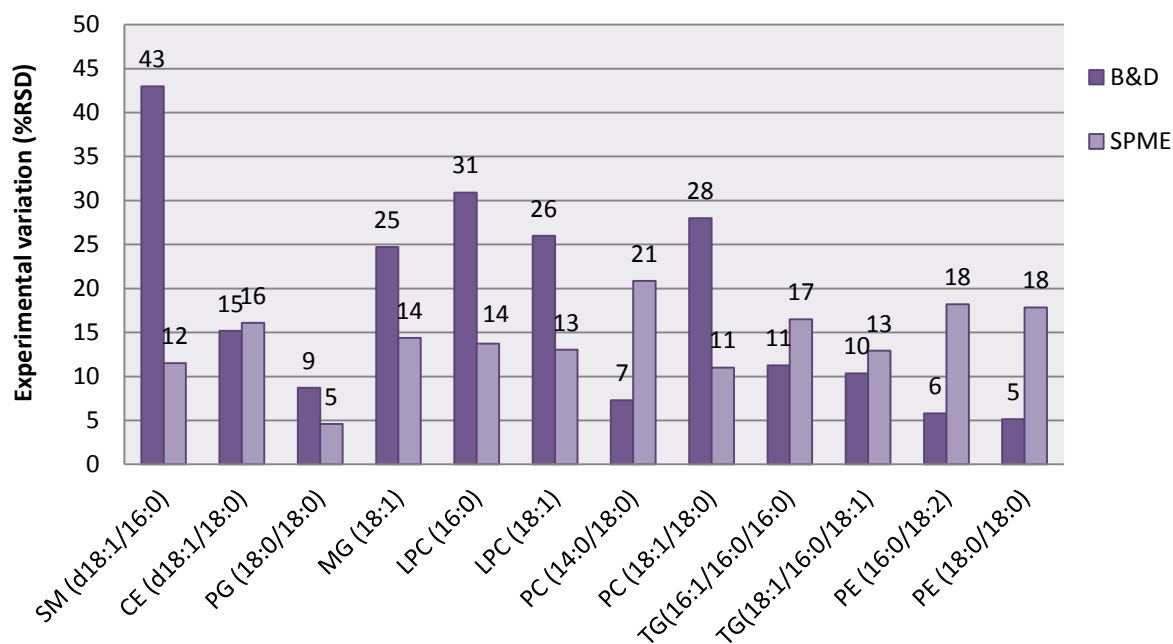


Figure 4-5 Comparison of method precision (expressed as % RSD for n=5 replicates) obtained for Bligh & Dyer with methanol/ chloroform and the validated SPME technique using C18 coatings

4.3.3 Lipidomics - SPME results versus conventional Bligh & Dyer

After data processing, analysis of two data sets from the results obtained for SPME indicated the presence of a total of 1922 ions in positive mode and 655 ions in negative ion mode, while for the Bligh & Dyer method, 1430 ions were detected in positive ion mode and 451 ion in negative ion mode on average in HCC cell samples for a mass range of 100 to 1200 D. It is noteworthy to mention that in an ESI source, a single lipid can give rise to more than one ion adduct. These ions may include proton, sodium, potassium, and ammonium adducts; considering the multiple-charged ions of each, and also the isotope peaks.^{48,293} Therefore, identification and selection of lipids was based on searches for the most probable ion adduct for each lipid category, and for the precise identification assurance of at least two adducts at the same retention time. This approach was followed for feature identification in section

4.3.6. Ion maps and histograms of the distribution of method precision for all unknown features with intensities higher than LOD levels are considered. For this purpose, six independent extraction replicates were used for each method to compare the data acquired by SPME to those of Bligh & Dyer for evaluation of method performance; the results are shown in Figure 4-6 and Figure 4-7. This type of representation is indicative of overall data quality for each method. In the perspective of data interpretation, high metabolite coverage is not useful when the method precision is poor, as in such cases, biological variability cannot be clearly distinguished from analytical variability.

For the evaluation of method performance, the absence of analytical variability must be assured; since acceptable RSD values are 15% for targeted analysis, and 20% for quantitative analysis, an RSD value of 30% or less should be of acceptable precision in LC-MS lipidomics.²²⁰ As observed in the Figure 4-6 and Figure 4-7, the distribution of % RSD for all features shows that both extraction methods represent RSDs below 30% in positive ion mode; in the case of SPME, this value was found to be below 5% for the majority of peaks. Moreover, in both cases, most features presented RSD values less than 30% in negative ESI mode, with only a small number of features exceeding 30% RSD. These data signify that SPME can match and in some cases exceed the accuracy of the data produced by the conventional method.

Analysis of samples using negative ESI mode resulted in a total of 655 and 451 peaks observed for SPME and Bligh & Dyer, respectively. The ion maps of both methods demonstrate relatively identical coverage of features, yet in general, the metabolite coverage in negative ion mode is poor in comparison to coverage obtained for positive ion mode. This is attributed to the better ionization efficiency of lipids in positive ESI mode, since most lipid

classes and subclasses show a great tendency for ionization in positive ESI polarities, while some classes such as glycerolipids solely generate ions in positive ESI mode. In fact, among all the lipid classes under study, only PI, PS, and fatty acids were ionized in negative ion mode. This is in line with the trends reported for LC/MS method development for lipid analysis in section 2.3.1, 3.3.1 and 4.3.1.

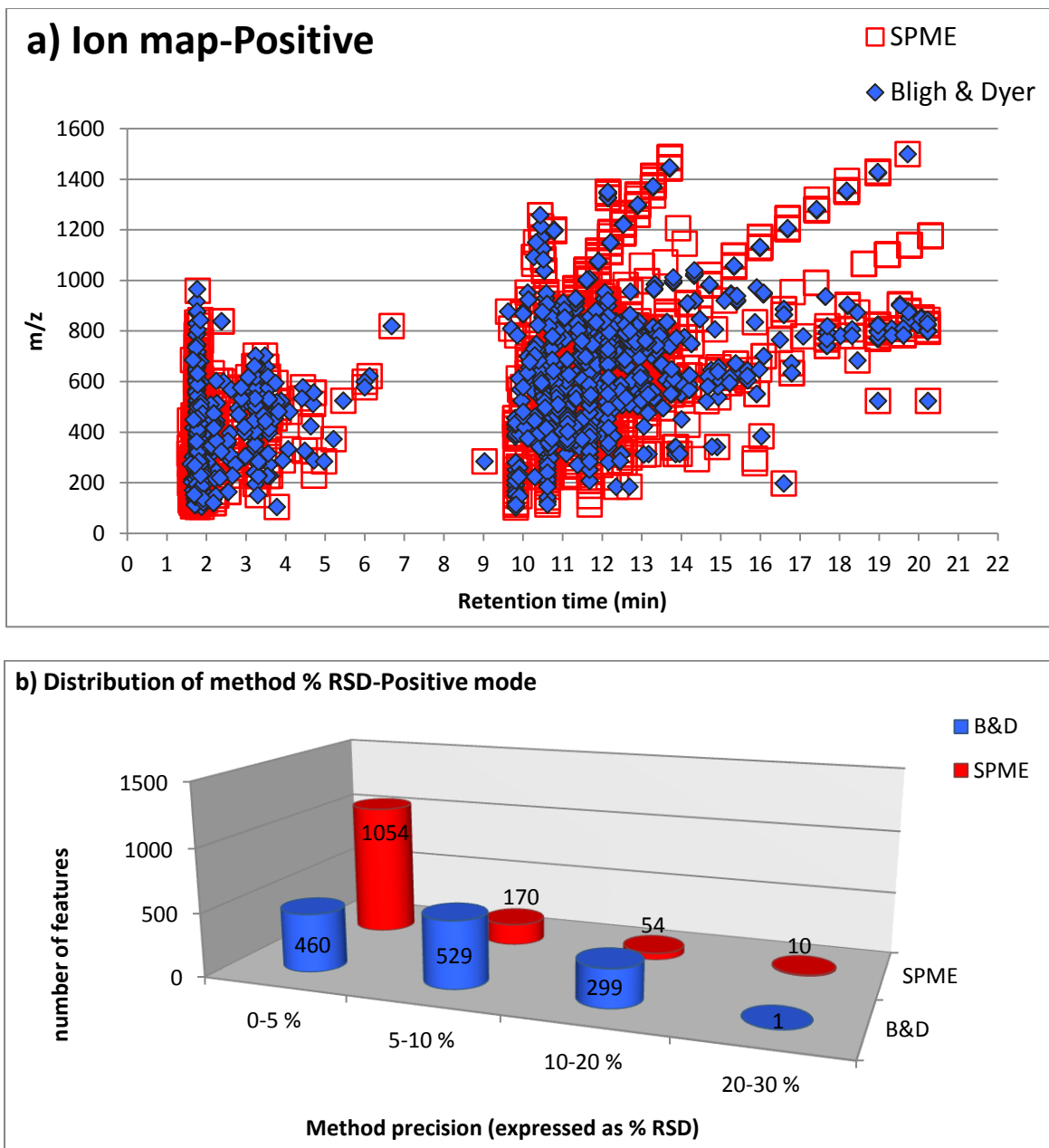


Figure 4-6 (a) Ion map (m/z versus retention time) for HUH7 cell samples extracted by Bligh&Dyer and SPME and analyzed using positive ESI-LC-MS method. (b) Number of peaks with given % RSD obtained for the two independent data sets.

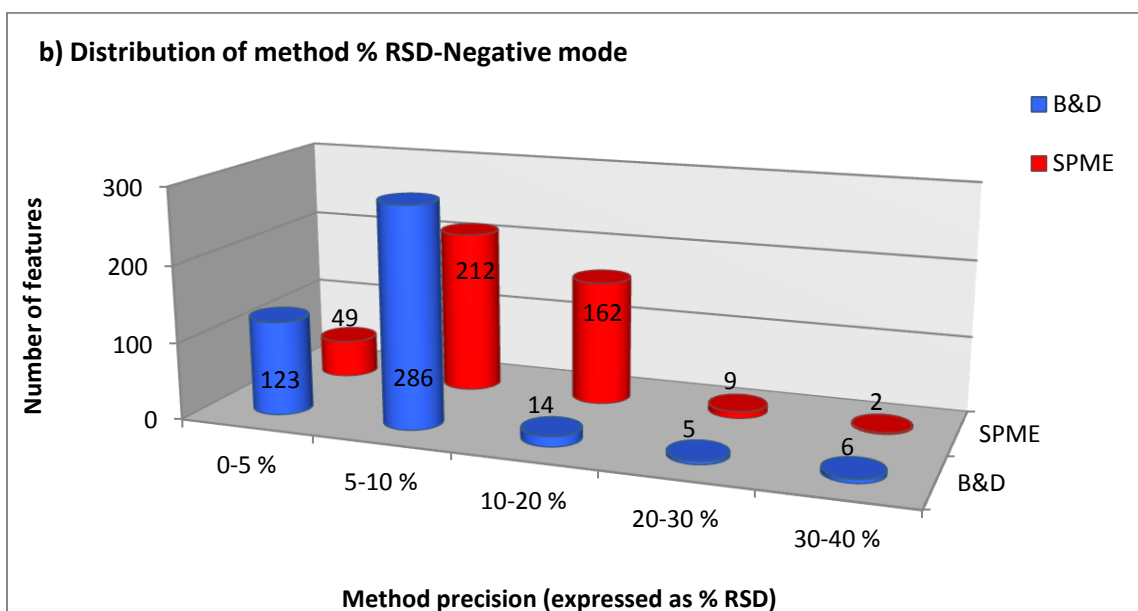
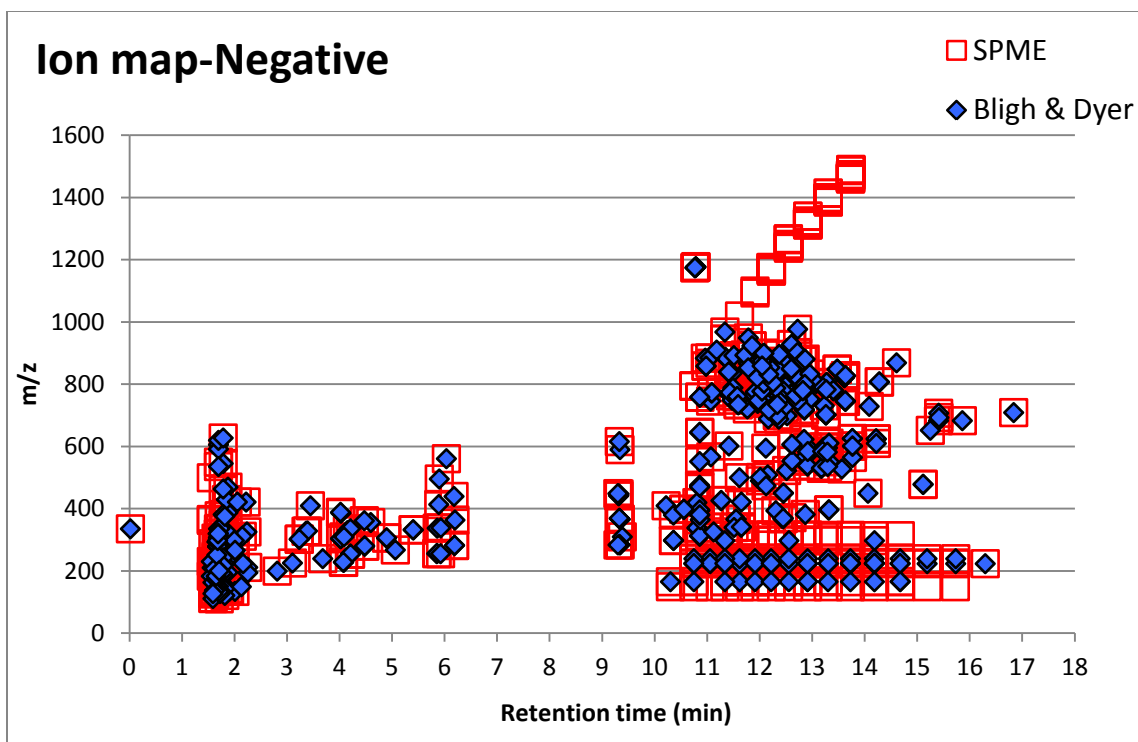


Figure 4-7 (a) Ion map (m/z versus retention time) for HUH7 cell samples extracted by Bligh&Dyer and SPME and analyzed using negative ESI-LC-MS method. (b) Number of peaks with given % RSD obtained for the two independent data sets.

4.3.4 **Quality control (QC) Monitoring- assessment of instrumental response robustness**

Quality control samples were prepared by combining aliquots of all samples, and injected frequently within the sample set. The results for this QC were used to ensure that no systematic drift occurred throughout the entire run time. Plots of signal intensity versus QC run order for known identified lipids for which authentic standards were available are shown in Figure 4-8. Lipids were selected so as to cover a wide range of signal intensities and the entire chromatographic retention times. QC1, QC2, QC3 and QC4 were considered part of the preconditioning procedure, and were included to show that the system was adequately pre-conditioned. Figure 4-8 shows a linear trend line for all QC injections for known lipids observed in the cell samples. The results indicate good performance of the entire LC-MS system.

In addition to targeted monitoring of instrument response during a 24 hour run sequence for the selected lipids, QC samples were also used to assess the quality of lipidomics data. This was performed by subjecting these QC samples to SIMCA processing into a PCA plot together with the entire treated and control cell samples extracted by both Bligh & Dyer and SPME. The results of PCA analysis for the current study, including QC samples, are shown in Figure 4-9. As can be seen, all QC injections (shown in yellow) cluster tightly together, with no evident outliers, which is a good indication of the quality of the data set. This verifies that the instrument response was robust throughout the entire sequence and further processing and interpretation of the dataset is reliable.

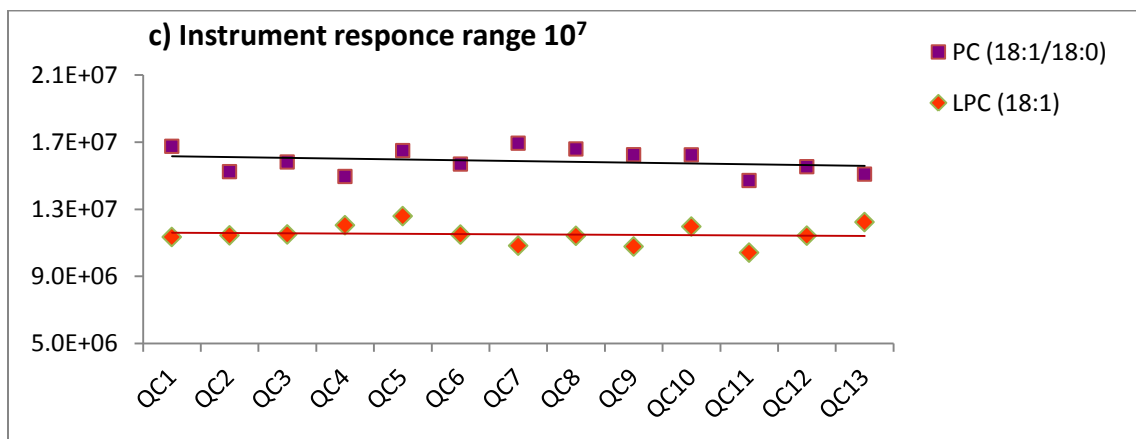
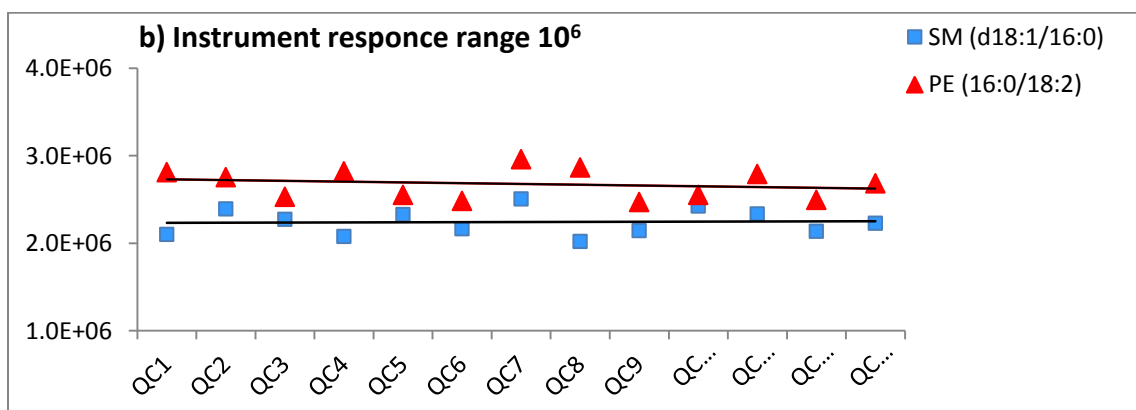
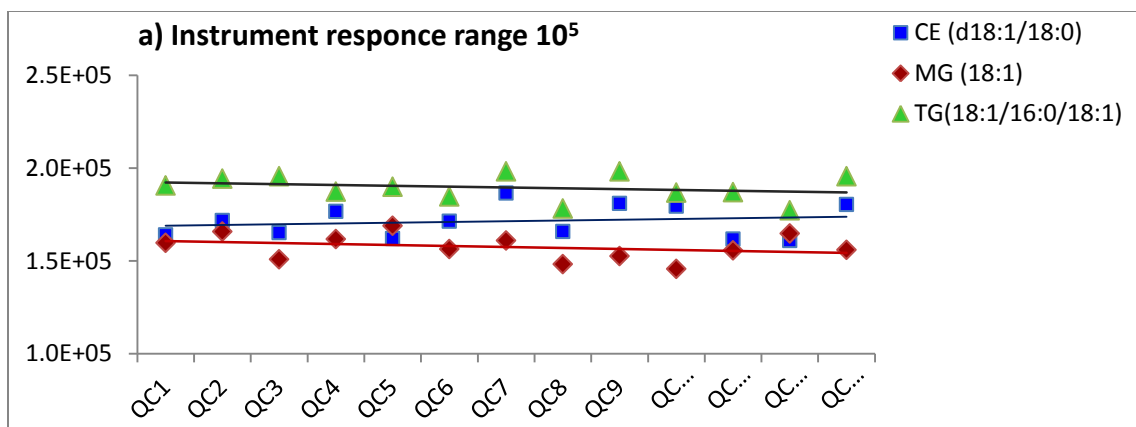


Figure 4-8 Instrumental response variability for several QC injections randomized within the run sequence for selected compounds (a) CE, MG, and TG (b) SM and PE (c) PC and LPC; compounds with different signal intensity ranges are represented in separate charts.

4.3.5 Statistical analysis

In this study, only lipid species whose levels were found to differ significantly between treated and control samples were reported. However, there were plenty of lipid features extracted by both B&D and SPME methods for which concentration levels were not significantly distinguished between groups; as such, these features were not included in the OPLS-DA model list. Principal Component Analysis was conducted on data obtained from HUH7-cell culture analysis, including control and treated cells extracted by both Bligh & Dyer and SPME methods in positive and negative ionization polarities. The purpose of this analysis was to evaluate the ability of the detected features to discriminate changes occurring between individual samples, and to compare differences between extraction methods. The PCA score plots displayed clear separation between different groups of samples. First, three components described 75.9% of the obtained variance, with apparent differentiation found between Bligh & Dyer and SPME, as shown in Figure 4-9.

Moreover, Orthogonal Partial Least Squares-Discriminant analysis (OPLS-DA) models were also obtained considering the score plots of the first and second components. Based on the OPLS-DA models and statistical analysis, samples were compared between control and treated cells. Data were modeled to visualize discrimination between control and treated cells using SPME and BD methods separately. The OPLS-DA score plot shows good separation between Bligh & Dyer versus SPME as different extraction methods; it also shows clear separation between control and treated cells using each method. A list was compiled of all the ions that failed to obtain a higher than VIP score of 1 on the score plots, as these ions were found to be driving the difference between groups in the OPLS-DA model. Numerous

tentatively identified ions were present as multiple adducts. Examples of PCA and OPLS-DA plots are illustrated in Figure 4-9 and Figure 4-10, respectively.

Based on the results obtained from both extraction methods, features that were significantly higher in the treated cells led to the identification of a group of linked phosphatidylcholine (PC) and phosphatidylethanolamine (PE) with a higher degree of unsaturation in their fatty acyl moieties. Moreover, group separation in the OPLS-DA model between the two extraction methods revealed different strengths and weakness of each method in analysis of lipids, which will be discussed further in this chapter.

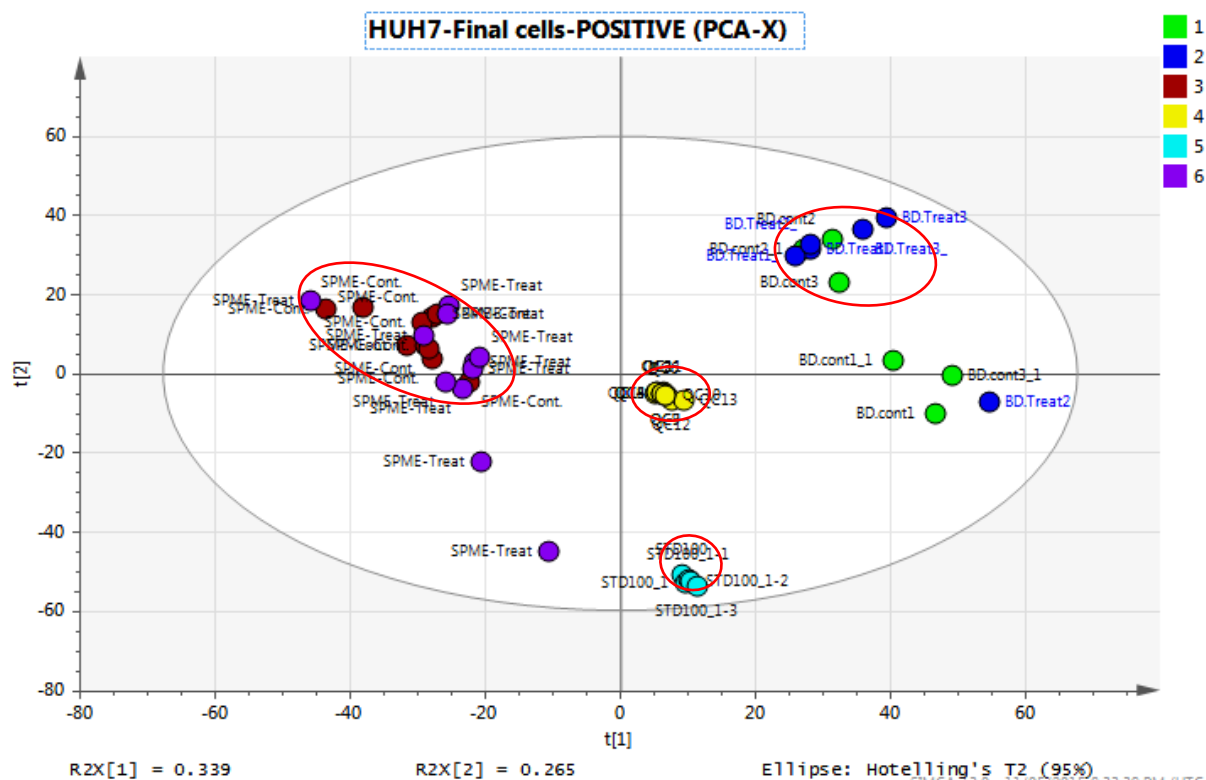


Figure 4-9 Score plots of PCA performed on samples of control and treated cells extracted by SPME (red and violet dots); and samples of control and treated cells extracted by Bligh & Dyer (blue and green dots), QCs (yellow dots) and standard lipids (tiffany blue). Clustering of the QC samples demonstrates the repeatability of the analytical system used. X-axis and Y-axis represent the score of the first and second principal component, respectively. This plot is run for the pool of ion features unselectively.

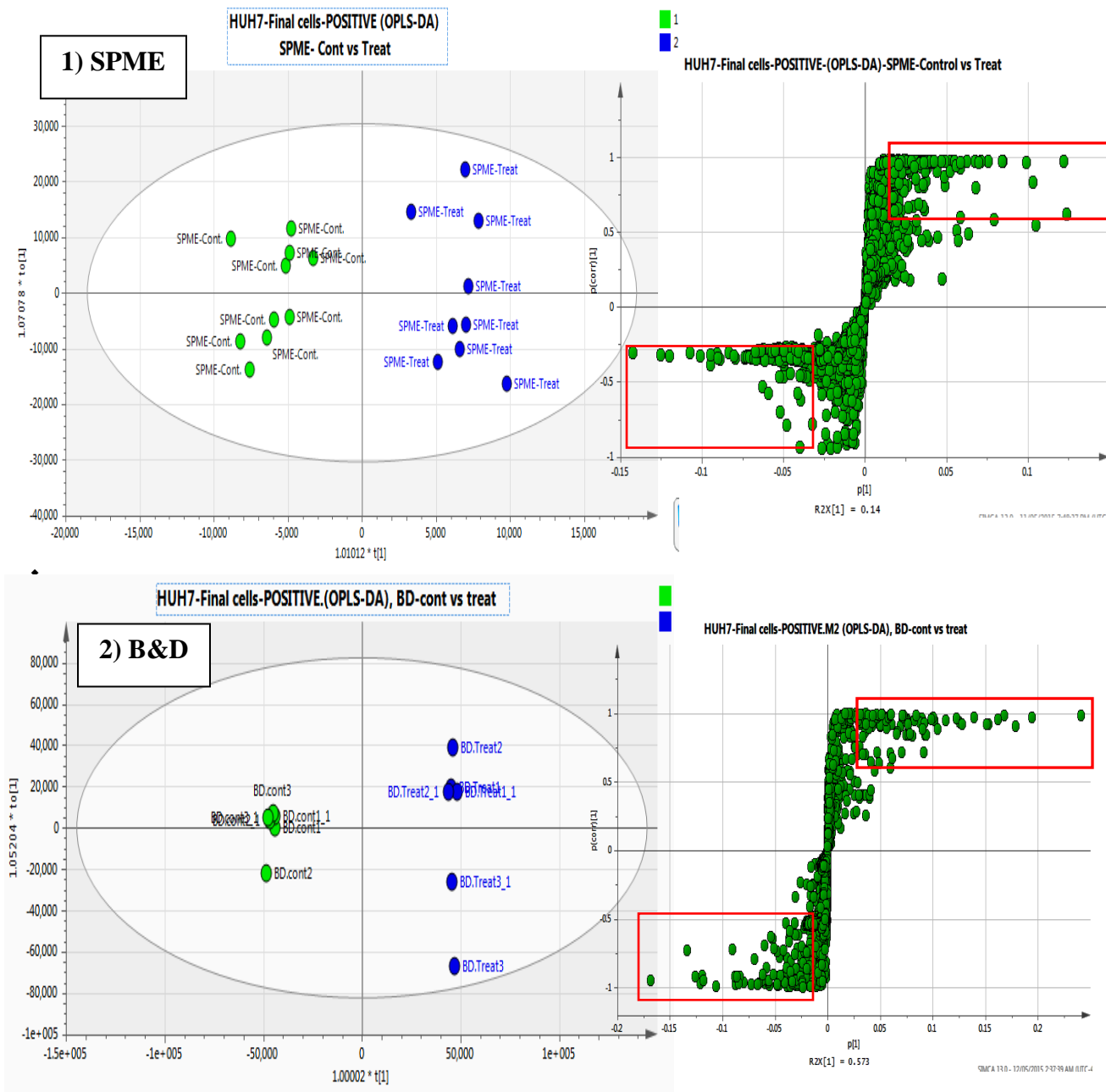


Figure 4-10 Example OPLS-Da models (right) and representative S-plots (left) in positive mode comparing control and treated cell samples by using: 1) SPME (top) and 2) Bligh & Dyer (bottom) extraction methods. Green and blue markers in the OPLS-DA models (right panels) represent the significant difference between profile of control and treated groups, respectively using both methods; each green dot on the S-plots (left panels) represents an ion feature that was detected. The green dots inside red boxes were the ions that drive group separation and screened for further identification

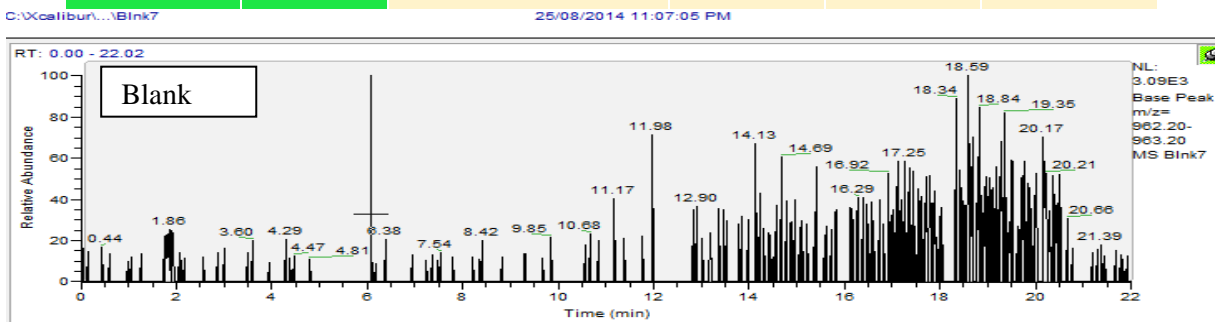
4.3.6 Feature Identification

A simple search of the Metlin and HMDB MS databases normally suggests multiple isobaric lipids for a single specific m/z ratio. A key criterion for narrowing down the selection is chromatographic retention time. As an example for the feature identification procedure, one of the recognized ion features which were significantly different in the OPLS-DA model between groups are illustrated with their XIC chromatograms (Figure 4-11) and the logistics for limiting the search is explained for this feature. For instance, a search through Metlin and HMDB presented numerous choices for different isobaric species for the ion feature with $m/z=780.55338$. However, this feature retained at 11.40 min, a retention time that falls into the region where the majority of the phospholipid species are found.

Notably, lipids originally elute based on their hydrophobicity (LogP) and related acyl chain groups. Within the same lipid sub-group, retention time increases with acyl chain length and degree of saturation. Therefore, the retention time obtained for an m/z value of 780.55338 that elute at min 11.40 could not possibly be a triglyceride, since all TG species elute after 13 min. However, the suggested adduct ions should still be taken into consideration. Some of the feature hints identify PC and PE species for $[M+ACN+H]$ or $[M+NH_4]$. Based on our developed LCMS method, phospholipids solely produce $[M+H]^+$ ions in high intensities. This property eliminates the majority of the remaining alternatives and further refines the list. Since the accuracy of the mass spectrometry was strictly monitored, and the instrument frequently calibrated, a maximum ion tolerance on 5ppm could be confidently selected, which helped to remove plenty of hint results. For example, when searching for structures that corresponded to the unknown ion mass of 780.55338 obtained in positive ion mode, features within 0-5 ppm accuracy of the exact mass determined isobaric phospholipids that

included 25 isomeric PC (36:5) species and 6 isomeric PE (39:5) species. The presence of isobaric species that are ions with the same mass and have different acyl compositions but the same nominal mass of 780.55338 (i.e. 20:5/16:0 PC and 20:5/19:0 PE), will give us the likelihood of both PE and PC phospholipid species. Meanwhile, the presence of isomeric species that have the same chemical formula and belong to the same phospholipid subcategory, but still have different FA localizations; create multiple hits in feature identification; (i.e. 20:5/16:0 PC and 20:4/16:1 PC). Owing to the fact that EPA (20:5) was used as the treating agent, it is expected that the up-regulated phospholipids, glycerolipids and sphingomyelins are more likely to form isomeric species with at least one FA moiety of EPA. For instance, among the possible isomeric moieties associated to ion m/z of 780.55338, the PC (20:5/16:0) is more likely than the PC (20:4/16:1) or PC (18:3/18:2) and such. To be clear, the aim here is to distinguish between lipid classes (PC, PE, and TG) based on retention times, and to narrow down the choices within each class based on mass. However, multiple isomers within each class cannot be discriminated; such further differentiation would require either MS/MS or MSⁿ instruments. In addition, for reassurance, the related peaks were inspected in the XIC chromatograms. One of the significant discriminative metabolites between control and treated HUH7 cell samples was found to be the peak with an m/z ion of 962.72301, detected by both SPME and BD methods in positive ion mode. The XIC of this ion is specified in the Figure 4-11 for the individual samples using both Bligh & Dyer and SPME methods.

Mz	Rt	Metabolite hint	Δ ppm	# of hints	Lipid class
962.72301	13.32	TG (60:15)	0	2	Glycerolipid

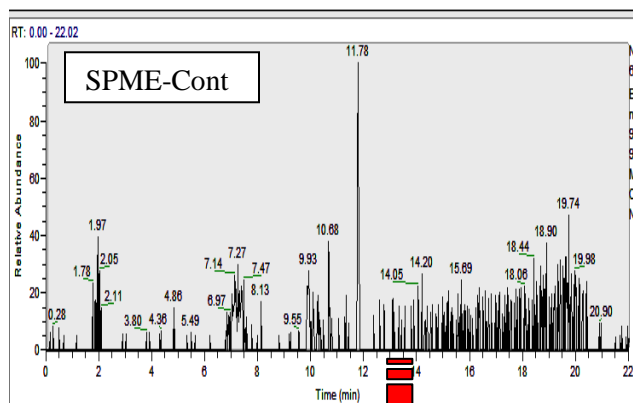


C:\Xcalibur\...Cont-NoSon1

25/08/2014 11:29:55 PM

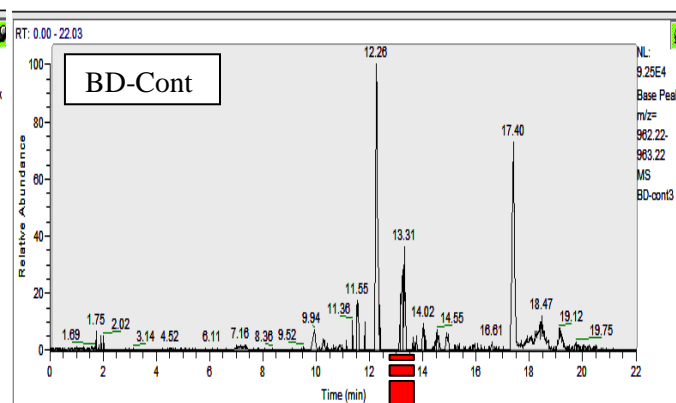
C:\Xcalibur\...BD-cont3

26/08/2014 12:26:07 PM



C:\Xcalibur\...Treat-NoSon1

26/08/2014 12:38:25 AM



C:\Xcalibur\...BD-Treat3

26/08/2014 12:03:17 PM

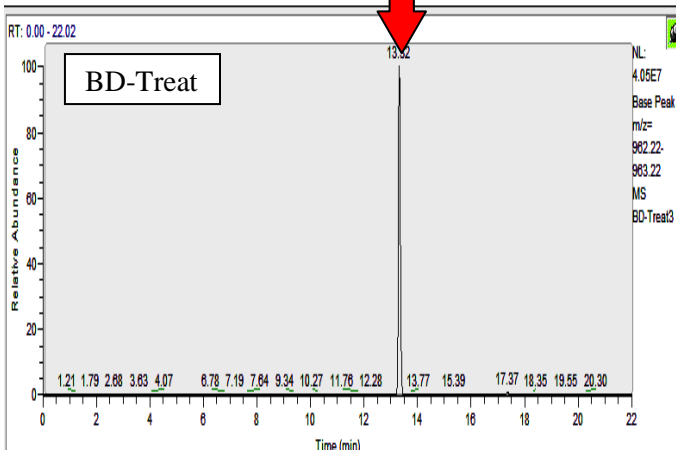
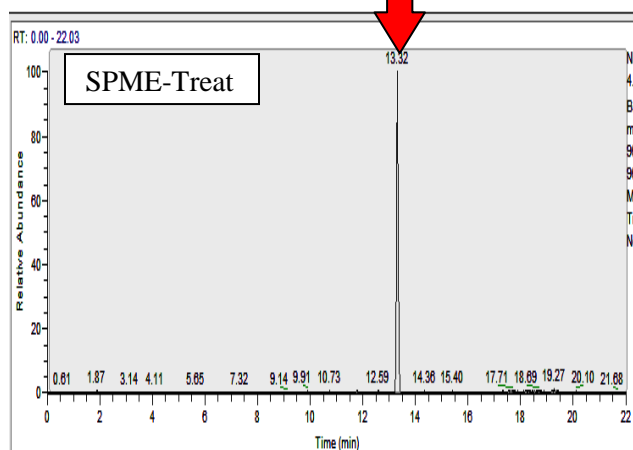


Figure 4-11 Example XIC chromatograms illustrates the ion 962.72301 in control vs. treated groups using SPME and B&D. The chromatograms clearly confirm the changes of this species which were not detectable in the control HUH7 cells cultured in normal condition. However, when the same cells were cultured while supplemented with EPA, this metabolite increased greatly and created a significant discrimination between cell groups in statistical analysis.

4.3.7 Comparison of extraction efficiency of two methods for the group coverage

The performance of the Bligh & Dyer method versus SPME methods for extraction of various lipid groups was compared, and the results of these studies are summarized in Figure 4-12. Several trends are easily apparent. Bligh & Dyer exhibit weak performance for the extraction of low abundant phospholipids such as LysoPCs and PGs which may be related to ESI saturation. The results of the matrix effect evaluation for the two methods supported the current findings by evaluation of ionization suppression/enhancement for LysoPCs and PGs, which can be found in section 4.3.10. In addition, the recognition of subspecies of the Sphingolipid class which contains ceramides and sphingomyelins suggest the superiority of the SPME technique in the extraction of these lipids. On the other hand, the Bligh & Dyer method had a distinct advantage for covering a larger number and diversity of high-abundant membrane phospholipids such as PC and PE. The amount of extracted total lipids is highly dependent on the solvent mixture used in solvent-based extraction methods. Given the high efficiency of chloroform and methanol as extracting solvents in B&D, it is not surprising that more coverage of membrane phospholipids was observed. This is due to the function of methanol in releasing lipids from their protein-lipid complexes, followed by their complete dissolution in chloroform.^{39,107,294} In SPME technique, the sample matrix remains undisturbed and it could be considered as a shortcoming for the extraction of membrane lipids. Both methods performed similarly in the extraction of triglycerides, although SPME worked better the extraction of less abundant glycerolipids, including Monoacylglycerols and Diacylglycerols.

Figure 4-12 shows in more detail the performance of the selected methods for coverage of various lipids. The results implicate that SPME could be a better choice for lipidomics in

regards to better coverage between groups of various lipid categories. Conversely, Bligh & Dyer was shown to be highly efficient in the lipidomic study within class-specific lipids of the same (sub) category such as PC or PEs. By and large, a comparison of the obtained results makes it clear that most lipids identified by Bligh & Dyer were also confirmed by the suggested SPME approach.

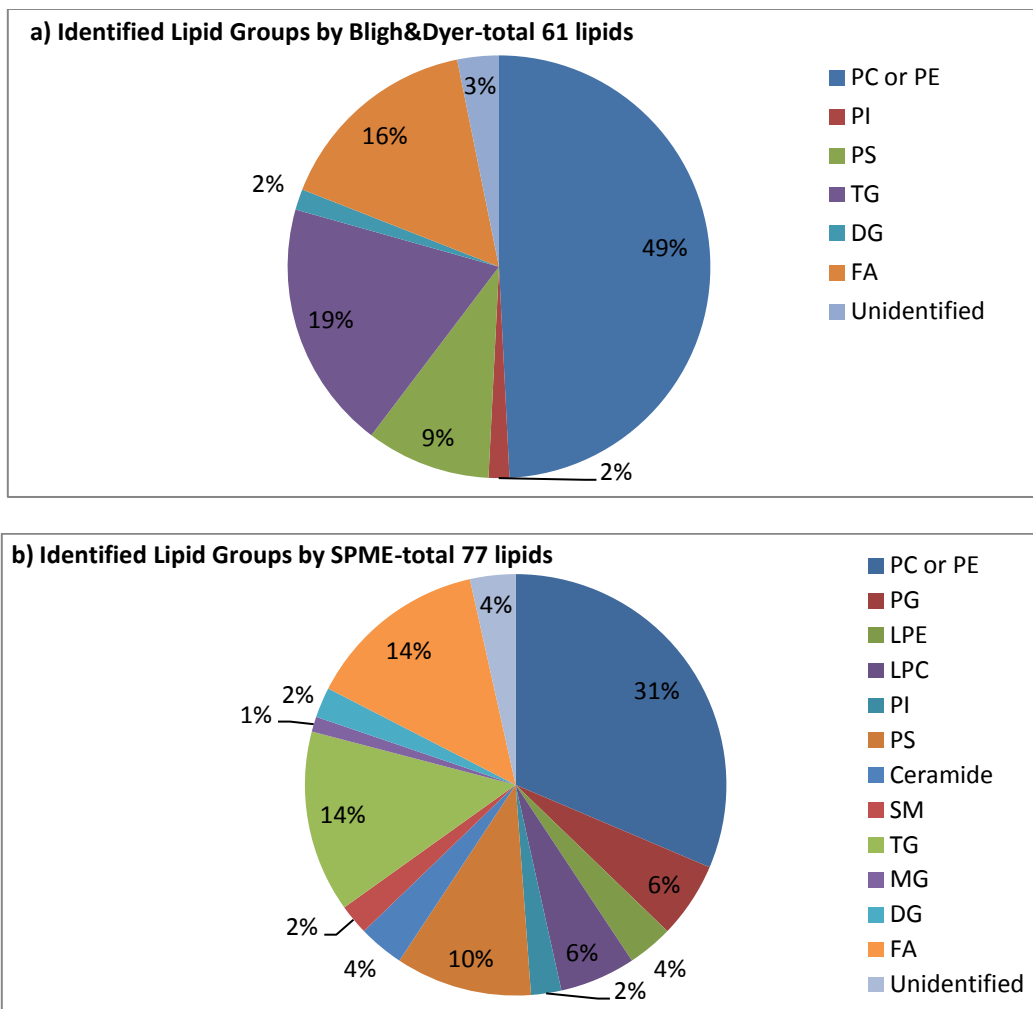


Figure 4-12 Comparison of extraction efficiency of a) Bligh & Dyer and b) SPME in covering a broad range of class-specific lipids.

4.3.8 Control vs. Treated Cells- Up-regulated lipids

Following a conservative and strict criteria, feature ions were confined to a list of significantly up/down-regulated lipids. Considering the lipid ions which were statistically higher in the

group of treated cells, the Bligh & Dyer method yielded a final list of 31 features in positive ion mode and 16 features in negative ion mode, while for the SPME method 39 features were identified in positive ion mode, and 24 features in negative ion mode. Relative quantification was performed by reporting fold changes between control and treated cells for each feature with significant up/down-regulation. For the given lipids, the obtained P-values were calculated using an unpaired t-test comparison of group means for each ion that yielded P-values between 8.90×10^{-3} to 1.06×10^{-25} . Table 4-2 and Table 4-3 summarizes the tentative identification of top lipids found in positive and negative ESI modes, respectively, using both SPME and Bligh & Dyer methods. Features that contributed to the differentiation of samples are listed according to their significant up-regulation as a result of cell treatment with EPA. The similarity of the obtained list of lipid ions by Bligh & Dyer and that of SPME indicates that these two extraction methods are closely comparable. Although the most dominant species were the same in both lists obtained by Bligh & Dyer and SPME, clear differences were apparent in the less abundant components. Through application of the SPME method, a distinct pattern of diversity between lipid categories and sub-categories could be observed. For instance, less abundant phospholipid species such as LysoPC, LysoPE, PS, PG, DG, and CE were detected by SPME, while these features were apparently overlooked with the use of the Bligh & Dyer method. On the other hand, the Bligh & Dyer was shown to be more efficient for the detection of triglycerides and membrane phospholipids. Furthermore, according to our results, application of either method allowed for identification of lipids that emerged as significantly different between the control and treated groups, competently representing sharp distinction of unsaturation and elongation in their fatty acyls chains.

Theoretically, phosphoglycerides, together with sterols and sphingolipids, represent the major structural components of biological membranes. Based on the current results, diversity of TGs with higher degree of unsaturation was clearly detected in the treated cells using both extraction methods. This observation could also be explained by the fact that triacylglycerides provide a reservoir of fatty acids that can be mobilized for energy generation through the action of a series of lipases.²⁹⁵ In this regard, it is possible that enhanced storage of triacylglycerides could be beneficial for cancer cells, as they may be used as a readily available fuel source after re-oxygenation. It has been previously reported that the cells supplemented with omega-3 fatty acids significantly accumulate PUFAs in triglyceride form in their cytoplasm, which can be seen as lipid droplets.^{284,296} Enhanced lipid peroxidation, in turn, results in accumulation of toxic lipid peroxide products in cells that eventually cause cell death. However, in spite of evidence revealing the tumoricidal action of various PUFAs, their exact mechanism(s) of action is still not clearly understood.^{108,286,296–298} To this extent, our findings, taken together with other works, support the necessity of more profound investigations on the potential pathophysiological roles of this class of lipids on cancer cell metabolism. The identified lipids that were located away from the S-plot centre were the most discriminant features involved in differentiation of analyzed samples, and are identified and listed in Table 4-2. Relative quantification was performed by reporting fold changes between control and treated cells for each feature with significant up/down-regulation. Figure 4-13 illustrates the level of difference between controls and treated groups using each extraction method.

Table 4-2 List of upregulated lipids with use of SPME and Bligh & dyer methods - positive mode; the input mz is the extracted mz ions by R program and the exact mass is the mass of lipid feature reported in Lipid Map Database and Metlin Database

Up-regulated- Positive							Fold Change	
	Input mz	Exact mz	RT (min)	Metabolite	# of hits	Class	SPME	B&D
1	780.55338	780.5538	11.41	PC (36:5) or PE (39:5)	33	Phospholipid	56	23
2	806.56897	806.5694	11.36	PC (38:6) or PE (41:6)	37	Phospholipid	41	8
3	990.75424	990.7545	13.80	TG (62:15)	6	Glycerolipid	2566	291
4	268.99826	-	1.88	Unidentified	-	-	5	ND
5	146.01881	-	1.86	Unidentified	-	-	2	ND
6	522.35518	522.3554	3.59	LPC(18:1)	20	Phospholipid	10	ND
7	949.72522	949.7280	16.08	TG (60:13)	14	Glycerolipid	3383	119
8	807.57242	807.5647	11.36	PE (40:7)	22	Phospholipid	43	8
9	854.56918	854.5694	10.71	PC (42:10)	9	Phospholipid	4653	64
10	834.60018	834.6007	11.72	PC (40:6) or PE (43:6)	30	Phospholipid	9	5
11	337.10448	337.1070	2.17	Isopsoralidin	1	Polyketide	6	ND
12	962.72301	962.7232	13.32	TG (60:15)	2	Glycerolipid	3763	353
13	802.53533	802.5381	11.41	PC (38:8)	8	Phospholipid	56	28
14	778.53784	778.5381	10.87	PC (36:6) or PE (39:6)	28	Phospholipid	44	18
15	1018.78551	1018.7858	14.33	TG (64:15)	6	Glycerolipid	2822	299
16	808.58482	808.5851	11.79	PC (38:5) or PE (41:5)	36	Phospholipid	2	8
17	703.57479	703.5749	12.36	PE-Cer(37:1) or SM(34:1)	6	Sphingolipid	11	ND
18	766.57443	766.5745	11.79	PC (36:4)	18	Phospholipid	40	30
19	752.52239	752.5225	10.88	PE (37:5) PC(34:5)	23	Phospholipid	2	103
20	856.58486	856.5851	11.07	PC (42:9)	14	Phospholipid	116	67
21	942.75437	942.7545	15.26	TG (58:11)	28	Glycerolipid	3398	251
22	916.73863	916.7389	15.41	TG (56:10)	26	Glycerolipid	3939	220
23	764.55849	764.5589	11.64	PC (36:5)	6	Phospholipid	96	26
24	921.69405	921.6967	15.41	TG (58:13)	8	Glycerolipid	2989	111
25	764.52227	764.5225	11.46	PE (38:6) or PC (35:6)	31	Phospholipid	21	10
26	970.78556	970.7858	15.91	TG (60:11)	30	Glycerolipid	2165	175
27	944.76997	994.7702	16.08	TG (58:10)	38	Glycerolipid	786	188
28	882.60059	882.6007	11.05	PC (44:10)	6	Phospholipid	1799	214
29	804.55328	804.5538	10.92	PC (36:4) PE (39:4)	21	Phospholipid	112	4
30	768.55314	768.5538	12:59	PE (38:4) or PC (35:4)	51	Phospholipid	2	1
31	738.50655	738.5068	11.51	PE (36:5) or PC (33:5)	24	Phospholipid	29	21
32	832.58469	832.5851	11:25	PC (40:7)	23	Phospholipid	17	4
33	792.58985	792.5902	11.71	PC (38:5)	19	Phospholipid	59	19
34	922.69748	922.7045	15.41	TG (58:10)	1	Glycerolipid	59	19

35	794.56952	794.5694	12.48	PE (40:5) or PC (37:5)	40	Phospholipid	4	3
36	750.54250	750.5432	12.16	PE (38:5)	15	Phospholipid	5	3
37	828.55350	828.5538	10.73	PC (40:9)	12	Phospholipid	295	96
38	480.30832	480.3085	3.83	Lyso PE (18:1)	3	Phospholipid	5	ND
39	721.50641	721.5014	13.39	PG (32:1)	14	Phospholipid	5	ND

Table 4-3 List of upregulated lipids obtained with use of SPME and Bligh & dyer methods- negative mode

Up-regulated-Negative								
	Input mz	Exact mz	RT (min)	Metabolite	# of hits	Class	SPME	B&D
1	301.21768	301.2173	3.23	EPA (20:5)	13	Fatty acid	356	219
2	283.26453	283.2643	9.34	Stearic Acid (18:0)	25	Fatty acid	4	1
3	255.23317	255.2330	5.85	Palmitic acid (14:0)	32	Fatty acid	6	1
4	329.24916	329.2486	4.15	DPA (22:5)	8	Fatty acid	28	28
5	331.26493	331.2643	5.41	Adrenic acid (22:4)	12	Fatty acid	13	1
6	281.24898	281.2486	6.19	Oleic acid, FA (18:1)	69	Fatty acid	11	1
7	303.23346	303.2330	4.02	Arachidonic acid (20:4)	67	Fatty acid	4	1
8	311.29630	311.2956	10.86	Fatty ester (20:0)	26	Fatty acid	5	1
9	279.23341	279.2330	4.48	Lineolic acid (18:2)	168	Fatty acid	4	1
10	253.21765	253.2173	4.21	palmitoleic acid (14:1)	65	Fatty acid	5	ND
11	818.59427	818.5917	12.72	PS (38:1)	7	Phospholipid	4	1
12	883.53685	883.5342	10.97	PI (38:5)	28	Phospholipid	3	3
13	885.55254	885.5499	11.35	PI (38:4)	24	Phospholipid	8	ND
14	892.61004	892.6073	11.72	PS (44:5)	2	Phospholipid	9	7
15	866.59438	866.5917	11.79	PS (42:4)	8	Phospholipid	5	ND
16	894.62626	894.6230	12.37	PS (44:4)	3	Phospholipid	3	ND
17	749.53427	794.5338	12.16	PG (34:0)	11	Phospholipid	6	ND
18	875.58528	875.5808	12.82	PG (44:7)	2	Phospholipid	9	ND
19	838.56301	838.5604	11.41	PS (40:4)	14	Phospholipid	48	36
20	804.61491	804.6124	13.28	PS (38:0)	3	Phospholipid	5	5
21	793.56064	793.5753	12.49	PA (43:4)	2	Phospholipid	8	ND
22	761.58353	761.5702	12.37	PG (36:0)	6	Phospholipid	10	ND
23	844.60968	844.6073	12.61	PS (40:1)	8	Phospholipid	7	1
24	886.55604	886.5604	11.35	PS (44:8)	3	Phospholipid	6	2

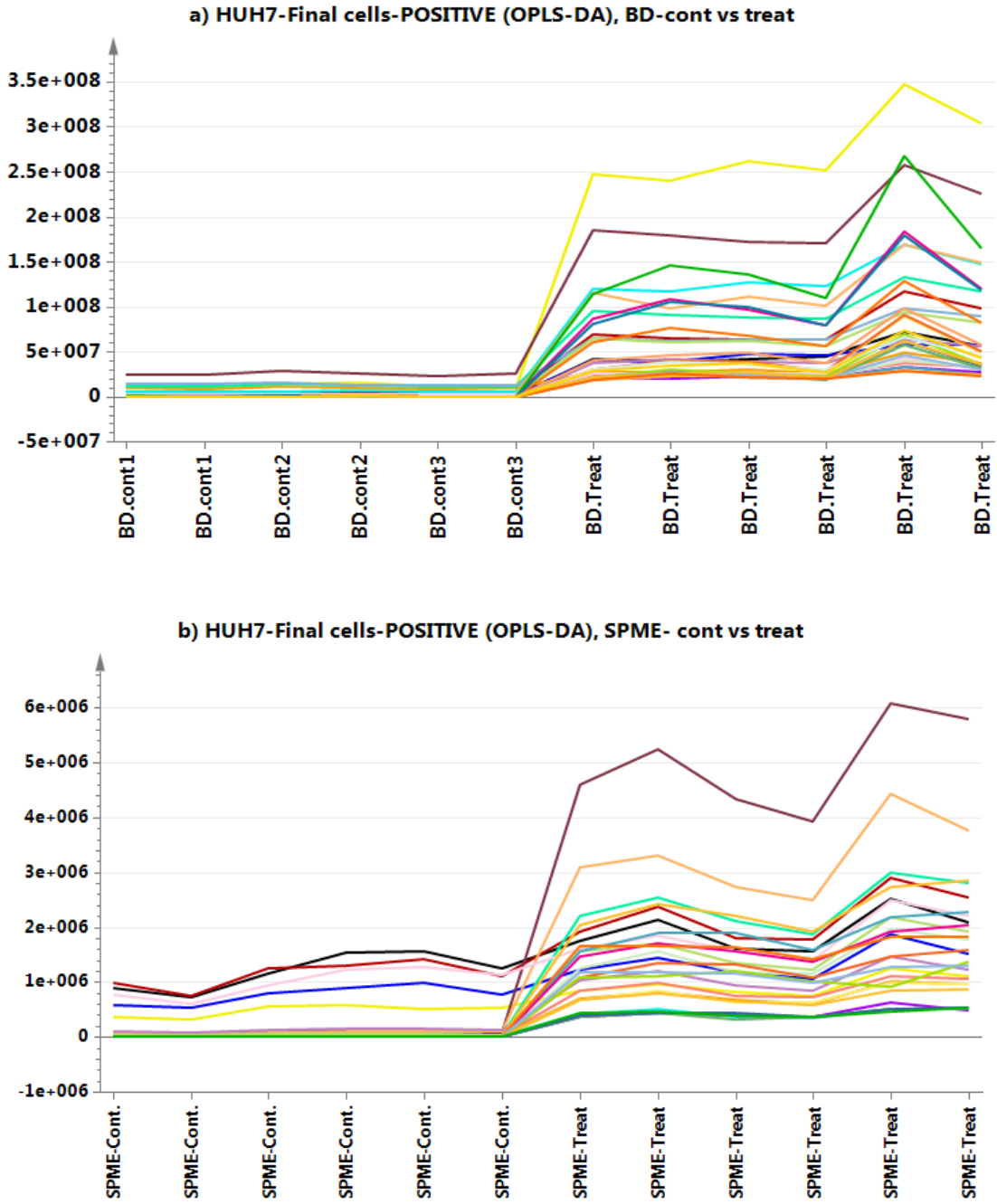


Figure 4-13 Comparison between control and treated cells which illustrate the significant increase in the level of the above listed lipid species with application of a) Bligh & Dyer and b) SPME extraction technique

4.3.9 Control vs. Treated Cells - Down-regulated lipids

By considering the lipid species, which were statistically down-regulated in the treated cells, both methods presented a list of 19 features in positive ion mode. These features were mostly groups of phospholipids with saturated and short hydrocarbon chains that were significantly higher in the control group and down-regulated in the treated cells as a result of treatment with the polyunsaturated fatty acid (EPA). Table 4-4 summarizes the tentative identification of important down-regulated lipids found in positive ESI modes using both SPME and Bligh & Dyer methods. Features that contributed to the differentiation of samples are listed according to their degree of down-regulation as a result of cell treatment. Based on the list, it could be clearly observed that all down-regulated lipid species were more saturated in control cells vs. treated cells. It also clearly shows that the control cancer cells produced phospholipids and glycerolipids with shorter fatty acyl moieties. In negative ion mode, although ions could be observed on the S-plot, none of these ions were achieving higher than VIP 1 on the score plots to drive the difference between groups in the OPLS-DA model.

Table 4-4 List of down-regulated lipids obtained with use of SPME and Bligh & dyer - positive mode

Down-regulated - Positive								
	Input mz	Exact mz	RT (min)	Metabolite	# of hits	Class	SPME	B&D
1	786.60055	786.6007	12.60	PC (36:2) or PE (39:2)	82	Phospholipid	2	10
2	760.58459	760.5861	12.71	PE (37:1) or PC (34:1)	47	Phospholipid	ND	5
3	788.61603	788.6164	13.46	PC (36:1) or PE (39:1)	55	Phospholipid	ND	3
4	782.56924	782.5694	11.85	PC (36:4) or PE (39:4)	60	Phospholipid	ND	8
5	678.50661	678.5068	11.48	PC (28:0) or PE (31:0)	32	Phospholipid	ND	4
6	758.56889	758.5694	12.07	PE (37:1) or PC (34:1)	68	Phospholipid	ND	6
7	732.55333	732.5538	12.06	PE (35:1) or PC (32:1)	40	Phospholipid	5	5
8	794.72296	794.7232	18.98	TG (46:1)	28	Glycerolipid	4	3
9	822.75435	822.7545	20.23	TG (48:1)	60	Glycerolipid	3	2
10	617.51151	617.5140	13.87	DG (34:1)	14	Glycerolipid	5	ND

11	468.30841	468.3085	2.83	LysoPC (14:0)	1	Phospholipid	3	ND
12	627.53450	627.4983	11.34	DG (37:6)	4	Glycerolipid	3	3
13	730.53777	730.5381	11:49	PE (35:2) or PC (32:2)	32	Phospholipid	3	9
14	761.58805	761.5691	12.71	PG (20:3)	5	Phospholipid	5	ND
15	772.58445	772.5851	12.27	PC (35:2)	56	Phospholipid	2	9
16	704.52201	704.5225	11.44	PE (33:1) or PC (30:1)	29	Phospholipid	3	3
17	1279.35114		17.47	Unidentified	-	-	3	ND
18	1205.33235		16.69	Unidentified	-	-	3	ND
19	687.19942		12.58	Unidentified	-	-	21	3

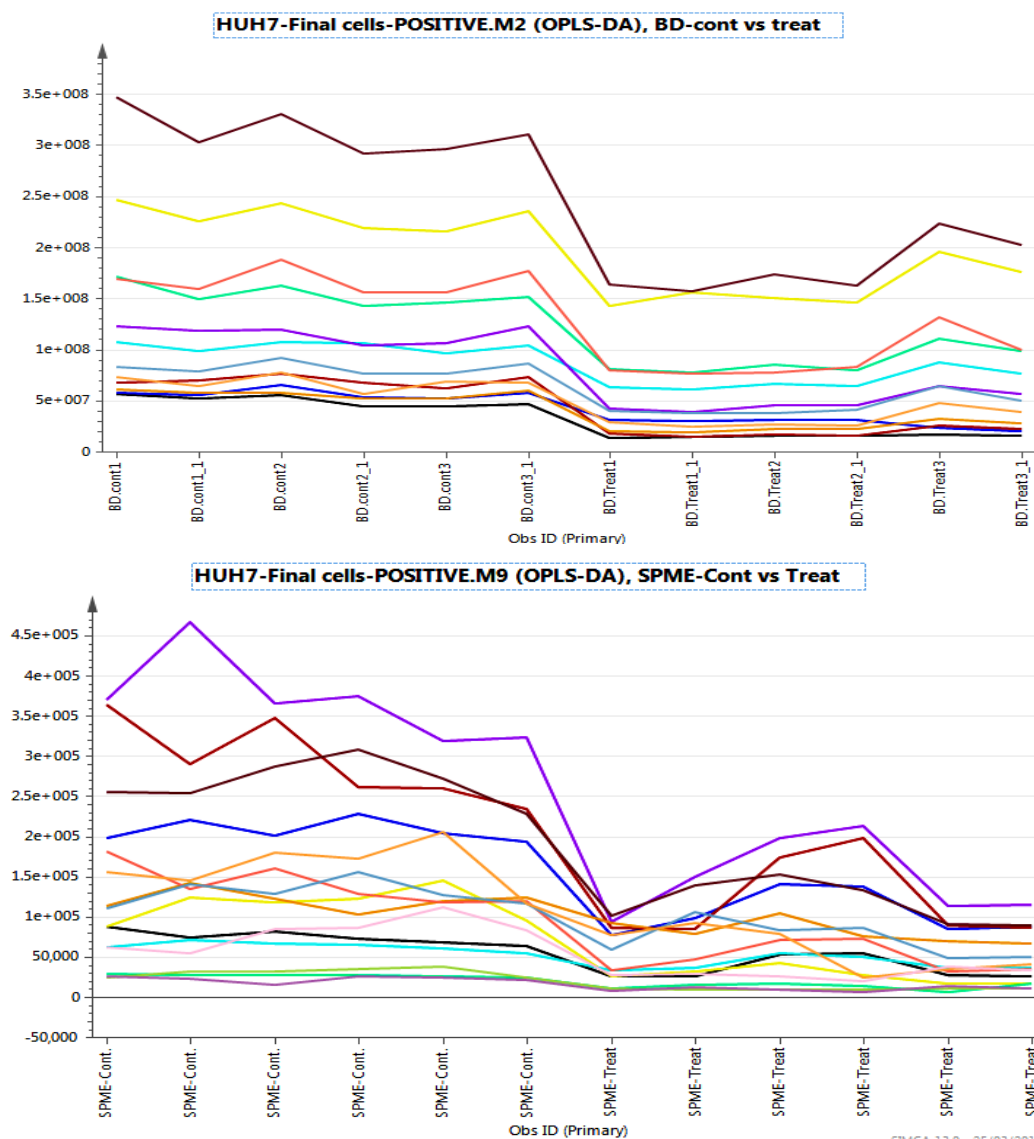


Figure 4-14 The two graphs illustrate the significant decrease of the above listed lipids in the treated cells extracted by top) Bligh & Dyer and bottom) SPME method.

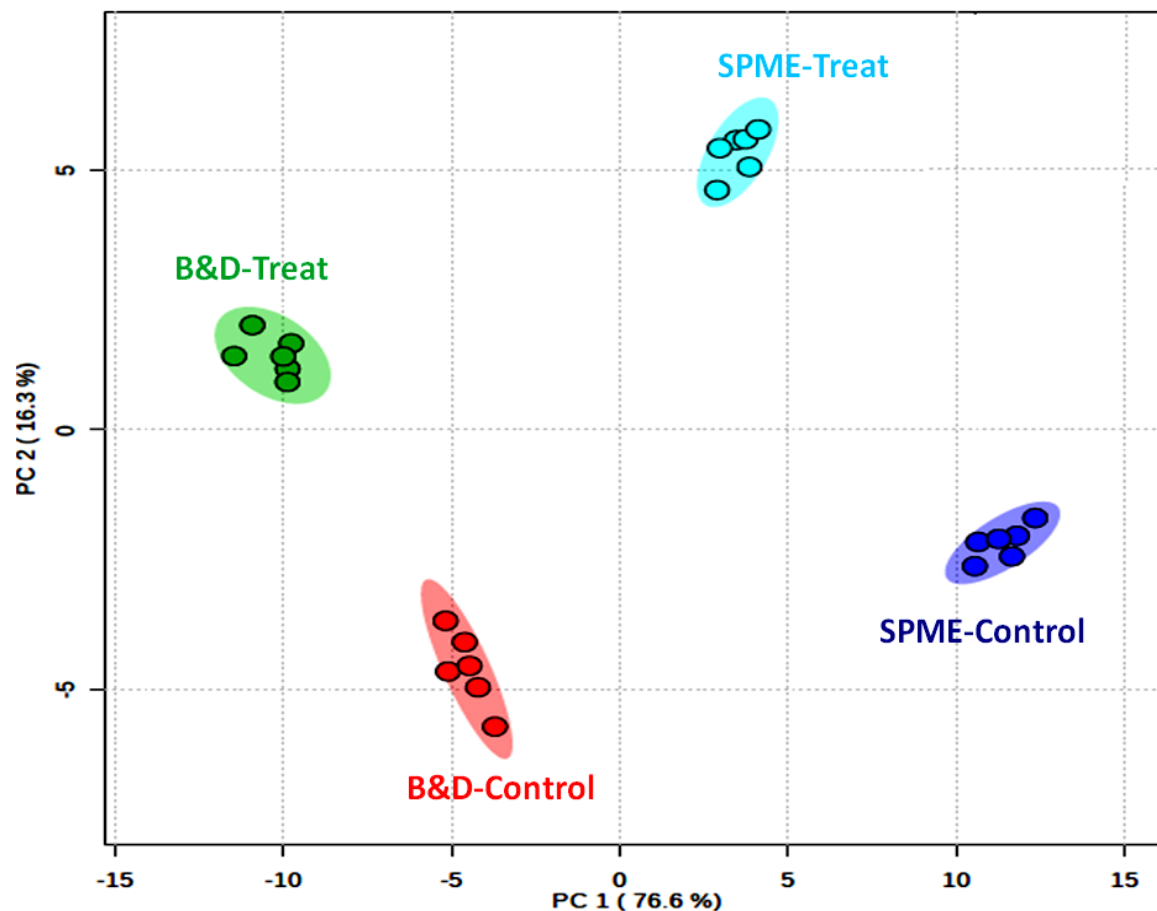


Figure 4-15 Score plots of PCA performed on the lipid features of most significant difference listed in Table 4-2, Table 4-3 and Table 4-4. Plot illustrates a clear separation between BD-control and SPME-control, BD-Treat and SPME-Treat. The x-axes and y-axes represent the score of the first and second principal component contributing 72.6% and 20.3% variances, respectively.

Figure 4-14 illustrates the level of difference between control and treated groups using each extraction method. The PCA score plots displayed clear separation between different groups of samples.

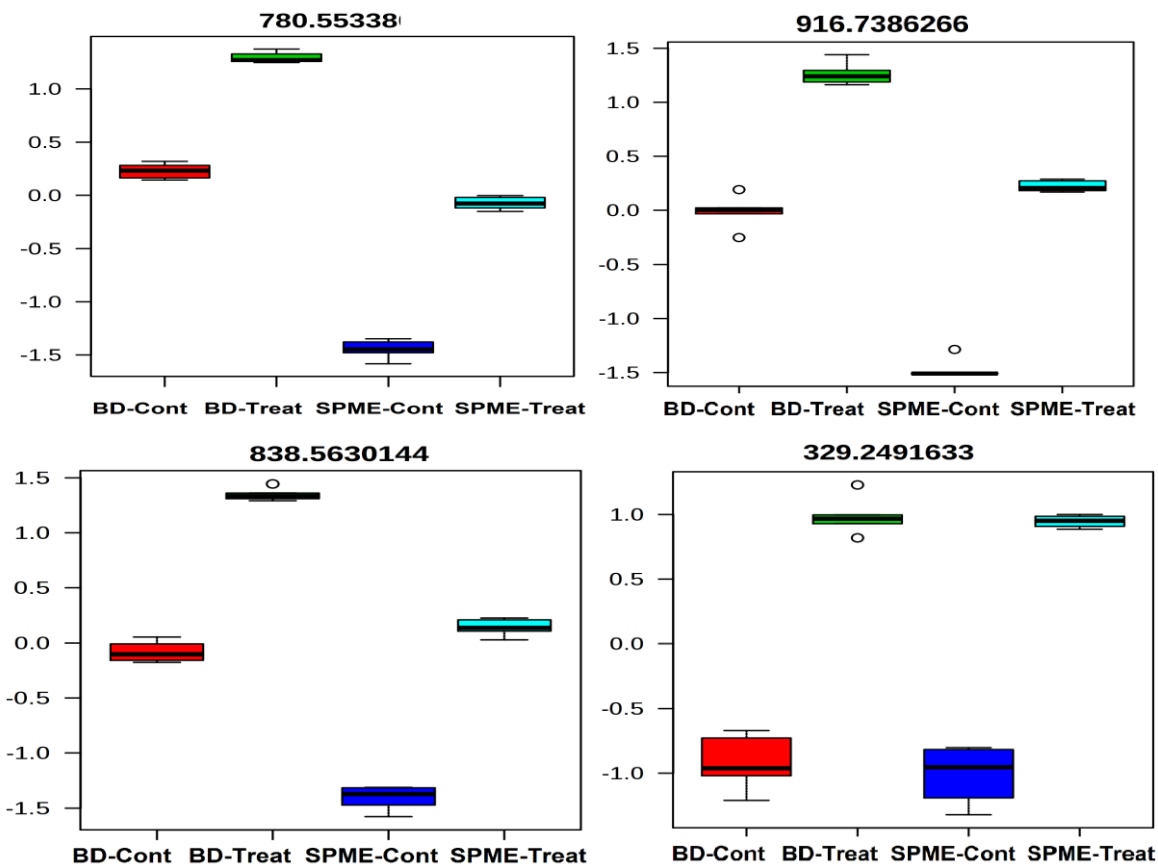


Figure 4-16 Example Box-whisker plots representing four potential lipid candidates with lowest p values between the control and treated cell groups: m/z 780.55338 for PC (20:5/16:0) or PE (20:5/19:0); m/z 916.738626 for TG (20:5/20:5/16:0), m/z 838.56301 for PS (22:4/18:0) and m/z 329.24916 for docosapentaenoic acid (22:5).

Representative box-whisker plots for some of the ion features are shown in Figure 4-16 and indicate the individual discrimination power between controls and treated cells using each method.

In cancer biology, massive amounts of lipids are required as building blocks of cell membranes in order to promote the high proliferation of tumor cells. To achieve this, special modifications occur in the lipid composition of cancer cells that distort the cellular adhesion properties and cause resistance to apoptosis. The importance of membrane synthesis in cancer cells has been highlighted by the excessive expression and activity of some enzymes that are involved in the synthesis of phosphatidylcholine (PC) and phosphatidylethanolamine (PE)

(the major phospholipids of cellular membranes).^{299,300} As mammalian cells are inefficient in synthesizing polyunsaturated fatty acids because of Δ^3 -desaturase enzyme deficiency, a high rate of *de novo* lipid synthesis in tumors elevates the relative amount of saturated and monounsaturated fatty acids. To support this hypothesis, the same group of lipids (containing short chain saturated fatty acyls) were detected more abundantly in the control cells and were diminished as a result of treatment with a highly unsaturated long chain fatty acid. This may lead to production of lipid species with longer aliphatic chains and multiple double bonds in their structure. Relying solely on the obtained data, a conclusion cannot be made that increased levels of polyunsaturated lipids (including those phosphatidylcholines and phosphatidylethanolamines) in treated cells could directly cause lipotoxicity and cell apoptosis. However, recently published research suggests that plasma membranes containing abundant quantities of polyunsaturated phospholipids are more prone to deformation and fission.³⁰¹ Accordingly, in addition to suggesting that these lipids may induce modification in cell metabolism and morphology, our data also supports the necessity of further chemotaxonomical investigations in this arena.

4.3.10 Matrix effect evaluation

Among all analytical methods employed for lipid analysis, LC-MS is the most commonly used technique for sensitive detection of a variety of lipids in biological matrices. However, phospholipids among all lipid categories may cause ionization suppression due to their high biological abundance, which results in suboptimal ionization of low-abundant lipid species. A matrix effect occurs when matrix molecules co-elute with the analyte of interest, competing for available charges, and consequently diminishing the ionization efficiency of the ESI interface. Absolute matrix effect was assessed using the post extraction spike method described by Matuszewski.²⁰⁹ As described in Equation 2-1, a calculation of matrix effect can be performed by relating the peak area of lipid standards in neat solvent to the peak area of the same lipid standards spiked in a matrix extract sample.

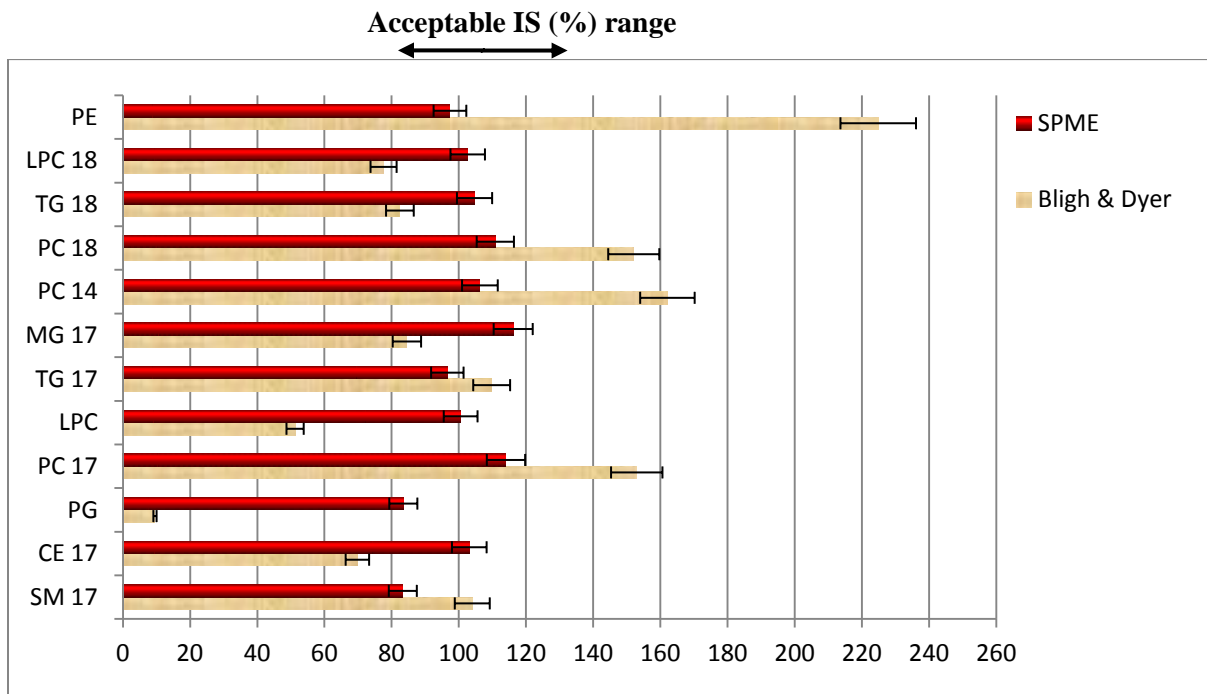


Figure 4-17 Evaluation of ionization suppression involved in the extraction of cell samples

IS mvalues larger than 120% and smaller than 80% represent significant ionization enhancement or suppression for a given analyte. In the Bligh & Dyer samples, signal suppression was observed for PG, CE, and LysoPC, while PE and PC indicated significant ionization enhancement. However, In SPME samples, neither of the lipid species demonstrated a notable matrix effect (Figure 10). This confirms the overall quality of the SPME method in regards to the reliability of the collected data.

4.4 Conclusion

Previous research has indicated that when tumor cells are supplemented with PUFAs, a modification in their phospholipid fraction occurs.^{286,302} This modification alters the lipid metabolism pattern, consequently interrupting the lipid bilayer membrane, changing the cell morphology, and suppressing cell growth. The current study considered these findings to investigate lipidome alterations in treated cells while comparing the proposed SPME method to conventional LLE methodology based on the Bligh & Dyer protocol. The use of SPME yielded a list of 77 lipid species that were found to differ significantly between control and treated cells, from which 63 lipids were up-regulated in treated cells. This list is nearly identical to the peer list obtained by the BD method. However, more diversity of lipid classes and subclasses such as LPC, ceramides, and prenol lipids were observed using SPME. Furthermore, in a comparison between control and treated cells, no single lipid was found to be significantly up-regulated or down-regulated to be determined as a potential biomarker; rather, a pattern of modifications emerged in the HCC cell lipidome profile, which clearly distinguished the control group from the cells supplemented with eicosapentaenoic acid (EPA).

Treated cell samples showed significant changes in the structure of lipids, primarily membrane lipids, including elongated triglycerides and sphingomyelins, both of whose fatty acyl moieties acquired a higher degree of unsaturation. Neither of the previously published studies investigated the modification of the whole lipidome profile of cancer cells when exposed to polyunsaturated fatty acids, mainly focusing on the effect of PUFAs on cell proliferation and metabolism pathways.^{286,303,304} In other work, it has been reported that cancer cells supplemented by EPA demonstrate morphological features of cell death characterized by cell shrinkage and detachment. This phenomenon could be explained according to the results of the present study, in that the significantly increased number of polyunsaturated phospholipids prevents orderly collocation and tight packing of these molecules into a neat lipid bilayer assembly, thus facilitating membrane deformation.³⁰¹ Moreover, a comparison of the SPME method with the Bligh and Dyer solvent extraction technique indicated the absence of a matrix effect (ionization enhancement/suppression) for all lipid classes for SPME applications. This constitutes an advantage of SPME method not only for isolation of lipid analytes from intrusive macromolecules, but also on prevention of the suppressive effect of highly abundant lipids in the ESI source on lipid species with lower abundance. The observed lipidome differences in our study were relatively considerable between the two groups of control and treated cells, yet the differences between the two applied techniques can be considered trivial for effective extraction of lipid components. The data presented within this paper supports the use of SPME in lipidomic studies of cell line. In comparison to Bligh & Dyer, SPME provided more comprehensive simultaneous coverage of less hydrophobic lipid species with lower abundance, while Bligh & Dyer performed well for the coverage of PC and PE as membrane phospholipids species with

diversity in their aliphatic chain. The strength of our study is in the use of the validated SPME method coupled with the LC–MS platform; the proposed protocol is simple, does not require any sample pre-treatment, provides excellent clean-up, and prevents matrix effects, which is one of the main drawbacks of standard procedures. Therefore, this method could be successfully used as an alternative approach for sample preparation and sample clean-up in lipidomic studies. The presented study was a first approach to establish improved alteration in lipidomics studies of cell lines, which may now be followed-up in an extensive cohort of HCC tumors or any other tumor tissue.

Chapter 5

Summary and future directions

5.1 Summary

Recent advancements in modern MS-based analytical technologies have allowed for the creation of a wealth of information in metabolomics and lipidomics studies. The created information should meet requirements of reliability, consistency, and authenticity, all of which are challenging to achieve due to the complexity of the “omic” workflow across multiple platforms. Also, the presence of high indulgence metabolite, peptide, and protein backgrounds makes target discrimination difficult.

It has been long established that the extended process of sample preparation with multiple steps involved can increase the risk of errors and pitfalls in the obtained results, since each step is susceptible to experimental artifacts. In this process, selectivity and sample clean-up can be challenged during sample handling, and consequently influence the diversity and integrity of the captured lipidome. Nonetheless, in spite of the growing rate of universal interest in clinical studies and biomarker discovery, none of the currently available sample preparation methods have been truly modified and developed to acquire the desired competency for *in vivo*, *ex vivo*, and *in vitro* lipidomics with no demand of additional steps. This thesis covers a collection of analytical method developments for *in vivo* and *in vitro* lipid analysis using multipurpose SPME approaches in complex biological matrices; from sampling and sample preparation, use of fiber and thin film coatings, to separation with RP-LC and detection by ESI/MS or tandem MS/MS. The presented work shows that modern

sample preparation approaches based on SPME can provide new insights in lipid analysis from complex biological samples.

In this context, SPME has been fulfilling remarkable transformations in availability, throughput, configuration, application flexibility, as well as compatibility with groundbreaking advancements in analytical instrumentation. This technique was initially developed for GC applications, but to-date it is routinely employed in combination with other analytical platforms such as LC, electrophoresis, NMR, and mass spectrometry. The most dramatic advancement of SPME is in particular the feasibility of this technique for in vivo clinical studies; by extracting directly from living organisms for in vivo analysis, the necessity of a quenching step is completely excluded from the total workflow, while the captured lipids are the exact snapshot of the metabolic state at the time of sampling. In addition, various headspace SPME platforms in combination with GC-MS and GC \times GC systems were used for the extraction and enrichment of volatile compounds in plant and food metabolomics.¹⁶¹⁻¹⁶⁸ Insofar, headspace SPME has been successfully applied for the determination of metabolic changes and potential biomarkers from the volatile emissions of breath, skin, cancer tissue, and cell line.¹⁶⁹⁻¹⁷³ However, due to the non-volatile and highly hydrophobic nature of lipids, headspace SPME cannot be considered as an option for comprehensive lipidomics. Here, we described a high throughput molecular lipidomics that benefits from the two available configurations of SPME, including the commercial SPME fibers suitable for in vivo studies, and the thin film geometry on a 96-blade device to potentiate high throughput ex vivo and in vitro lipid analyses. In this thesis, both approaches are comprehensively validated for absolute quantification targeted lipid analysis, as well as untargeted lipidomic profiling of several hundreds of molecular lipid species in diverse and

complex biological systems from biological fluids to cell culture. As a starting point, free fatty acids were selected as a class-specific lipid group. Commercial rod-fiber C18 SPME fibers were tentatively used *in vitro* to validate the extraction procedure from human and fish plasma, followed by use of LCMS using an ion-trap simple platform for accurate measurement and monitoring of polyunsaturated fatty acids in plasma samples of several patients during cardiac surgery. Afterwards, the 96-well robot-assisted SPME with the use of thin film geometry was employed for whole lipid analysis based on bioanalytical method validation guidelines. This was an attempt to minimize and automate the sample handling procedure while covering sensitive extraction of all lipid categories. Lipid extracts were next analyzed on a triple quadruple MS/MS for exact quantification of target lipids in human plasma, since it is likely that circulating plasma lipids can be used as predictive and diagnostic hallmarks in several disease states. Finally, in the last effort, the validity of the proposed thin film protocol was further examined on a group of cultured human hepatocellular cells for lipid profiling and “discovery lipidomics” assay. In this part, the list of extracted lipids was successfully compared with that obtained by use of traditional liquid-liquid extraction based on the Bligh & Dyer protocol. The validation and key features of SPME methodology were discussed in comparison with Bligh & Dyer, emphasizing practical issues associated with operating the platform, and differences in the obtained results. By implementing lipid class extraction and separation prior to MS analysis, quantitative lipidomics of a wide range of cells and tissues can be achieved. The research presented herein highlights the efficacy of both fiber and thin film geometries by discussing their application for both low-throughput *in vivo* and high-throughput *ex vivo/in vitro* lipidomics studies. Just like any other counterpart methodologies, the presented SPME protocols come

along with several shortcomings, leaving room for improvement in the future studies. For instance, owing to its non-exhaustive nature, SPME renders lower extraction amounts that interpret into lower instrumental intensity and inferior overall sensitivity when comparing to other conventional sample preparation methods. Regardless of this shortcoming, SPME still suggests an identical precision in the quantitative and qualitative evaluations, indicating that smaller amounts of extracted lipids are still sufficient for trustworthy and consistent measurements. Looking at the glass half-full, non-exhaustive sampling with lower extracted amounts is somehow beneficial. The top-level advantages of this feature were clearly reflected in the results of matrix effect studies throughout the entire thesis, starting from fatty acids, whole lipid quantitative MS/MS, to lipidomics profiling. This is further beneficial not only from an ESI ionization efficiency point of view, but also concentration wise; abundant lipids with higher concentrations cannot conceal the peak of lipids existing in lower concentrations with lower signal intensities. One may suggest performing final extract dilutions for counterpart exhaustive methods to prevent this phenomenon; on one hand, dilution reduces the concentration of low abundant analytes to below-detection limits, while on the other hand, it is one additional step added to the sample preparation procedure, which increases the chance of contamination and artifact encounters.

Despite the success of SPME in efficient extraction of lipid species from various biological matrices, for ex-vivo and in vitro sampling, there are inherent challenges particularly if the method is anticipated for the extraction of unstable lipids fast turn-over lipid metabolites. The current sampling time of 90 min may not be appropriate for monitoring rapid changes in extracellular lipids. Moreover, the long extraction time may result in deterioration and decomposition of lipoproteins and other bonded lipids. This seemingly problem will require further studies in order to improve the extraction time. A possible approach may be exploration

of the extraction under pre-equilibrium or kinetic calibration condition which will allow for improved time resolution. The other SPME coating may also need to be evaluated for increasing the efficiency and coverage of lipid metabolites. Optimization of coating composition will lead to better extraction of more polar lipid components as it has been previously demonstrated for metabolomics studies.³⁰⁵ For instance, the new mixed-mode coatings include less hydrophobic lipids such as lyso phospholipids. Lastly, the non-exhaustive SPME is of benefit to in vivo sampling methodologies, since it minimizes the system disturbance and provides the opportunity of using small probe dimensions inserted directly into living system organs. In this thesis, several methodological improvements were achieved throughout the new SPME protocols for usefulness and practicability of lipidomics sample preparation. First and foremost, the extraction procedure was simplified; second, a broader range of lipids with diversity in their classes and subclasses was achieved; third, direct extraction from biological samples was attainable without the need of multi-step sample pre-treatment and sampling; fourth, a better sample clean-up was achieved, and fifth, an improved, fully automated method for measurement of all lipid categories over a broad range was introduced.

Last but not least, standard addition calibration using SPME provided accurate measurement of total and free lipid concentrations in biological samples. Meanwhile, a valuable insight into the lipid-protein interaction mechanisms is conceivable, and study of different binding affinities in complex biofluids is no longer a challenge. Finally, the SPME method offers important information on bioavailable concentrations of the analytes in plasma samples.

5.2 Future directions

The future of lipidomics holds massive deliverable output, which is essential to delineate disease mechanisms for the scientific community across the biological, clinical, and

biomedical research fields. As a consequence, it is critical for the 96-well format SPME to automatically handle intensive tasks and also be expanded to larger formats so as to speed up the extraction pipelines, and as a result, increase the throughput of the system.

One of the future directions of the currently presented thesis could be the development of more efficient SPME coatings with improved selectivity and sensitivity for the extraction of individual groups of specific lipids. For instance, several phospholipids among all other lipid categories are of special interest in biomarker discovery lipidomics studies. These phospholipids contain a hydrophilic positively-charged ammonium head group (choline) which is connected to one or two hydrophobic tail(s). Accordingly, hydrophilic-lipophilic balanced (HLB) particles can be used as a potential sorbent coating in both thin-film and fiber geometries to facilitate more selective and effective extraction of this group of lipids. Several effective coatings were provided and reported in our lab for the extraction of quaternary ammonium compounds (QACs), which are structurally similar to some phospholipids;³⁰⁶ they also can be the potential choice for specified lipid extractions in the near future. However, newly emerging components of the SPME workflow will have to undergo systematic validation before routine adoption for complex matrices.

Moreover, the presented lipid extraction protocol can also be expanded to the *in vivo* SPME platform, using the available needle-supported SPME fiber for extraction of lipids from tissue or organ of live and freely-moving animals for disease discovery research. It is noteworthy to mention that even though the presented SPME protocol herein is validated based on equilibrium extraction, kinetic calibration could be also considered for *in vivo* and *in vitro* applications so as to minimize the disturbance of the system under study by reducing the time of extraction.^{160,174,197,228,307} In addition, the validated method should not be

restricted to clinical analysis of lipids; it can be also employed towards the analysis of lipid content of food or plant for nutrition lipidomics purposes.

In conclusion, the present study was a first approach to establish promising alterations in the clinical lipidomics workflow, which may now be followed-up in an extensive cohort of various biological matrices.

Bibliography

- (1) Fahy, E.; Subramaniam, S.; Brown, H. A.; Glass, C. K.; Merrill, A. H.; Murphy, R. C.; Raetz, C. R. H.; Russell, D. W.; Seyama, Y.; Shaw, W.; Shimizu, T.; Spener, F.; Van Meer, G.; VanNieuwenhze, M. S.; White, S. H.; Witztum, J. L.; Dennis, E. a. *J Lipid Res* **2005**, *46*, 839–861.
- (2) Fahy, E.; Subramaniam, S.; Murphy, R. C.; Nishijima, M.; Raetz, C. R. H.; Shimizu, T.; Spener, F.; van Meer, G.; Wakelam, M. J. O.; Dennis, E. a. *J. Lipid Res.* **2009**, *50 Suppl*, S9–S14.
- (3) Yetukuri, L. R. *Bioinformatics approaches for the analysis of lipidomics data*; 2010.
- (4) Fahy, E.; Sud, M.; Cotter, D.; Subramaniam, S. *Nucleic Acids Res.* **2007**, *35*, W606–W612.
- (5) Kasuga, K.; Suga, T.; Mano, N. *J. Pharm. Biomed. Anal.* **2015**, *113*, 151–162.
- (6) Kamphorst, J. J.; Fan, J.; Lu, W.; White, E.; Rabinowitz, J. D. **2011**, 9114–9122.
- (7) van der Vusse, G. J.; van Bilsen, M.; Glatz, J. F. *Cardiovasc. Res.* **2000**, *45*, 279–293.
- (8) Beaudoin, F.; Michaelson, L. V.; Hey, S. J.; Lewis, M. J.; Shewry, P. R.; Sayanova, O.; Napier, J. a. *Proc. Natl. Acad. Sci. U. S. A.* **2000**, *97*, 6421–6426.
- (9) Kennedy, E. P. *Klin. Wochenschr.* **1987**, *65*, 205–212.
- (10) Peretó, J.; López-García, P.; Moreira, D. *Trends Biochem. Sci.* **2004**, *29*, 469–477.
- (11) Bishop, W. R.; Bell, R. M. *Annu. Rev. Cell Biol.* **1988**, *4*, 579–610.
- (12) Barenholz, Y.; Thompson, T. E. *Chem. Phys. Lipids* **1999**, *102*, 29–34.
- (13) Hevonoja, T.; Pentikäinen, M. O.; Hyvönen, M. T.; Kovanen, P. T.; Ala-Korpela, M. *Biochim. Biophys. Acta - Mol. Cell Biol. Lipids* **2000**, *1488*, 189–210.
- (14) Sastry, P. S. *Prog. Lipid Res.* **1985**, *24*, 69–176.
- (15) Sabourdy, F.; Astudillo, L.; Colacios, C.; Dubot, P.; Mrad, M.; Ségui, B.; Andrieu-Abadie, N.; Levade, T. *Biochim. Biophys. Acta* **2015**, *1851*, 1040–1051.
- (16) Gilham, D.; Lehner, R. *Rev. Endocr. Metab. Disord.* **2004**, *5*, 303–309.
- (17) Miller, N. E. *Eur. Heart J.* **1990**, *11 Suppl H*, 1–3.
- (18) Rueckert, D. G.; Schmidt, K. *Chem. Phys. Lipids* **1990**, *56*, 1–20.
- (19) Ahmadian, M.; Duncan, R. E.; Jaworski, K.; Sarkadi-Nagy, E.; Sul, H. S. *Future Lipidol.* **2007**, *2*, 229–237.
- (20) Gibbons, G. F.; Islam, K.; Pease, R. J. *Biochim. Biophys. Acta* **2000**, *1483*, 37–57.
- (21) Smith, L. C.; Pownall, H. J.; Gotto, a M. *Annu. Rev. Biochem.* **1978**, *47*, 751–757.
- (22) Brown, W. V. *J. Clin. Lipidol.* *1*, 7–19.
- (23) N.M. Weijers, R. *Curr. Diabetes Rev.* **2012**, *8*, 390–400.
- (24) Olbricht, C. J. *Klin. Wochenschr.* **1991**, *69*, 455–462.
- (25) Layre, E.; Moody, D. B. *Biochimie* **2013**, *95*, 109–115.

- (26) Santos, C. R.; Schulze, A. *FEBS J.* **2012**, *279*, 2610–2623.
- (27) Wijesinghe, D. S.; Chalfant, C. E. *Adv. wound care* **2013**, *2*, 538–548.
- (28) Abel, E. D.; O’Shea, K. M.; Ramasamy, R. *Arterioscler. Thromb. Vasc. Biol.* **2012**, *32*, 2068–2076.
- (29) Haoula, Z.; Ravipati, S.; Stekel, D. J.; Ortori, C. A.; Hodgman, C.; Daykin, C.; Rainefenning, N.; Barrett, D. A.; Atiomo, W. **2014**.
- (30) Brown, H. A. *Chem. Rev.* **2011**, *111*, 5817–5820.
- (31) Hoischen, C.; Ihn, W.; Gura, K.; Gumpert, J. *J. Bacteriol.* **1997**, *179*, 3437–3442.
- (32) Carrier, A.; Parent, J. *J. Liq. Chromatogr. Relat. Technol.* **2001**, *24*, 97–107.
- (33) Hauff, S.; Vetter, W. *Anal. Chim. Acta* **2009**, *636*, 229–235.
- (34) Aradottir, S.; Olsson, B. L. *BMC Biochem.* **2005**, *6*, 18.
- (35) Nakanishi, H.; Ogiso, H.; Taguchi, R. *Methods Mol. Biol.* **2009**, *579*, 287–313.
- (36) Liebisch, G.; Lieser, B.; Rathenber, J.; Drobnik, W.; Schmitz, G. *Biochim. Biophys. Acta - Mol. Cell Biol. Lipids* **2004**, *1686*, 108–117.
- (37) Burdge, G. C.; Wright, P.; Jones, a E.; Wootton, S. a. *Br. J. Nutr.* **2000**, *84*, 781–787.
- (38) Merlin, J.-F.; Gresti, J.; Bellenger, S.; Narce, M. *Anal. Chim. Acta* **2006**, *565*, 163–167.
- (39) Houjou, T.; Yamatani, K.; Imagawa, M.; Shimizu, T.; Taguchi, R. *Rapid Commun. Mass Spectrom.* **2005**, *19*, 654–666.
- (40) Horvath, S. E.; Daum, G. *Prog. Lipid Res.* **2013**, *52*, 590–614.
- (41) Hokazono, E.; Tamezane, H.; Hotta, T.; Kayamori, Y.; Osawa, S. *Clin. Chim. Acta.* **2011**, *412*, 1436–1440.
- (42) Morita, S.; Shirakawa, S.; Kobayashi, Y.; Nakamura, K.; Teraoka, R.; Kitagawa, S.; Terada, T. *J. Lipid Res.* **2012**, *53*, 325–330.
- (43) Ohkawa, R.; Kishimoto, T.; Kurano, M.; Dohi, T.; Miyauchi, K.; Daida, H.; Nagasaki, M.; Uno, K.; Hayashi, N.; Sakai, N.; Matsuyama, N.; Nojiri, T.; Nakamura, K.; Okubo, S.; Yokota, H.; Ikeda, H.; Yatomi, Y. *Clin. Biochem.* **2012**, *45*, 1463–1470.
- (44) Bessonneau, V.; Bojko, B.; Azad, A.; Keshavjee, S.; Azad, S.; Pawliszyn, J. *J. Chromatogr. A* **2014**, *1367*, 33–38.
- (45) Fuchs, B.; Süß, R.; Teuber, K.; Eibisch, M.; Schiller, J. *J. Chromatogr. A* **2011**, *1218*, 2754–2774.
- (46) Privett, O. S.; Blank, M. L.; Coddling, D. W.; Nickell, E. C. *J. Am. Oil Chem. Soc.* **1965**, *42*, 381–393.
- (47) Hidaka, H.; Hanyu, N.; Sugano, M.; Kawasaki, K.; Yamauchi, K.; Katsuyama, T. *Ann. Clin. Lab. Sci.* **2007**, *37*, 213–221.
- (48) Milne, S.; Ivanova, P.; Forrester, J.; Alex Brown, H. *Methods* **2006**, *39*, 92–103.
- (49) Han, X.; Gross, R. W. *Mass Spectrom. Rev.* *24*, 367–412.
- (50) Yang, K.; Han, X. *Metabolites* **2011**, *1*, 21–40.

- (51) Brugger, B.; Erben, G.; Sandhoff, R.; Wieland, F. T.; Lehmann, W. D. *Proc. Natl. Acad. Sci.* **1997**, *94*, 2339–2344.
- (52) Han, X.; Gross, R. W. *Proc. Natl. Acad. Sci. U. S. A.* **1994**, *91*, 10635–10639.
- (53) Ejsing, C. S.; Duchoslav, E.; Sampaio, J.; Simons, K.; Bonner, R.; Thiele, C.; Ekroos, K.; Shevchenko, A. *Anal. Chem.* **2006**, *78*, 6202–6214.
- (54) Han, X. *Anal. Biochem.* **2002**, *302*, 199–212.
- (55) McAnoy, A. M.; Wu, C. C.; Murphy, R. C. *J. Am. Soc. Mass Spectrom.* **2005**, *16*, 1498–1509.
- (56) Ståhlman, M.; Ejsing, C. S.; Tarasov, K.; Perman, J.; Borén, J.; Ekroos, K. *J. Chromatogr. B. Analyt. Technol. Biomed. Life Sci.* **2009**, *877*, 2664–2672.
- (57) Lintonen, T. P. I.; Baker, P. R. S.; Suoniemi, M.; Ubhi, B. K.; Koistinen, K. M.; Duchoslav, E.; Campbell, J. L.; Ekroos, K. *Anal. Chem.* **2014**, *86*, 9662–9669.
- (58) Schwudke, D.; Schuhmann, K.; Herzog, R.; Bornstein, S. R.; Shevchenko, A. *Cold Spring Harb. Perspect. Biol.* **2011**, *3*, a004614.
- (59) Birjandi, A. P.; Mirnaghi, F. S.; Bojko, B. .
- (60) Li, M.; Zhou, Z.; Nie, H.; Bai, Y.; Liu, H. *Anal. Bioanal. Chem.* **2011**, *399*, 243–249.
- (61) Ruiz-Rodriguez, A.; Reglero, G.; Ibañez, E. *J. Pharm. Biomed. Anal.* **2010**, *51*, 305–326.
- (62) Kopf, T.; Schmitz, G. *J. Chromatogr. B. Analyt. Technol. Biomed. Life Sci.* **2013**, *938*, 22–26.
- (63) Christie, W. W. *GAS CHROMATOGRAPHY AND LIPIDS A Practical Guide*; 1990.
- (64) Brondz, I. *Anal. Chim. Acta* **2002**, *465*, 1–37.
- (65) Laakso, I.; Hiltunen, R. **2002**, *465*, 39–62.
- (66) Lisa, M.; Cífková, E.; Holčápek, M. *J. Chromatogr. A* **2011**, *1218*, 5146–5156.
- (67) Salivo, S.; Beccaria, M.; Sullini, G.; Tranchida, P. Q.; Dugo, P.; Mondello, L. *J. Sep. Sci.* **2015**, *38*, 267–275.
- (68) Li, X.; Xu, Z.; Lu, X.; Yang, X.; Yin, P.; Kong, H.; Yu, Y.; Xu, G. *Anal. Chim. Acta* **2009**, *633*, 257–262.
- (69) Halket, J. M.; Waterman, D.; Przyborowska, A. M.; Patel, R. K. P.; Fraser, P. D.; Bramley, P. M. *J. Exp. Bot.* **2005**, *56*, 219–243.
- (70) Bird, S. S.; Marur, V. R.; Sniatynski, M. J.; Greenberg, H. K.; Kristal, B. S. *Anal. Chem.* **2011**, *83*, 940–949.
- (71) Taguchi, R.; Ogiso, H.; Suzuki, T. *Anal. Biochem.* **2008**, *375*, 124–131.
- (72) Cajka, T.; Fiehn, O. *Trends Analyt. Chem.* **2014**, *61*, 192–206.
- (73) Namie, J.; Kot-wasik, A. **2014**, *1362*, 62–74.
- (74) Hermansson, M.; Uphoff, A.; Käkälä, R.; Somerharju, P. *Anal. Chem.* **2005**, *77*, 2166–2175.
- (75) Xu, F.; Zou, L.; Lin, Q.; Ong, C. N. *Rapid Commun. Mass Spectrom.* **2009**, *23*, 3243–

3254.

- (76) Sandra, K.; Pereira, A. D. S.; Vanhoenacker, G.; David, F.; Sandra, P. *J. Chromatogr. A* **2010**, *1217*, 4087–4099.
- (77) Fauland, A.; Köfeler, H.; Trötz Müller, M.; Knopf, A.; Hartler, J.; Eberl, A.; Chitraju, C.; Lankmayr, E.; Spener, F. *J. Lipid Res.* **2011**, *52*, 2314–2322.
- (78) Chamorro, L.; García-Cano, A.; Busto, R.; Martínez-González, J.; Albillos, A.; Lasunción, M. Á.; Pastor, O. *Clin. Chim. Acta.* **2013**, *421*, 132–139.
- (79) Isaac, G. *Development of Enhanced Analytical Methodology for Lipid Analysis from Sampling to Detection A Targeted Lipidomics Approach*; 2005.
- (80) Hu, C.; Dommelen, J. Van; Heijden, R. Van Der; Spijksma, G.; Reijmers, T. H.; Wang, M.; Slee, E.; Lu, X.; Xu, G.; Greef, J. Van Der; Hankemeier, T. **2008**, 4982–4991.
- (81) Liebisch, G.; Binder, M.; Schifferer, R.; Langmann, T.; Schulz, B.; Schmitz, G. *Biochim. Biophys. Acta* **2006**, *1761*, 121–128.
- (82) Fahy, E.; Subramaniam, S.; Brown, H. A.; Glass, C. K.; Merrill, A. H.; Murphy, R. C.; Raetz, C. R. H.; Russell, D. W.; Seyama, Y.; Shaw, W.; Shimizu, T.; Spener, F.; van Meer, G.; VanNieuwenhze, M. S.; White, S. H.; Witztum, J. L.; Dennis, E. a. *J. Lipid Res.* **2005**, *46*, 839–861.
- (83) Murphy, R. C.; Fiedler, J.; Hevko, J. *Chem. Rev.* **2001**, *101*, 479–526.
- (84) Kliman, M.; May, J. C.; McLean, J. A. *Biochim. Biophys. Acta* **2011**, *1811*, 935–945.
- (85) Paglia, G.; Kliman, M.; Claude, E.; Geromanos, S.; Astarita, G. *Anal. Bioanal. Chem.* **2015**, *407*, 4995–5007.
- (86) Xu, H.; Valenzuela, N.; Fai, S.; Figeys, D.; Bennett, S. A. L. *FEBS J.* **2013**, *280*, 5652–5667.
- (87) Fernández, J. A.; Ochoa, B.; Fresnedo, O.; Giralt, M. T.; Rodríguez-Puertas, R. *Anal. Bioanal. Chem.* **2011**, *401*, 29–51.
- (88) Spengler, B. *J. Mass Spectrom.* **1997**, *32*, 1019–1036.
- (89) Stübiger, G.; Aldover-Macasaet, E.; Bicker, W.; Sobal, G.; Willfort-Ehringer, A.; Pock, K.; Bochkov, V.; Widhalm, K.; Belgacem, O. *Atherosclerosis* **2012**, *224*, 177–186.
- (90) Zhao, Z.; Xu, Y. *J. Lipid Res.* **2010**, *51*, 652–659.
- (91) J. Folch, M. Lees, G. H. S. S. *J. Biol. Chem.* **1957**, *226*, 497–509.
- (92) Bligh, E. G.; Dyer, W. J. *Can. J. Biochem. Physiol.* **1959**, *37*, 911–917.
- (93) Speijer, H.; Giesen, P. L.; Zwaal, R. F.; Hack, C. E.; Hermens, W. T. *Biophys. J.* **1996**, *70*, 2239–2247.
- (94) Lísá, M.; Holcapek, M. *Anal. Chem.* **2015**, 150620100944000.
- (95) Metherel, A. H. **2012**.
- (96) Min, H. K.; Lim, S.; Chung, B. C.; Moon, M. H. *Anal. Bioanal. Chem.* **2011**, *399*, 823–830.

- (97) Cui, L.; Lee, Y. H.; Kumar, Y.; Xu, F.; Lu, K.; Ooi, E. E.; Tannenbaum, S. R.; Ong, C. N. *PLoS Negl. Trop. Dis.* **2013**, *7*, e2373.
- (98) Hilvo, M.; Gade, S.; Hyötyläinen, T.; Nekljudova, V.; Seppänen-Laakso, T.; Sysi-Aho, M.; Untch, M.; Huober, J.; von Minckwitz, G.; Denkert, C.; Orešič, M.; Loibl, S. *Int. J. Cancer* **2014**, *134*, 1725–1733.
- (99) Chen, F.; Maridakis, V.; O'Neill, E. A.; Hubbard, B. K.; Strack, A.; Beals, C.; Herman, G. A.; Wong, P. *Biomarkers* **2011**, *16*, 321–333.
- (100) Shah, V.; Castro-Perez, J. M.; McLaren, D. G.; Herath, K. B.; Previs, S. F.; Roddy, T. P. *Rapid Commun. Mass Spectrom.* **2013**, *27*, 2195–2200.
- (101) Scherer, M.; Schmitz, G.; Liebisch, G. *Clin. Chem.* **2009**, *55*, 1218–1222.
- (102) Matyash, V.; Liebisch, G.; Kurzchalia, T. V.; Shevchenko, A.; Schwudke, D. *J. Lipid Res.* **2008**, *49*, 1137–1146.
- (103) Löfgren, L.; Ståhlman, M.; Forsberg, G.-B.; Saarinen, S.; Nilsson, R.; Hansson, G. I. *J. Lipid Res.* **2012**, *53*, 1690–1700.
- (104) Carlson, L. A. *Clin. Chim. Acta* **1985**, *149*, 89–93.
- (105) Matyash, V.; Liebisch, G.; Kurzchalia, T. V.; Shevchenko, A.; Schwudke, D. *J. Lipid Res.* **2008**, *49*, 1137–1146.
- (106) Xu, H.; Valenzuela, N.; Fai, S.; Figeys, D.; Bennett, S. a L. *FEBS J.* **2013**, *280*, 5652–5667.
- (107) Liebisch, G.; Lieser, B.; Rathenber, J.; Drobnik, W.; Schmitz, G. *Biochim. Biophys. Acta* **2004**, *1686*, 108–117.
- (108) Fukasawa, M.; Tanaka, Y.; Sato, S.; Ono, Y.; Nitahara-Kasahara, Y.; Suzuki, T.; Miyamura, T.; Hanada, K.; Nishijima, M. *Biol. Pharm. Bull.* **2006**, *29*, 1958–1961.
- (109) Hardy, S.; El-Assaad, W.; Przybytkowski, E.; Joly, E.; Prentki, M.; Langelier, Y. *J. Biol. Chem.* **2003**, *278*, 31861–31870.
- (110) Pfleger, R. C.; Anderson, N. G.; Snyder, F. *Biochemistry* **1968**, *7*, 2826–2833.
- (111) Teo, C. C.; Chong, W. P. K.; Tan, E.; Basri, N. B.; Low, Z. J.; Ho, Y. S. *TrAC Trends Anal. Chem.* **2015**, *66*, 1–18.
- (112) Kim, H.; Salem, N. *J. Lipid Res.* **1990**, *31*, 2285–2289.
- (113) Panagiotopoulou, P. M.; Tsimidou, M. *Grasas y Aceites* **2007**, *53*, 84–95.
- (114) Hamilton, J. G.; Comai, K. *Lipids* **1988**, *23*, 1146–1149.
- (115) Chen, Y.; Liu, Q.; Yong, S.; Teo, H. L.; Lee, T. K. *Clin. Chim. Acta* **2014**, *428*, 20–25.
- (116) Cha, D.; Cheng, D.; Liu, M.; Zeng, Z.; Hu, X.; Guan, W. *J. Chromatogr. A* **2009**, *1216*, 1450–1457.
- (117) Acar, N.; Berdeaux, O.; Grégoire, S.; Cabaret, S.; Martine, L.; Gain, P.; Thuret, G.; Creuzot-Garcher, C. P.; Bron, A. M.; Bretillon, L. *PLoS One* **2012**, *7*.
- (118) Shin, J.-H.; Shon, J. C.; Lee, K.; Kim, S.; Park, C. S.; Choi, E. H.; Lee, C. H.; Lee, H. S.; Liu, K.-H. *Anal. Bioanal. Chem.* **2014**, *406*, 1917–1932.

- (119) Liu, X.; Wang, F.; Liu, X.; Chen, Y.; Wang, L. *Eur. J. Lipid Sci. Technol.* **2011**, *113*, 775–779.
- (120) Uddin, M. S.; Kishimura, H.; Chun, B.-S. *J. Food Sci.* **2011**, *76*, C350–C354.
- (121) Uchikata, T.; Matsubara, A.; Fukusaki, E.; Bamba, T. *J. Chromatogr. A* **2012**, *1250*, 69–75.
- (122) Flores, E. M. M. *Microwave-Assisted Sample Preparation for Trace Element Determination*; Newnes, 2014.
- (123) Gonzalez-Illan, F.; Ojeda-Torres, G.; Diaz-Vazquez, L. M.; Rosario, O. *J. Anal. Toxicol.* **2011**, *35*, 232–237.
- (124) Khoomrung, S.; Chumnanpuen, P.; Jansa-Ard, S.; Ståhlman, M.; Nookaew, I.; Borén, J.; Nielsen, J. *Anal. Chem.* **2013**, *85*, 4912–4919.
- (125) Tsochatzidis, N. A.; Guiraud, P.; Wilhelm, A. M.; Delmas, H. *Chem. Eng. Sci.* **2001**, *56*, 1831–1840.
- (126) Liu, Y.; Chen, T.; Qiu, Y.; Cheng, Y.; Cao, Y.; Zhao, A.; Jia, W. *Anal. Bioanal. Chem.* **2011**, *400*, 1405–1417.
- (127) Pizarro, C.; Arenzana-Rámila, I.; Pérez-del-Notario, N.; Pérez-Matute, P.; González-Sáiz, J.-M. *Anal. Chem.* **2013**, *85*, 12085–12092.
- (128) Liu, L.; Na, L.; Niu, Y.; Guo, F.; Li, Y.; Sun, C. *J. Chromatogr. Sci.* **2013**, *51*, 376–382.
- (129) Péres, V. F.; Saffi, J.; Melecchi, M. I. S.; Abad, F. C.; de Assis Jacques, R.; Martinez, M. M.; Oliveira, E. C.; Caramão, E. B. *J. Chromatogr. A* **2006**, *1105*, 115–118.
- (130) Teo, C. C.; Chong, W. P. K.; Tan, E.; Basri, N. B.; Low, Z. J.; Ho, Y. S. *TrAC Trends Anal. Chem.* **2015**, *66*, 1–18.
- (131) Chen, J.; Pawliszyn, J. B. *Anal. Chem.* **1995**, *67*, 2530–2533.
- (132) Zhang, Z.; Yang, M. J.; Pawliszyn, J. *Anal. Chem.* **1994**, *66*, 844A – 853A.
- (133) Arthur, C. L.; Pawliszyn, J. *Anal. Chem.* **1990**, *62*, 2145–2148.
- (134) Szultka, M.; Szeliga, J.; Jackowski, M.; Buszewski, B. *Anal. Bioanal. Chem.* **2012**, *403*, 785–796.
- (135) Bojko, B.; Wąsowicz, M.; Pawliszyn, J. *J. Pharm. Anal.* **2014**, *4*, 6–13.
- (136) Mirnaghi, F. S.; Chen, Y.; Sidisky, L. M.; Pawliszyn, J. *Anal. Chem.* **2011**, *83*, 6018–6025.
- (137) Mirnaghi, F. S.; Mousavi, F.; Rocha, S. M.; Pawliszyn, J. *J. Chromatogr. A* **2013**, *1276*, 12–19.
- (138) Musteata, M. L.; Musteata, F. M.; Pawliszyn, J. *Anal. Chem.* **2007**, *79*, 6903–6911.
- (139) Togunde, O. P.; Lord, H.; Oakes, K. D.; Servos, M. R.; Pawliszyn, J. *J. Sep. Sci.* **2013**, *36*, 219–223.
- (140) Mirnaghi, F. S.; Pawliszyn, J. *Anal. Chem.* **2012**, *84*, 8301–8309.
- (141) Boyacı, E.; Gorynski, K.; Rodriguez-Lafuente, A.; Bojko, B.; Pawliszyn, J. *Anal.*

- Chim. Acta* **2014**, 809, 69–81.
- (142) Cudjoe, E.; Pawliszyn, J. *J. Chromatogr. A* **2014**, 1341, 1–7.
- (143) Musteata, F. M.; Pawliszyn, J. *TrAC Trends Anal. Chem.* **2007**, 26, 36–45.
- (144) Vuckovic, D.; Shirey, R.; Chen, Y.; Sidisky, L.; Aurand, C.; Stenerson, K.; Pawliszyn, J. *Anal. Chim. Acta* **2009**, 638, 175–185.
- (145) Lord, H. L.; Zhang, X.; Musteata, F. M.; Vuckovic, D.; Pawliszyn, J. *Nat. Protoc.* **2011**, 6, 896–924.
- (146) Vuckovic, D.; Cudjoe, E.; Musteata, F. M.; Pawliszyn, J. *Nat. Protoc.* **2010**, 5, 140–161.
- (147) Pawliszyn, J. *Handbook of Solid Phase Microextraction*; Elsevier, 2011; Vol. 29.
- (148) Risticvic, S.; Lord, H.; Górecki, T.; Arthur, C. L.; Pawliszyn, J. *Nat. Protoc.* **2010**, 5, 122–139.
- (149) Ouyang, G. *Anal. Chim. Acta* **2008**, 627, 184–197.
- (150) Vuckovic, D.; Pawliszyn, J. *J. Pharm. Biomed. Anal.* **2009**, 50, 550–555.
- (151) Musteata, F. M.; Pawliszyn, J. *J. Proteome Res.* **2005**, 4, 789–800.
- (152) Boyacı, E.; Rodríguez-Lafuente, Á.; Gorynski, K.; Mirnaghi, F.; Souza-Silva, É. a.; Hein, D.; Pawliszyn, J. *Anal. Chim. Acta* **2014**.
- (153) Wang, S.; Oakes, K. D.; Bragg, L. M.; Pawliszyn, J.; Dixon, G.; Servos, M. R. *Chemosphere* **2011**, 85, 1472–1480.
- (154) Vuckovic, D.; Risticvic, S.; Pawliszyn, J. *Angew. Chem. Int. Ed. Engl.* **2011**, 50, 5618–5628.
- (155) Barbara Bojkoa, Krzysztof Gorynskia, German Augusto Gomez-Riosa, Jan Matthias Knaakb, Tiago Machucac, Vincent Nikolaus Spetzlerb, Erasmus Cudjoea, Michael Hsinc, Marcelo Cypelc, M. S.; Mingyao Liuc, Shaf Keshavjeec, J. P. *Anal. Chim. Acta* **2013**, 803, 75–81.
- (156) Cudjoe, E.; Vuckovic, D.; Hein, D.; Pawliszyn, J. *Anal. Chem.* **2009**, 81, 4226–4232.
- (157) Vuckovic, D.; Cudjoe, E.; Hein, D.; Pawliszyn, J. **2010**, 80, 6870–6880.
- (158) Bojko, B.; Vuckovic, D.; Mirnaghi, F.; Cudjoe, E.; Wasowicz, M.; Jerath, A.; Pawliszyn, J. **2012**, 34, 31–37.
- (159) Reyes-Garcés, N.; Bojko, B.; Pawliszyn, J. *J. Chromatogr. A* **2014**, 1374, 40–49.
- (160) Togunde, O. P.; Oakes, K. D.; Servos, M. R.; Pawliszyn, J. *J. Chromatogr. A* **2012**, 1261, 99–106.
- (161) Weingart, G.; Kluger, B.; Forneck, A.; Krska, R.; Schuhmacher, R. *Phytochem. Anal.* **23**, 345–358.
- (162) Liberto, E.; Ruosi, M. R.; Cordero, C.; Rubiolo, P.; Bicchi, C.; Sgorbini, B. *J. Agric. Food Chem.* **2013**, 61, 1652–1660.
- (163) Gonçalves, J.; Figueira, J.; Rodrigues, F.; Câmara, J. S. *J. Sep. Sci.* **2012**, 35, 2282–2296.

- (164) Figueira, J.; Câmara, H.; Pereira, J.; Câmara, J. S. *Food Chem.* **2014**, *145*, 653–663.
- (165) Nicolotti, L.; Cordero, C.; Cagliero, C.; Liberto, E.; Sgorbini, B.; Rubiolo, P.; Bicchi, C. *Anal. Chim. Acta* **2013**, *798*, 115–125.
- (166) Pontes, M.; Pereira, J.; Câmara, J. S. *Food Chem.* **2012**, *134*, 2509–2520.
- (167) Sánchez, G.; Venegas-Calcrón, M.; Salas, J. J.; Monforte, A.; Badenes, M. L.; Granell, A. *BMC Genomics* **2013**, *14*, 343.
- (168) Cagliero, C.; Bicchi, C.; Cordero, C.; Rubiolo, P.; Sgorbini, B.; Liberto, E. *Food Chem.* **2012**, *132*, 1071–1079.
- (169) Riazanskaia, S.; Blackburn, G.; Harker, M.; Taylor, D.; Thomas, C. L. P. *Analyst* **2008**, *133*, 1020–1027.
- (170) Abaffy, T.; Möller, M. G.; Riemer, D. D.; Milikowski, C.; DeFazio, R. A. *Metabolomics* **2013**, *9*, 998–1008.
- (171) Buszewski, B.; Ulanowska, A.; Ligor, T.; Jackowski, M.; Kłodzińska, E.; Szeliga, J. *J. Chromatogr. B. Analyt. Technol. Biomed. Life Sci.* **2008**, *868*, 88–94.
- (172) Wang, Y.; Hu, Y.; Wang, D.; Yu, K.; Wang, L.; Zou, Y.; Zhao, C.; Zhang, X.; Wang, P.; Ying, K. *Cancer Biomark.* **2012**, *11*, 129–137.
- (173) Ligor, M.; Ligor, T.; Bajtarevic, A.; Ager, C.; Pienz, M.; Klieber, M.; Denz, H.; Fiegl, M.; Hilbe, W.; Weiss, W.; Lukas, P.; Jamnig, H.; Hackl, M.; Buszewski, B.; Miekisch, W.; Schubert, J.; Amann, A. *Clin. Chem. Lab. Med.* **2009**, *47*, 550–560.
- (174) Vuckovic, D.; Pawliszyn, J. *Anal. Chem.* **2011**, *83*, 1944–1954.
- (175) Vuckovic, D.; De Lannoy, I.; Gien, B.; Shirey, R. E.; Sidisky, L. M.; Dutta, S.; Pawliszyn, J. *Angew. Chemie - Int. Ed.* **2011**, *50*, 5344–5348.
- (176) Van Bilsen, M.; van der Vusse, G. J.; Reneman, R. S. *Eur. J. Physiol.* **1998**, *437*, 2–14.
- (177) van der Vusse, G. J.; Glatz, J. F.; Stam, H. C.; Reneman, R. S. *Physiol. Rev.* **1992**, *72*, 881–940.
- (178) Gao, X.; Li, K.; Hui, X.; Kong, X.; Sweeney, G.; Wang, Y.; Xu, A.; Teng, M.; Liu, P.; Wu, D. *Biochem. J.* **2011**, *435*, 723–732.
- (179) Kahn, S. E.; Hull, R. L.; Utzschneider, K. M. *Nature* **2006**, *444*, 840–846.
- (180) McGarry, J. D. *Diabetes* **2002**, *51*, 7–18.
- (181) Novgorodtseva, T. P.; Karaman, Y. K.; Zhukova, N. V.; Lobanova, E. G.; Antonyuk, M. V.; Kantur, T. A. *Lipids Health Dis.* **2011**, *10*, 82.
- (182) Zhou, Y.; Tian, C.; Jia, C. *Br. J. Nutr.* **2012**, *108*, 408–417.
- (183) Lacaze, J.-P. C. L.; Stobo, L. A.; Turrell, E. A.; Quilliam, M. A. *J. Chromatogr. A* **2007**, *1145*, 51–57.
- (184) Pusvaskiene, E.; Januskevicius, B.; Prichodko, A.; Vickackaite, V. *Chromatographia* **2008**, *69*, 271–276.
- (185) Brondz, I. *Anal. Chim. Acta* **2002**, *465*, 1–37.

- (186) Tsikas, D.; Zoerner, A.; Mitschke, A.; Homsy, Y.; Gutzki, F.-M.; Jordan, J. J. *Chromatogr. B. Analyt. Technol. Biomed. Life Sci.* **2009**, *877*, 2895–2908.
- (187) Hellmuth, C.; Weber, M.; Koletzko, B.; Peissner, W. *Anal. Chem.* **2012**, *84*, 1483–1490.
- (188) Kamphorst, J. J.; Fan, J.; Lu, W.; White, E.; Rabinowitz, J. D. *Anal. Chem.* **2011**, *83*, 9114–9122.
- (189) Kallenbach, M.; Baldwin, I. T.; Bonaventure, G. *Plant Methods* **2009**, *5*, 17.
- (190) Kotani, A.; Fuse, T.; Kusu, F. *Anal. Biochem.* **2000**, *284*, 65–69.
- (191) Gutnikov, G. *J. Chromatogr. B Biomed. Sci. Appl.* **1995**, *671*, 71–89.
- (192) Battistutta, F.; Buiatti, S.; Zenarola, C.; Zironi, R. *J. High Resolut. Chromatogr.* **1994**, *17*, 662–664.
- (193) Bailey, A. L.; Southon, S. *Anal. Chem.* **1998**, *70*, 415–419.
- (194) Simpson, N. J. K. *Solid-Phase Extraction: Principles, Techniques, and Applications*; CRC Press, 2000.
- (195) Poole, C. F.; Gunatilleka, A. D.; Sethuraman, R. *J. Chromatogr. A* **2000**, *885*, 17–39.
- (196) Kataoka, H. *J. Pharm. Biomed. Anal.* **2011**, *54*, 926–950.
- (197) Bojko, B.; Cudjoe, E.; Pawliszyn, J.; Wasowicz, M. *TrAC Trends Anal. Chem.* **2011**, *30*, 1505–1512.
- (198) Bojko, B.; Reyes-Garcés, N.; Bessonneau, V.; Goryński, K.; Mousavi, F.; Souza Silva, E. a.; Pawliszyn, J. *TrAC Trends Anal. Chem.* **2014**, *61*, 168–180.
- (199) Bojko, B.; Pawliszyn, J. *Bioanalysis* **2014**, *6*, 1227–1239.
- (200) Ábalos, M.; Bayona, J. .; Pawliszyn, J. *J. Chromatogr. A* **2000**, *873*, 107–115.
- (201) Mitropoulou, A.; Hatzidimitriou, E.; Paraskevopoulou, A. *Food Res. Int.* **2011**, *44*, 1561–1570.
- (202) Sharma, V.; Fan, J.; Jerath, a; Pang, K. S.; Bojko, B.; Pawliszyn, J.; Karski, J. M.; Yau, T.; McCluskey, S.; Wąsowicz, M. *Anaesthesia* **2012**, *67*, 1242–1250.
- (203) Bojko, B.; Vuckovic, D.; Cudjoe, E.; Hoque, M. E.; Mirnaghi, F.; Wąsowicz, M.; Jerath, A.; Pawliszyn, J. *J. Chromatogr. B* **2011**, *879*, 3781–3787.
- (204) Wąsowicz, M.; Jerath, A.; Bojko, B.; Sharma, V.; Pawliszyn, J.; McCluskey, S. *Can. J. Anaesth.* **2012**, *59*, 14–20.
- (205) Ashbrook, J. D.; Spector, A. A.; Santos, E. C.; Fletcher, J. E. *J. Biol. Chem.* **1975**, *250*, 2333–2338.
- (206) Matuszewski, B. K.; Constanzer, M. L.; Chavez-Eng, C. M. *Anal. Chem.* **2003**, *75*, 3019–3030.
- (207) Mirnaghi, F. S.; Pawliszyn, J. *J. Chromatogr. A* **2012**, *1261*, 91–98.
- (208) Bojko, B.; Vuckovic, D.; Pawliszyn, J. *J. Pharm. Biomed. Anal.* **2012**, *66*, 91–99.
- (209) Matuszewski, B. K.; Constanzer, M. L.; Chavez-Eng, C. M. *Anal. Chem.* **2003**, *75*, 3019–3030.

- (210) Kortz, L.; Dorow, J.; Becker, S.; Thiery, J.; Ceglarek, U. *J. Chromatogr. B. Analyt. Technol. Biomed. Life Sci.* **2013**, *927*, 209–213.
- (211) Oro, N. E.; Whittal, R. M.; Lucy, C. A. *Anal. Chim. Acta* **2012**, *741*, 70–77.
- (212) Cavaliere, C.; Foglia, P.; Gubbiotti, R.; Sacchetti, P.; Samperi, R.; Laganà, A. *Rapid Commun. Mass Spectrom.* **2008**, *22*, 3089–3099.
- (213) Cavaliere, C.; Foglia, P.; Gubbiotti, R.; Sacchetti, P.; Samperi, R.; Lagana, A. **2008**, 3089–3099.
- (214) van der VUSSE, G. J. *Drug Metab. Pharmacokinet.* **2009**, *24*, 300–307.
- (215) Fredrickson, D. S.; Gordon, R. S. *J. Clin. Invest.* **1958**, *37*, 1504–1515.
- (216) Hervé, F.; Urien, S.; Albengres, E.; Duché, J. C.; Tillement, J. P. *Clin. Pharmacokinet.* **1994**, *26*, 44–58.
- (217) Stewart, A. ; Fujiwara, S.; Amisaki, T. *Biochim. Biophys. Acta - Gen. Subj.* **2013**, *1830*, 5427–5434.
- (218) Musteata, F. M.; Pawliszyn, J.; Qian, M. G.; Wu, J.-T.; Miwa, G. T. *J. Pharm. Sci.* **2006**, *95*, 1712–1722.
- (219) Brodersen, R.; Andersen, S.; Vorum, H.; Nielsen, S. U.; Pedersen, a O. *Eur. J. Biochem.* **1990**, *189*, 343–349.
- (220) Food and Drug Administration. *Biopharm. Fed. Regist.* **2001**, *66*.
- (221) Mai, J.; Kinsella, J. E. *J. Food Sci.* **1979**, *44*, 1101–1105.
- (222) Mai, J.; Kinsella, J. E. *J. Food Biochem.* **1980**, *3*, 229–239.
- (223) Philibert, A.; Vanier, C.; Abdelouahab, N.; Chan, H. M.; Mergler, D. *Am J Clin Nutr* **2006**, *84*, 1299–1307.
- (224) Tuunanen, H.; Ukkonen, H.; Knuuti, J. *Curr. Cardiol. Rep.* **2008**, *10*, 142–148.
- (225) Turer, A. T.; Stevens, R. D.; Bain, J. R.; Muehlbauer, M. J.; van der Westhuizen, J.; Mathew, J. P.; Schwinn, D. A.; Glower, D. D.; Newgard, C. B.; Podgoreanu, M. V. *Circulation* **2009**, *119*, 1736–1746.
- (226) Ouyang, G.; Vuckovic, D.; Pawliszyn, J. *Chem. Rev.* **2011**, *111*, 2784–2814.
- (227) Musteata, F. M.; Pawliszyn, J. *J. Biochem. Biophys. Methods* **2007**, *70*, 181–193.
- (228) Cudjoe, E.; Togunde, P.; Pawliszyn, J. **2012**, 2605–2619.
- (229) Bojko, B.; Gorynski, K.; Gomez-Rios, G. a; Knaak, J. M.; Machuca, T.; Cudjoe, E.; Spetzler, V. N.; Hsin, M.; Cypel, M.; Selzner, M.; Liu, M.; Keshjavee, S.; Pawliszyn, J. *Lab. Invest.* **2014**, *94*, 586–594.
- (230) Jung, H. R.; Sylvänne, T.; Koistinen, K. M.; Tarasov, K.; Kauhanen, D.; Ekroos, K. *Biochim. Biophys. Acta* **2011**, *1811*, 925–934.
- (231) Brown, H. A. *Lipidomics and Bioactive Lipids: Mass Spectrometry Based Lipid Analysis*; Elsevier, 2007; Vol. 26.
- (232) Haag, M.; Schmidt, A.; Sachsenheimer, T.; Brügger, B. *Metabolites* **2012**, *2*, 57–76.
- (233) Moore, J. D.; Caufield, W. V; Shaw, W. a. *Methods Enzymol.* **2007**, *432*, 351–367.

- (234) Tautenhahn, R.; Patti, G. J.; Rinehart, D.; Siuzdak, G. *Anal. Chem.* **2012**, *84*, 5035–5039.
- (235) Deutsch, E. *Proteomics* **2008**, *8*, 2776–2777.
- (236) Destailats, F. *Lipid Technol.* **2010**, *22*, 119–119.
- (237) Koivusalo, M.; Haimi, P.; Heikinheimo, L.; Kostianen, R.; Somerharju, P. *J. Lipid Res.* **2001**, *42*, 663–672.
- (238) Tulipani, S.; Llorach, R.; Urpi-Sarda, M.; Andres-Lacueva, C. *Anal. Chem.* **2013**, *85*, 341–348.
- (239) Bylda, C.; Thiele, R.; Kobold, U.; Volmer, D. A. *Analyst* **2014**, *139*, 2265–2276.
- (240) Abbott, S. K.; Jenner, A. M.; Mitchell, T. W.; Brown, S. H. J.; Halliday, G. M.; Garner, B. *Lipids* **2013**, *48*, 307–318.
- (241) Chen, W.; Zhang, C.; Song, L.; Sommerfeld, M.; Hu, Q. *J. Microbiol. Methods* **2009**, *77*, 41–47.
- (242) Hodson, L.; Skeaff, C. M.; Fielding, B. A. *Prog. Lipid Res.* **2008**, *47*, 348–380.
- (243) Wang, L. Y.; Summerhill, K.; Rodriguez-Canas, C.; Mather, I.; Patel, P.; Eiden, M.; Young, S.; Forouhi, N. G.; Koulman, A. *Genome Med.* **2013**, *5*, 39.
- (244) Salihovic, S.; Kärrman, A.; Lindström, G.; Lind, P. M.; Lind, L.; van Bavel, B. *J. Chromatogr. A* **2013**, *1305*, 164–170.
- (245) Kim, H. Y.; Salem, N. *J. Lipid Res.* **1990**, *31*, 2285–2289.
- (246) Separation of Lipids by Solid Phase Extraction (SPE) : Protocol Exchange <http://www.nature.com/protocolexchange/protocols/2156> (accessed Aug 28, 2015).
- (247) Nilsson, K.; Andersson, M.; Beck, O. *J. Chromatogr. B. Analyt. Technol. Biomed. Life Sci.* **2014**, *970*, 31–35.
- (248) M. Ritchie, M. Mal, S. W. *Waters Corp. Milford* **2012**.
- (249) Yang, Y.; Cruickshank, C.; Armstrong, M.; Mahaffey, S.; Reisdorph, R.; Reisdorph, N. *J. Chromatogr. A* **2013**, *1300*, 217–226.
- (250) Cudjoe, E.; Vuckovic, D.; Hein, D.; Pawliszyn, J. *Anal. Chem.* **2009**, *81*, 4226–4232.
- (251) Bessonneau, V.; Bojko, B.; Azad, A.; Keshavjee, S.; Azad, S.; Pawliszyn, J. *J. Chromatogr. A* **2014**, *1367*, 33–38.
- (252) Mirnaghi, F. S.; Pawliszyn, J. *Anal. Chem.* **2012**, *84*, 8301–8309.
- (253) Togunde, O. P.; Cudjoe, E.; Oakes, K. D.; Mirnaghi, F. S.; Servos, M. R.; Pawliszyn, J. *J. Chromatogr. A* **2012**, *1262*, 34–42.
- (254) Ejsing, C. S.; Duchoslav, E.; Sampaio, J.; Simons, K.; Bonner, R.; Thiele, C.; Ekroos, K.; Shevchenko, A. *Anal. Chem.* **2006**, *78*, 6202–6214.
- (255) Bessonneau, V.; Boyaci, E.; Maciazek-jurczyk, M.; Pawliszyn, J. *Anal. Chim. Acta* **2015**, *856*, 35–45.
- (256) Bojko, B.; Gorynski, K.; Gomez-Rios, G. A.; Knaak, J. M.; Machuca, T.; Spetzler, V. N.; Cudjoe, E.; Hsin, M.; Cypel, M.; Selzner, M.; Liu, M.; Keshavjee, S.; Pawliszyn,

- J. Anal. Chim. Acta* **2013**, *803*, 75–81.
- (257) Zeng, E. Y.; Noblet, J. a. *Environ. Sci. Technol.* **2002**, *36*, 3385–3392.
- (258) Gouliarmou, V.; Smith, K. E. C.; de Jonge, L. W.; Mayer, P. *Anal. Chem.* **2012**, *84*, 1601–1608.
- (259) Bandow, N.; Altenburger, R.; Brack, W. *Chemosphere* **2010**, *79*, 1070–1076.
- (260) Górecki, T.; Pawliszyn, J. *Analyst* **1997**, *122*, 1079–1086.
- (261) Boyacı, E.; Sparham, C.; Pawliszyn, J. *Anal. Bioanal. Chem.* **2014**, *406*, 409–420.
- (262) Patterson, R. E.; Ducrocq, A. J.; Mcdougall, D. J.; Garrett, T. J.; Yost, R. A. **2015**, *1002*, 260–266.
- (263) Speijer, H.; Giesen, P. L.; Zwaal, R. F.; Hack, C. E.; Hermens, W. T. *Biophys. J.* **1996**, *70*, 2239–2247.
- (264) Bangham, A. D. *Adv. Lipid Res.* **1963**, *1*, 65–104.
- (265) Cai, S.; Syage, J. A. *J. Anal. Chem.* **2006**, *78*, 1191–1199.
- (266) Yang, Y.; Cruickshank, C.; Armstrong, M.; Mahaffey, S.; Reisdorph, R.; Reisdorph, N. *J. Chromatogr. A* **2013**, *1300*, 217–226.
- (267) Birjandi, A. P.; Bidari, A.; Rezaei, F.; Hosseini, M. R. M.; Assadi, Y. *J. Chromatogr. A* **2008**, *1193*, 19–25.
- (268) Cudjoe, E.; Bojko, B.; de Lannoy, I.; Saldivia, V.; Pawliszyn, J. *Angew. Chemie Int. Ed.* **2013**, *52*, 12124–12126.
- (269) Vuckovic, D. *Anal. Bioanal. Chem.* **2012**, *403*, 1523–1548.
- (270) Bojko, B.; Wąsowicz, M.; Pawliszyn, J. *J. Pharm. Anal.* **2013**.
- (271) Heringa, M. B.; Hermens, J. L. M. *TrAC Trends Anal. Chem.* **2003**, *22*, 575–587.
- (272) Górecki, T.; Pawliszyn, J. *Analyst* **1997**, *122*, 1079–1086.
- (273) Rueckert, D. G. *Chem. Phys. lipids, 1990, Vol.56(1), pp.1-20* **1990**, *56*, 1–20.
- (274) Tall, a. *Annu. Rev. Biochem.* **1995**, *64*, 235–257.
- (275) Stein, O.; Stein, Y. *Atherosclerosis* **2005**, *178*, 217–230.
- (276) Koster, E. H. M.; Wemes, C.; Morsink, J. B.; De Jong, G. J. *J. Chromatogr. B Biomed. Sci. Appl.* **2000**, *739*, 175–182.
- (277) Kratochwil, N. a.; Huber, W.; Müller, F.; Kansy, M.; Gerber, P. R. *Biochem. Pharmacol.* **2002**, *64*, 1355–1374.
- (278) Lambrinidis, G.; Vallianatou, T.; Tsantili-Kakoulidou, A. *Adv. Drug Deliv. Rev.* **2015**.
- (279) International Conference on Harmonisation of Technical Requirements for Registration of Pharmaceuticals for Human Use. *ICH Harmonized Guideline on “validation of analytical procedures: text and methodology” Q2 (R1)*.
- (280) Thompson, M.; Ellison, S. L. R.; Wood, R. *Pure Appl. Chem.* **2002**, *74*, 835–855.
- (281) El-Serag, H. B. *N. Engl. J. Med.* **2011**, *365*, 1118–1127.
- (282) Anthony, P. P. *Histopathology* **2001**, *39*, 109–118.

- (283) Llovet, J. M.; Burroughs, A.; Bruix, J. *Lancet* **2003**, *362*, 1907–1917.
- (284) Lim, K.; Han, C.; Dai, Y.; Shen, M.; Wu, T. *Mol. Cancer Ther.* **2009**, *8*, 3046–3055.
- (285) Siddiqui, R. A.; Harvey, K.; Stillwell, W. *Chem. Phys. Lipids* **2008**, *153*, 47–56.
- (286) Chénais, B.; Blanckaert, V. *Int. J. Breast Cancer* **2012**, *2012*, 712536.
- (287) Pardini, R. S. *Chem. Biol. Interact.* **2006**, *162*, 89–105.
- (288) Wenk, M. R. *Nat. Rev. Drug Discov.* **2005**, *4*, 594–610.
- (289) Sandra, K.; Sandra, P. *Curr. Opin. Chem. Biol.* **2013**, *17*, 847–853.
- (290) Vuckovic, D.; de Lannoy, I.; Gien, B.; Shirey, R. E.; Sidisky, L. M.; Dutta, S.; Pawliszyn, J. *Angew. Chem. Int. Ed. Engl.* **2011**, *50*, 5344–5348.
- (291) Patti, G. J.; Tautenhahn, R.; Siuzdak, G. *Nat. Protoc.* **2012**, *7*, 508–516.
- (292) Patti, G. J.; Tautenhahn, R.; Siuzdak, G. *Nat. Protoc.* **2012**, *7*, 508–516.
- (293) Blanksby, S. J.; Mitchell, T. W. *Annu. Rev. Anal. Chem. (Palo Alto, Calif.)* **2010**, *3*, 433–465.
- (294) Iverson, S. J.; Lang, S. L.; Cooper, M. H. *Lipids* **2001**, *36*, 1283–1287.
- (295) Li, Y.; Ghasemi Naghdi, F.; Garg, S.; Adarme-Vega, T. C.; Thurecht, K. J.; Ghafor, W. A.; Tannock, S.; Schenk, P. M. *Microb. Cell Fact.* **2014**, *13*, 14.
- (296) Dai, J.; Shen, J.; Pan, W.; Shen, S.; Das, U. N. *Lipids Health Dis.* **2013**, *12*, 71.
- (297) Itoh, S.; Taketomi, A.; Harimoto, N.; Tsujita, E.; Rikimaru, T.; Shirabe, K.; Shimada, M.; Maehara, Y. *J. Clin. Biochem. Nutr.* **2010**, *47*, 81–90.
- (298) Chi, T.-Y.; Chen, G. G.; Lai, P. B. S. *Cancer J.* **2004**, *10*, 190–200.
- (299) Iorio, E.; Ricci, A.; Bagnoli, M.; Pisanu, M. E.; Castellano, G.; Di Vito, M.; Venturini, E.; Glunde, K.; Bhujwalla, Z. M.; Mezzanzanica, D.; Canevari, S.; Podo, F. *Cancer Res.* **2010**, *70*, 2126–2135.
- (300) Ramírez de Molina, A.; Gutiérrez, R.; Ramos, M. A.; Silva, J. M.; Silva, J.; Bonilla, F.; Sánchez, J. J.; Lacal, J. C. *Oncogene* **2002**, *21*, 4317–4322.
- (301) Pinot, M.; Vanni, S.; Pagnotta, S.; Lacas-Gervais, S.; Payet, L. -a.; Ferreira, T.; Gautier, R.; Goud, B.; Antonny, B.; Barelli, H. *Science (80-)* **2014**, *345*, 693–697.
- (302) Dai, J.; Shen, J.; Pan, W.; Shen, S.; Das, U. N. *Lipids Health Dis.* **2013**, *12*, 71.
- (303) Vinciguerra, M.; Sgroi, A.; Veyrat-Durebex, C.; Rubbia-Brandt, L.; Buhler, L. H.; Foti, M. *Hepatology* **2009**, *49*, 1176–1184.
- (304) Lim, K.; Han, C.; Dai, Y.; Shen, M.; Wu, T. *Mol. Cancer Ther.* **2009**, *8*, 3046–3055.
- (305) Mousavi, F.; Bojko, B.; Pawliszyn, J. *Anal. Chim. Acta* **2015**, *892*, 95–104.
- (306) Boyacı, E.; Pawliszyn, J. *Anal. Chem.* **2014**, *86*, 8916–8921.
- (307) Wang, S.; Oakes, K. D.; Bragg, L. M.; Pawliszyn, J.; Dixon, G.; Servos, M. R. *Chemosphere* **2011**, *85*, 1472–1480.